2010

DEPARTAMENTO DE CIÊNCIAS DA VIDA

FACULDADE DE CIÊNCIAS E TECNOLOGIA
UNIVERSIDADE DE COIMBRA

Validation of primary hippocampal cultures for the study of neuronal dynamics

Marta Santos Esteves da Silva

2010

Marta Santos Esteves da Silva Validation of primary hippocampal cultures for the study of neuronal dynamics.

DEPARTAMENTO DE CIÊNCIAS DA VIDA

FACULDADE DE CIÊNCIAS E TECNOLOGIA
UNIVERSIDADE DE COIMBRA

Validation of primary hippocampal cultures for the study of neuronal dynamics

Dissertação apresentada à Universidade de Coimbra para cumprimento dos requisitos necessários à obtenção do grau de Mestre em Biologia Celular e Molecular. O trabalho foi realizado sob a orientação científica do Doutor Rony Nuydens (Janssen Pharmaceutica NV) e do Professor Doutor Carlos Duarte (Universidade de Coimbra)

Marta Santos Esteves da Silva

2010

The following work is the result of a partnership between the University of Coimbra, Portugal and Janssen Pharmaceutica N.V. (a division of Johnson & Johnson Pharmaceutical Research & Development), Belgium, from September 2009 to June 2010.

Acknowledgments

I would first like to thank Dr Rony Nuydens for accepting me in his team, for the interesting scientific discussions we had and for the experience transmitted. I also thank Peter Verstraelen for accepting me in his project, for the enthusiastic discussions and brainstorming we had, and for the support and some of the data presented in this work.

I express my gratitude to Professor Carlos Duarte, not only for providing me such an opportunity, but also for the support and amazing guidance given to me since I started the Masters, and especially during this year. I also thank Professora Emília Duarte for always being available to help me and answer my questions.

I especially want to thank Christoph Tombeur. I cannot be grateful enough for all the support in the lab, for always trying to answer my questions, finding the best solutions, and of course all the great (serious and not so serious) conversations we had.

A very heartfelt acknowledgment goes to Aga. I really appreciate getting to know you, your help, concern, advices, great tips, and joy really meant a lot to me. I especially want to thank all the emotional support, and the professional and most importantly, life experience that you so gracefully transmitted to me.

I thank all the helping minds and hands I met during my stay at Janssen. I want to thank Dr. Dieder Moechars, An, Eve, and Villy for all the support you gave me in so many different ways. A very kind thank you goes to Marc Vandermeeren, for always been so thoughtful and concerned with the well being of the three Portuguese girls.

I want to thank Dr Sandra Santos, for the important help given to me from Portugal. You were very kind in helping me in whatever you could at such a long distance.

To the friends I made during this year in Janssen, Turnhout and around – Raquel, Christelle, Nima, Geert, Andrea, and Daniele: thank you very much for our Friday evenings, weekend travels and especially smiles and pure joy that fill me with happiness as I recall how good it was to have you around to share this experience.

To my good friend Soraia. I lack the words to thank you for this year. Your happy spirit, strong personality, true friendship and patience to live with my bad mood were really important in every step of this experience. That I am truly grateful I could share with you.

I want to thank Hugo, for once again proving to be such a good friend, for giving me his support, for the great conversations, and of course for the essential help as my representative in Coimbra.

To my crazy friends in Portugal. I want to thank Raquel, Daniel, Miguel, Ana, Frederico, Carolina, Edgar, Marta, Bruno, Pedro and Sofia for all the phone calls, mails or visits, for the serious talks and silly moments, for your support, and for making me feel like I was not far away from you.

Por último, quero agradecer aos meus pais e à minha irmã. Por terem sempre acreditado em mim e nas minhas capacidades e por me terem proporcionado esta experiência. O vosso apoio incondicional tem sido fundamental desde sempre, ainda mais durante este ano tão desafiante. Todas as conversas que tivemos, os momentos cibernáuticos partilhados, os sorrisos que conseguiram mostrar quando mais precisava e as recepções calorosas quando estive de visita, não me deixam quaisquer dúvidas de que sou uma sortuda porque tenho a melhor família do mundo. Obrigada.

Table of contents

Abbreviations

AAV	adeno-associated virus
AMPAR	α-amino-3-hydroxyl-5-methyl-4-isoxazole-propionate receptor
Arc	activity-regulated cytoskeletal protein
BDNF	brain-derived neurotrophic factor
BSA	bovine serum albumin
βIII-tubulin	neuronal class III β-tubulin
C6-CM	1:1 mix of N2 medium and C6 glioma conditioned N2 medium
CAZ	cytoskeleton of the active zone
$[Ca^{2+}]_i$	intracellular calcium concentration
Ca^{2+}	calcium
CAM	cell adhesion molecule
CaMKII	Ca^{2+}/calmodulin-dependent protein kinase II
CASK	Ca^{2+}/calmodulin-dependent serine protein kinase
CM-DiI	1,1'-dioctadecyl-3,3,3',3'-tetramethylindocarbocyanine perchlorate
CNS	central nervous system
CO_2	carbon dioxide
CV	coated vesicles
DAPI	4',6-diamidino-2-phenylindole
DIV	days *in vitro*
DMEM	Dulbecco's modified Eagle's medium
DMSO	dimethylsulfoxide
DNA	deoxyribonucleic acid
EM	electron microscopy
ER	endoplasmic reticulum
FCS	fetal calf serum
Fluo3-AM	Fluo3 acetoxymethylester
GABA	γ-aminobutyric acid
GABAR	GABA receptor
GFAP	glial fibrillary acidic protein
eGFP	enhanced green fluorescent protein
GKAP	guanylate-kinase-associated protein
GRIP	glutamate-receptor-interacting protein
HBSS	Hank's balanced salt solution
$InsP_3R$	inositol-1,4,5-trisphosphate receptor
K^+	potassium
KA	kainate
Kali-7	Kalirin-7
L-LTP	late-phase long-term potentiation

LTD	long-term depression
LTP	long-term potentiation
MAP	microtubule-associated protein
MEM	minimum essential medium
Mg^{2+}	magnesium
mGluR	metabotropic glutamate receptor
MOI	multiplicity of infection
mRNA	messenger RNA
Na^{+}	sodium
NGF	nerve growth factor
NMDAR	N-methyl-D-aspartate receptor
PBS	phosphate buffered saline
PDL	poly-D-lysine
PEI	polyethyleneimine
PKC	protein kinase C
PSD	postsynaptic density
RNA	ribonucleic acid
ROI	region of interest
SER	smooth endoplasmic reticulum
SPAR	spine-associated RapGAP
SynGAP	synaptic Ras-GTPase activating protein
VGAT	vesicular GABA transporter
VGLUT1	vesicular glutamate transporter 1
VSCC	voltage-sensitive Ca^{2+} channel
YFP	yellow fluorescent protein

Resumo

As culturas primárias de neurónios dissociados são uma ferramenta popular em neurobiologia. Muita da informação acerca do desenvolvimento e refinamento dos circuitos neuronais foi obtida usando culturas primárias de neurónios isoladas a partir de diferentes regiões cerebrais. Estas culturas facilitam o acesso a neurónios individuais, permitindo a aplicação de métodos bioquímicos, electrofisiológicos ou de imagiologia. O efeito de manipulações farmacológicas pode ser inferido pela quantificação de alterações fenotípicas na cultura.

Prepararam-se culturas primárias de neurónios de hipocampo de rato em microplacas de 96 poços. Para a optimização das culturas diferentes condições foram testadas, entre elas o uso de diferentes meios de cultura e substratos para revestimento das placas. O meio C6-CM e revestimento de Poli-D-Lisina são as condições mais indicadas para o crescimento das culturas que podem ser usadas até aos 11DIV. O nível de morte celular e agregação de neurónios é elevado depois dos 11DIV.

Uma vez que se pretende usar estas culturas como modelo celular, a preparação foi caracterizada ao longo do tempo, através do uso de diferentes técnicas. As populações celulares presentes na cultura foram discriminadas através de marcadores celulares específicos. De 1DIV a 11DIV não há alteração no número de neurónios, embora o número de astrócitos e outras células aumente de 7DIV para 11DIV. Avaliou-se também o desenvolvimento neuronal e o crescimento de neurites, tendo-se observado a polarização dos neurónios em cultura e o alongamento das neurites, tal como descrito em estudos anteriores. O tamanho das neurites por neurónio aumenta para cada um dos tempos considerados.

Foram analizadas as alterações fenotípicas resultantes da estimulação de neurónios do hipocampo com NGF (*nerve growth factor*) ou com JNJ#X. O NGF (10ng/ml) teve um efeito protector no primeiro dia da cultura, tendo aumentado o número de neurónios. As restantes concentrações testadas (de 1 a 100 ng/ml) não alteraram significativamente o número de neurónios em cultura e o comprimento dos prolongamentos. Para concentrações entre 10^{-6} M e $3x10^{-8}$ M o composto JNJ#X aumentou o crescimento de neurites aos 1DIV, efeito que foi também detectado aos 4DIV para a concentração de $3x10^{-8}$ M. Na presença de concentrações mais elevadas de JNJ#X (10^{-5} M e 10^{-6} M) foi observada uma diminuição do número de neurónios em cultura após 7DIV. Para a maior concentração testada (10^{-5} M) o JNJ#X diminuiu o crescimento de neurites aos 7DIV, indicando que esta concentração é neurotóxica. Estes efeitos são uma indicação de que as técnicas previamente descritas são válidas na detecção de alterações fenotípicas na cultura primária.

A formação e maturação de sinapses durante o desenvolvimento foram avaliadas pela observação de proteínas pré- e pós-sinápticas. Tal como em estudos anteriores, os componentes pré-sinápticos foram observados a partir dos 4DIV, enquanto que os componentes pós-sinápticos foram observados apenas a partir dos 7DIV. As sinapses excitatórias foram analisadas em maior detalhe aos 7DIV e aos 11DIV. Não se verificaram diferenças significativas no número de proteínas pré- ou pós-sinápticas nem na colocalização dos marcadores sinápticos. Foram também usadas diferentes metodologias para a quantificação de espículas dendríticas. A marcação com CM-DiI permite a visualização de protuberâncias ao longo das neurites. Marcações combinadas com CM-DiI estão no momento a ser testadas para a caracterização das mesmas.

A funcionalidade da cultura primária foi também investigada. Para a análise da actividade eléctrica espontânea, foram feitos estudos de imagiologia em células individuais,

recorrendo ao uso de uma sonda fluorescente sensível a Ca^{2+}. As células foram estimuladas com glutamato e as alterações da $[Ca^{2+}]_i$ foram usadas com o objectivo de distinguir diferentes populações celulares. No entanto, foram poucas as preparações onde se observaram alterações da $[Ca^{2+}]_i$ resultantes da actividade eléctrica espontânea.

Abstract

Dissociated primary neuronal cultures are a popular research tool in neurobiology. Much of our understanding on the development and refinement of the neural circuitry sprung from the use of primary neuronal cultures isolated from different brain regions. These cultures allow the easy access to individual neurons for the application in biochemical, electrophysiological or imaging techniques. Furthermore, the effect of pharmacological manipulations can be assessed by quantifying phenotypical changes in the culture.

Primary neuronal hippocampal cultures from wild type animals were prepared and grown in 96-well microplates. For the optimization of the cultures, different conditions were tested, such as different sustaining media or substrates for well coating. The best sustaining medium is C6-CM and the best well coating is Poly-D-Lysine. In these conditions the cultures can be used until 11DIV. After 11DIV, the degree of cell death and neuronal clustering is high.

In order to be used as a cellular model, the cultures were characterized over time, by using different techniques. Cell populations were discriminated with the use of cell-type specific markers. From 1 to 11DIV, the number of neurons does not change, as the number of astrocytes and other cells increases from 7DIV to 11DIV. Neuronal development and neurite outgrowth were also assessed. It was observed that neurons in culture polarize and extend their processes, as described in previous studies. Neurite length per neuron is increasing in each of the timepoints considered.

Phenotypical changes in the primary cultures after stimulation with NGF (*nerve growth factor*) or JNJ#X were assessed. NGF (10ng/ml) seems to be neuroprotective at

1DIV. Other NGF concentrations tested (from 1 to 100ng/ml) did not induce significant changes neither in the number of neurons, nor in neurite outgrowth. Doses from 10^{-6} M to $3x10^{-8}$ M of JNJ#X increase neurite growth at 1DIV, an effect that is also detectable after 4DIV for $3x10^{-8}$ M of JNJ#X. High doses of JNJ#X (10^{-5} M and 10^{-6} M) decrease the number of neurons in culture at 7DIV. The highest tested dose of JNJ#X (10^{-5} M) also decreases neurite outgrowth at 7DIV, providing an indication that such dose is neurotoxic. The described changes in neuronal population and neurite outgrowth after the stimulations provide the indication that the used techniques are effective in the detection of phenotypical changes in the primary culture.

Further insight on synapse formation and maturation was assessed by evaluating the distribution of pre- and postsynaptic markers during development. As previously reported, presynaptic markers were detected after 4DIV, whereas postsynaptic markers were only observed at 7DIV. Excitatory synapses were further analyzed at 7DIV and 11DIV. There were no significant changes in the number of the markers and colocalizations in this timeframe. Different methodologies were applied for the quantification of dendritic spines. Labeling with CM-DiI allows for a clear visualization of protrusions along neurites. Combined stainings with CM-DiI for the further characterization of such protrusions are currently ongoing.

The functionality of the primary culture was also assessed. For the study of spontaneous electrical activity, live-cell imaging experiments were performed, with the use of a fluorescent Ca^{2+}-sensitive probe. Cells were stimulated with glutamate and changes in $[Ca^{2+}]_i$ were used for the discrimination of different cell types. However, traces of spontaneous electrical activity were very rare at any of the timepoints considered.

CHAPTER 1 Introduction

1.1. Brain function and neuronal communication

The mammalian brain relies on the communication between nerve cells for all its tasks, from the most simple to the most complex. However, there are still many unresolved questions as to how the brain works. Contemporary neuroscientists focus their attention on the circuit anatomy that underlies brain functions and the electrical patterns that bring these circuits to life, in an attempt to understand how assemblies of nerve cells can generate thought and motor activity (Südhof, 2006).

The great complexity of the brain, with an estimate of hundreds of billions of neurons, demands for a high degree of spatial, structural and functional organization. This is made possible by the remarkable flexibility of the nervous system which allows for precise communication between cells (Harms and Dunaeusky, 2007; Kasai et al**.,** 2003; Margeta and Shen, 2010; Sheng and Hoogenraad, 2007). Proposed for the first time by Santiago Ramón y Cajal more than a century ago, it is now known that such communication occurs through highly specialized intercellular junctions called synapses, which bring into contact a presynaptic axon and a postsynaptic dendrite, or a presynaptic neuron and a postsynaptic effector (Sheng and Hoogenraad, 2007; Südhof, 2006). In humans, the majority of synapses are formed during prenatal and early postnatal development, until about one year after birth. Subsequently, synapse numbers gradually decreases, even though new synapse formation still occurs throughout adulthood. Growing evidence shows that modifications in synapse function provide information on how the brain encodes the major events responsible for development from birth to adulthood, and how neural events related to learning and memory are controlled (Harms and Dunaeusky, 2007). Synapses are characterized by specificity and plasticity providing the structural and

the functional basis for formation and maintenance of the complex neural network comprising the brain. There is a high degree of control in the number, location and type of synapses formed.

Plasticity may be achieved by changing the properties of the existing synapses, by modifying the strength of synaptic transmission, the morphology or physical pattern of connectivity, or through the formation of new synapses and elimination of existing ones. These modifications occur in an activity-dependent manner, as a response to sensory experiences, and allow the long-term storage of information in the neural network (Sheng and Hoogenraad, 2007; Südhof, 2006). This is considered to be the underlying mechanism of learning and memory storage in the brain. Increasing evidence suggests that many neurological disorders affect synapses and synaptic plasticity. Therefore, steps towards a better understanding of synaptic function are needed for the design of novel therapeutical strategies.

1.2. What happens before synaptogenesis? Neural circuit assembly and development

The assembly of correct neuronal connections is crucial for the correct functioning of the nervous system (Stepanyants et al., 2004; Yamamoto et al., 2002). Neural circuits are the primary supracellular mediators of the brain's diverse functional capacities. A neural circuit can be defined as a cluster of neurons which receive, process and transmit electrochemical information, or in a higher perspective, a neural circuit can be formed by a network of interconnected brain regions that together integrate vast amounts of information and perform complex cognitive and regulatory functions (Tau and Peterson, 2010).

The structure and function of neural circuits constantly changes. The assembly starts with the first contact between nerve cells soon after birth. The developmental mechanisms

responsible for the formation of the adult vertebrate central nervous system (CNS) require an immense set of neurodevelopmental events dependent or independent of activity. The constant interaction between neurons and other cells and the surrounding environment also influence circuit formation. It was initially thought that the earliest stages of development of the CNS were exclusively controlled by genetically programmed clues for proliferation, migration and maturation of neurons, thus activity independent. The following synaptic refinement would be guided by neuronal activity driven by sensory inputs, and therefore considered activity-dependent (Cohen and Greenberg, 2008; Roerig and Feller, 2000). However, this traditional model is slowly being replaced by the possibility that the interplay of inherited genetic influences with a wide range of environmental exposures and experiences specifies the composition and organization of rudimentary neural circuits during all stages of development, leading to the widespread formation of connections between neurons (Blankenship and Feller, 2010; Tau and Peterson, 2010).

1.2.1. Initial steps of the neural circuit formation

Early neuronal and glial development starts at the embryonic period with proliferation from stem cells of the neural tube. At this stage, a large number of neurons are generated, followed by neuronal migration to their final location in the brain and neuronal differentiation (Ray et al., 1993; Spitzer, 2006). Many processes defining connectivity and ultimately neuronal functions are modulated by electrical activity. Activity-dependent processes influence neuronal network via a feedback loop mechanism. A given network may generate activity patterns which alter the organization of the network, causing modifications in the activity patterns that could further affect structural or functional characteristics (Roerig and Feller, 2000; Spitzer, 2006).

Neurons and neuronal precursors exhibit spontaneous activity at very early stages of development, well before synapses are formed. At this stage, activity occurs on a cell-by-cells basis and it is not typically correlated across cells. As the synaptic connections and functional circuits begin to emerge, spontaneous activity becomes correlated across large groups of neighbouring cells. It consists of rhythmic bursts of action potentials occurring with a timescale of minutes to hours, and provides modulatory information about the accuracy of the synapses formed, which will account for diverse connectivity configurations and functions (Blankenship and Feller, 2010; Cohen and Greenberg, 2008; Feller, 1999; Tau and Peterson, 2010; van Ooyen and van Pelt, 1994). Changes and oscillations in intracellular calcium concentration ($[Ca^{2+}]_i$) are the main mechanism by which spontaneous activity regulates neuronal development (Aguado et al., 2002; O'Donovan, 1999). In addition, the depolarizing action of γ-aminobutyric acid (GABA) in neural circuit development also accounts for Ca^{2+} influx and Ca^{2+} waves (Ben-Ari, 2002; Spitzer, 2002, 2006; Zhang and Poo, 2001), by changes in membrane polarization, activation or inactivation of ionic channels and neurotransmitter receptors (Fiszman et al., 1999; Liu and Wong-Riley, 2005) among other events.

1.2.2. Neuronal polarity

During migration, neurons undergo complex morphological rearrangements and become polarized, forming neurites that will differentiate either in axons or dendrites and eventually connect to other neurons forming synapses. The mechanisms involved in neuronal polarization are still not completely elucidated, mostly because of the limitations of *in situ* studies, complicating the manipulation of individual neurons. The development of *in vitro* systems allowed for significant advances in this area (da Silva and Dotti, 2002;

Dent and Gertler, 2003). It has been shown that neuronal polarization is not completely coincident in both situations. This is most likely due to the distribution of extracellular signals that control neurite sprouting *in situ* that are absent in neuronal cultures. However, as the basic architectural rearrangements are maintained and direct manipulation of differentiating neurons are possible, a great wealth of data have come from studies on neuronal cultures. In embryonic rat hippocampal cultures neurons are initially spherical, with a large nucleus, little cytoplasm and surrounded by thin lamellipodium. Later they extend at particular sites and have dynamic growth cones at their tips. One of these processes elongates rapidly while the others remain stationary, elongating later and to a lesser extent. The former would most likely become the axon and the latter the dendrites (Dotti et al., 1988; Tahirovic and Bradke, 2009). Such events involve cytoskeleton elements and many cytoskeletal associated proteins, with downstream regulation of different signaling cascades (Dent and Gertler, 2003). Spontaneous activity also regulates neuronal differentiation, controlling the level of excitability of cells, axon guidance, and dendrite outgrowth. Thus, a developing neural circuit is a dynamic system where the structure, the number of elements, and the functional characteristics of the elements are variable and partly under control of the system's own activity (Spitzer, 2006; van Ooyen and van Pelt, 1994).

1.3. Refinement of circuit connectivity: synapse formation and maturation

Efficient synaptic transmission in the CNS depends on the contact between the presynaptic axon and the postsynaptic dendrite, the recruitment of pre- and postsynaptic proteins to the site of contact, and the stabilization of the axodendritic interaction to initiate

the assembly of a functional synapse (Cohen and Greenberg, 2008; Lardi-Studler and Fritschy, 2007).

Despite the extensive wealth of studies on synapses, very little is known about their origin and evolution. This is due to the lack of tools available to study synapses in an evolutionary perspective. However, recent progress in proteomics and genomics, coupled with molecular phylogenetic approaches, are stimulating the interest in this subject (Ryan and Grant, 2009).

A single neuron may form many synapses. Additionally, synapses formed by one single neuron have large differences in properties, depending on the target neuron with which these synapses are formed. The number, location and distinct functional properties of synapses confer high degree of complexity to synaptic circuits, which is essential for information processing by these circuits (Südhof, 2006).

The coupling of two neurons through a synapse is a complex phenomenon. In a very simplified view, an electrical signal arrives at the pre-synaptic terminal and is transformed into a chemical signal which is released into the synaptic cleft, and recognized by receptors on the membrane of the postsynaptic neuron (Sudhof, 2004; Südhof, 2006), triggering a response. The chemical signal corresponds to the release of a chemical neurotransmitter by exocytosis of neurotransmitter-filled vesicles, under a tight temporal and spatial control (Fig.1). There are also additional antero- and retrograde signals regulating synapse properties and size (Südhof, 2006).

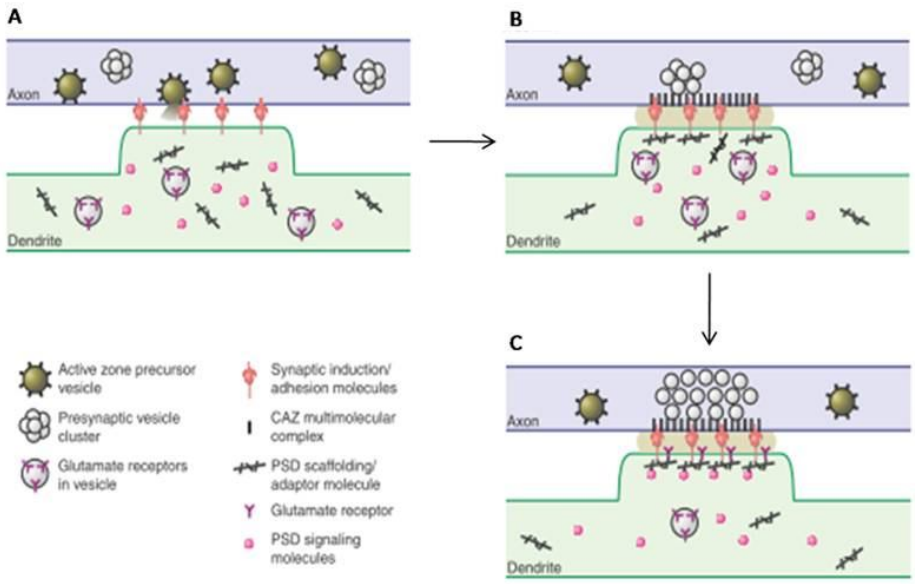

Figure 1. Simulated 'time-lapse sequence' representing synaptic differentiation.

The differentiation process is presumed to be initiated by interaction between the external regions of membrane molecules of both terminals. The insertion of presynaptic precursor vesicles in the active zone (A) activates cytoskeleton complexes in that area. This initiates the presynaptic reorganization that will lead to the formation of functional active zones, where the neurotransmitter will be released into the synaptic cleft by exocytosis of the presynaptic vesicles (B). Postsynaptic differentiation occurs latter by the sequential recruitment of PSD scaffolding molecules followed by glutamate receptors and PSD signaling molecules (C). This leads to the maturation of the synapse. CAZ, cytoskeleton of the active zone; PSD, postsynaptic density (Ziv and Garner, 2001)

Most synapses are formed during development, but synaptogenesis also occurs in the adult brain, as individual synapses in the brain have a life span of days to months and synapse formation and pruning in brain circuits occur during the entire life (Lardi-Studler and Fritschy, 2007). The majority of synapses in the brain are either excitatory or inhibitory. In excitatory synapses, the most important neurotransmitter is glutamate and the

receptors are either ionotropic N-methyl-d-aspartate receptors (NMDAR), α-amino-3-hydroxyl-5-methyl-4-isoxazole-propionate receptors (AMPAR) and kainate (KA) receptors, or metabotropic receptors (mGluRs). In inhibitory synapses, GABA and glycine act on ligand-gated chloride channels, the $GABA_A$ and glycine receptors, respectively. Excitatory transmission mediates information transfer across the brain, whereas inhibitory transmission shapes the patterns of neuronal activity in neuronal networks and prevents them from synchronous discharges (Lardi-Studler and Fritschy, 2007). Most of the excitatory synapses are formed in specialized dendritic protrusions called spines, whereas inhibitory synapses occur in the dendritic shaft, cell body and the axon initial segment (Fig.2).

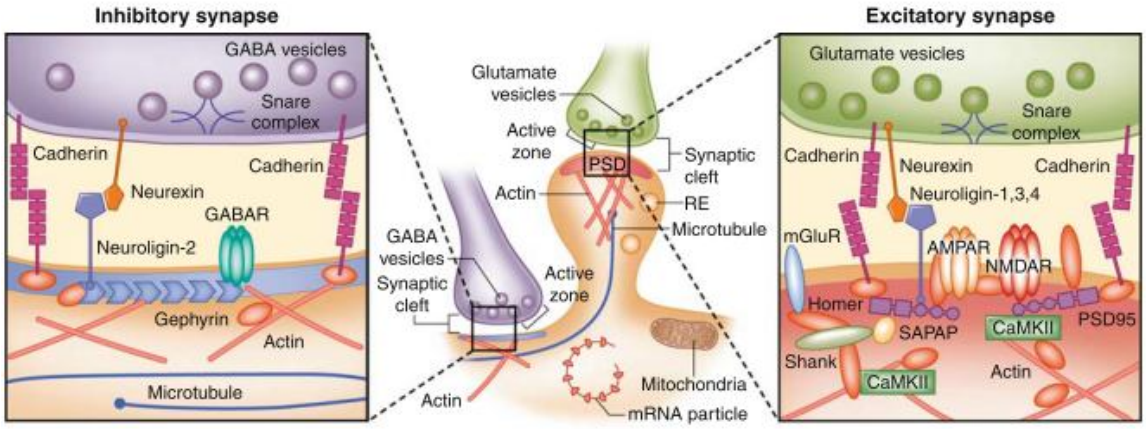

Figure 2. Molecular architecture of inhibitory and excitatory synapses.
GABAergic and glutamatergic synapses are formed in different locations in dendrites (central panel), as the former are located in the dendritic shaft (left panel), while the latter are usually formed in dendritic spines (right panel). In addition, there is a great difference in the composition of each synapse: excitatory synapses have a prominent PSD and spines are abundant in actin cytoskeleton, while inhibitory synapses do not have PSDs. GABAR, GABA Receptor; CaMKII, Ca^{2+}/calmodulin-dependent kinase II; RE, recycling endosome; SAPAP, synapse-associated protein 90/PSD-95 associated protein (van Spronsen and Hoogenraad, 2010).

1.3.1. Microanatomy of an excitatory synapse

Like other intercellular junctions, synapses contain diverse transmembrane proteins, neurotransmitter receptors, cytoskeletal elements and signaling molecules. However, unlike most other junctions they are typically asymmetric (Yamagata et al., 2003). Ultrastructural studies through electron microscopy (EM) allow for the clear distinction between the pre- and the postsynaptic fractions of the synapse. The active zone of the presynaptic terminal contains clusters of synaptic vesicles with about 40nm in diameter, that are exocytosed in the synaptic cleft In the postsynaptic side is the postsynaptic density (PSD), an electron-dense thickening of the membrane (Sala et al., 2008; Sheng and Hoogenraad, 2007). The active zone and the PSD are very close and precisely opposed to each other. Cell-adhesion molecules (CAMs) stabilize synapses by ensuring the appropriate proximity between the pre- and postsynaptic membranes (Fig. 2) (Sheng and Hoogenraad, 2007).

1.4. Activity-dependent adaptations of the neural circuit: plasticity

One of the most critical properties of the mammalian brain is its plasticity, that is the ability to modify neural circuit function and consequently thoughts, feelings and behaviour, as a response to neuronal activity generated by experience (Citri and Malenka, 2008; Lee, 2006). Synaptic plasticity particularly refers to activity-dependent modifications of the strength or efficacy of synaptic connections at pre-existing synapses (Citri and Malenka, 2008; Hamdache and Labadie, 2009). For more than a century synaptic plasticity has been proposed to play an important role in the brain's capacity to convert transient experiences into persistent memory traces.

Many mechanisms and forms of synaptic plasticity have already been described. Synaptic transmission can be enhanced or depressed within milliseconds or minutes (short-

term plasticity) to hours, days, weeks or even longer (long-term plasticity). There is increasing evidence that long-lasting changes in synapses are associated to learning and memory processes (Hamdache and Labadie, 2009). Virtually all excitatory synapses can simultaneously express different forms of synaptic plasticity (Citri and Malenka, 2008). Besides its temporal distinction, synaptic plasticity can either operate on specific sets of synapses, known as synapse-specific plasticity, or act on global variables to affect the function of all synapses on a given neuron – homeostatic plasticity (Lee, 2006).

Whichever the type considered, synaptic plasticity can be mediated by many mechanisms affecting either the pre- or postsynaptic components, like changes in excitability and gene expression, but also through non-neuronal events, such as changes in glial or vascular interactions with the neurons (Lee, 2006). Most of the results on synaptic plasticity come from studies focusing on long-term synapse-specific plasticity.

1.4.1. Long-term synaptic plasticity

In 1949 Donald Hebb proposed that associative memories form in the brain by synaptic modifications, which strengthens connections when presynaptic activity correlates with postsynaptic firing (Citri and Malenka, 2008). This idea lacked experimental support until 1973 when Bliss and colleagues proved that repetitive activation of excitatory synapses in the hippocampus caused a potentiation of synaptic strength that could last hours or days, a phenomenon then termed as long-term potentiation (LTP) (Bliss and Gardner-Medwin, 1973; Bliss and Lomo, 1973). Since then, LTP has been the object of a lot of interest and research, as it is believed that it may be an important key to understanding the cellular and molecular mechanisms underlying learning and memory (Bourne and Harris, 2007; Citri and Malenka, 2008; Sanes and Lichtman, 1999). LTP is a long lasting increase

in synaptic strength in response to a brief patterned high-frequency stimulus or a pairing of pre-and postsynaptic activation. It is now accepted that most synapses exhibiting LTP also show long-term depression (LTD). LTD is a long lasting decrease in synaptic strength following a brief patterned low-frequency stimulus. This implies that synaptic strength at excitatory synapses is susceptible to bidirectional modifications by different patterns of connectivity (Sabatini et al., 2002; Segal, 2005).

Most knowledge on the molecular mechanisms of synaptic plasticity comes from studies of LTP in hippocampal slices and dissociated cultures focusing on the excitatory synapses of CA1 pyramidal neurons. Studies in the hippocampus are important because of the large amount of evidence associating the hippocampus to various forms of long-term memory. Similar or identical forms of LTP have been observed at excitatory synapses throughout the brain, and the conclusions drawn from studying LTP in the hippocampus are often extrapolated to other brain regions (Citri and Malenka, 2008). Spines are the major receptor for excitatory synapses and have been shown to express plastic properties similar to those believed to occur during learning and memory formation. Therefore spines are believed to be the locus of long-term synaptic plasticity associated with memory storage (Segal, 2005). Further insight on excitatory synapses, and in particular on dendritic spines and the relation with synaptic plasticity, should be elucidated.

1.5. Synaptic plasticity: lessons from dendritic spines

The relation between spines and synaptic plasticity has been the focus of many experimental observations. In order to understand the cellular basis of memory storage, it is important to clarify how the structure and function of spines are regulated by molecular

interactions. It is also important to study the role of the local interactions surrounding the spines, and the global neural-network activity (Matsuzaki, 2007).

Spines are tiny protrusions arising from the dendrites of excitatory neurons (Harms and Dunaeusky, 2007). They are considered subcellular, highly specialized structures, apparently a compartment that biochemically responds to activation of individual synapses (Carlisle and Kennedy, 2005). These structures are quite frequent on dendrites of many types of neurons, including cerebral pyramidal cells, striatal neurons, granule cells of the dentate gyrus, and cerebral Purkinje cells (Fiala et al., 2008). About 90% of the excitatory synapses in mature mammalian brain are located in spines. There are approximately 1-10 spines per micrometer of dendrite length on principal neurons but spine density varies according to the neuron type and also along the length of the dendritic segment (Harris, 1999; Sala et al., 2008; Sheng and Hoogenraad, 2007).

Accumulating evidence using modern imaging techniques shows that neuronal activity is associated to changes in spine number, volume or shape. In recent years, the dynamic nature of spines has been vividly demonstrated by microscopy of living cells. The first glimpses of the dynamic nature of spines came to light with the studies of Smith and colleagues (Dailey and Smith, 1996).Using confocal time-lapse microscopy in culture and in organotypic slices from different brain regions it was demonstrated that spines emerge and retract on a time scale of seconds to minutes (Bhatt et al., 2009; Polleux and Gosh, 2008). Additionally, other reports showed that some mature spines undergo rapid changes in the shape of their heads (spine morphing), and also that filopodia emerge from the spine head (Dunaevsky and Mason, 2003a; Dunaevsky et al., 1999; Fischer et al., 1998). Rapid changes in spine morphology are believed to be based on rearrangements of the actin cytoskeleton (Dunaevsky et al., 1999). These results were then evaluated in the intact brain

with transgenic mice expressing fluorescent proteins (Polleux and Gosh, 2008). New spines can be formed, while existing ones can be eliminated. It is of major interest to understand how these events are modulated during synaptic activity (Kasai et al., 2003) specially given the growing evidence of a correlation between changes in spines and neurological disorders (Fiala et al., 2002).

1.5.1. Spine structure and function

Spines are formed by a bulbous head and a neck that ensures the connection to the parent dendrite (Hering and Sheng, 2001; Sala et al., 2008). There is a high degree of diversity and spines are often classified according to their morphology. Different types of spines can be found at the same time and in the same dendrite (Fig. 3) (Sala et al., 2008). Live imaging studies reveal that spines are highly dynamic, changing their size and shape within timescales ranging from seconds to days (Dunaevsky et al., 2001; Dunaevsky et al., 1999; Hering and Sheng, 2001). Increasing evidence suggests a relationship between the heterogeneous morphology and developmental stages, distance to the cell body or altered strength of synapses, which has led to an increased interest in investigating the underlying mechanism of synaptic strength and spine morphology (Bourne and Harris, 2007; Tada and Sheng, 2006).

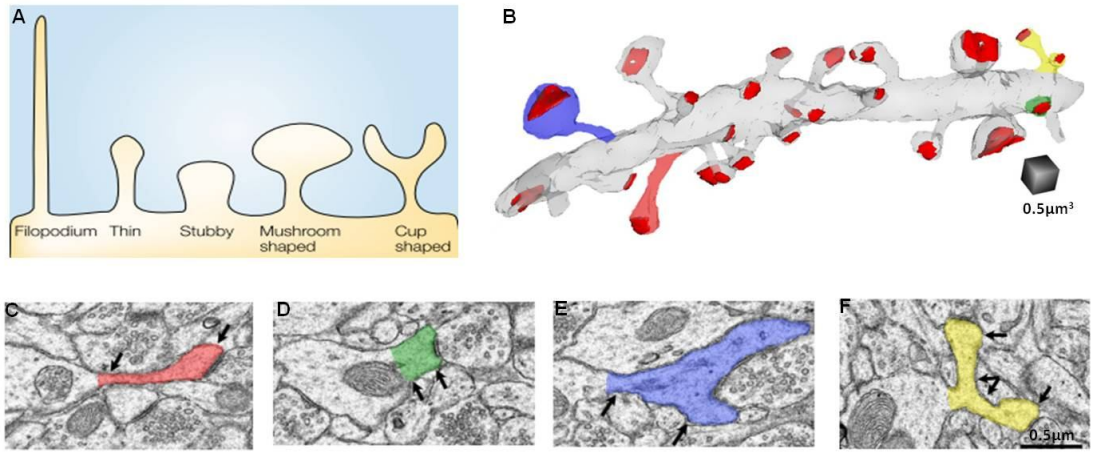

Figure 3. Morphological classification of dendritic spines.

Usually spines are ~0.5µm in diameter and 0.5-2.0µm in length, with a total volume ranging from less than 0.01µm^3 to 0.8µm^3 (Carlisle and Kennedy, 2005; Sorra and Harris, 2000). Spines have diverse morphologies (A). Developing neurons are abundant in filopodia, considered to be spine precursors. Filopodia are typically much longer and thinner than spines and headless (Parnass et al., 2000). Most spines are either thin-shaped with smaller heads attached to the dendrite by a fine neck(red B, C) or mushroom-shaped (blue B, E) with large heads, exceeding more than 0.6µm in diameter (Bourne and Harris, 2008; Parnass et al., 2000). PSDs (red) also vary in size and shape (B). The neck works as a constrictor and can be thin or thick. Neck geometry is important to signal transduction and protein trafficking from and to the spine (Carter and Sabatini, 2008). EM studies revealed other spine forms, such as stubby (green B, D), cup-shaped, or branched (yellow B, F) spines with two or more heads or single protrusion with multiple synapses along their head and neck (Bourne and Harris, 2008; Hering and Sheng, 2001; Sala et al., 2008). Accumulating evidence reveals that there is a continuum between categories (Garcia-Lopez et al., 2007; Sheng and Hoogenraad, 2007) (A adapted from Hering and Sheng, 2001; B to F adapted from Bourne and Harris, 2008).

The synaptic contact occurs between the presynaptic terminal and the spine head, which harbours the PSD and some organelles (Sheng and Hoogenraad, 2007). The constricted neck compartmentalizes the spine, hindering the diffusion of ions and signaling

molecules to and from the parent dendritic shaft (Fig. 3). This is a way to assure the relative isolation of the biochemical changes regarding one individual synapse, to prevent other synapses of the same neuron being influenced, and also to protect the parent dendrite from excitotoxic inputs that may affect the spine following synaptic activation (Bourne and Harris, 2008; Harris, 1999; Hayashi and Majewska, 2005; Hering and Sheng, 2001; Noguchi et al., 2005).

The structural changes to which spines are subjected are accompanied by alterations in the intracellular composition and organization (Hering and Sheng, 2001; Sala et al., 2008). The PSD occupies a privileged position at the head of the spine, usually occupying 10% of its surface area (Harris, 1999). It contains hundreds of proteins including a considerable concentration of the ionotropic and metabotropic glutamate receptors, scaffolding and adapter proteins, protein kinases and phosphatases and other signaling molecules, actin-binding proteins, and CAMs (Fig.4) (Sheng and Hoogenraad, 2007; Ziv and Garner, 2001).

Spine cytoskeleton is mainly formed by polymers of filamentous actin (F-actin). Actin cytoskeleton is highly dynamic, under the influence of Ca^{2+} transients. Rapid Ca^{2+}-induced changes greatly affect spine size, shape, motility, and stability (Sheng and Hoogenraad, 2007). Larger spines harbour larger PSDs and are also more likely to contain more membrane-bound organelles (Fig. 4).

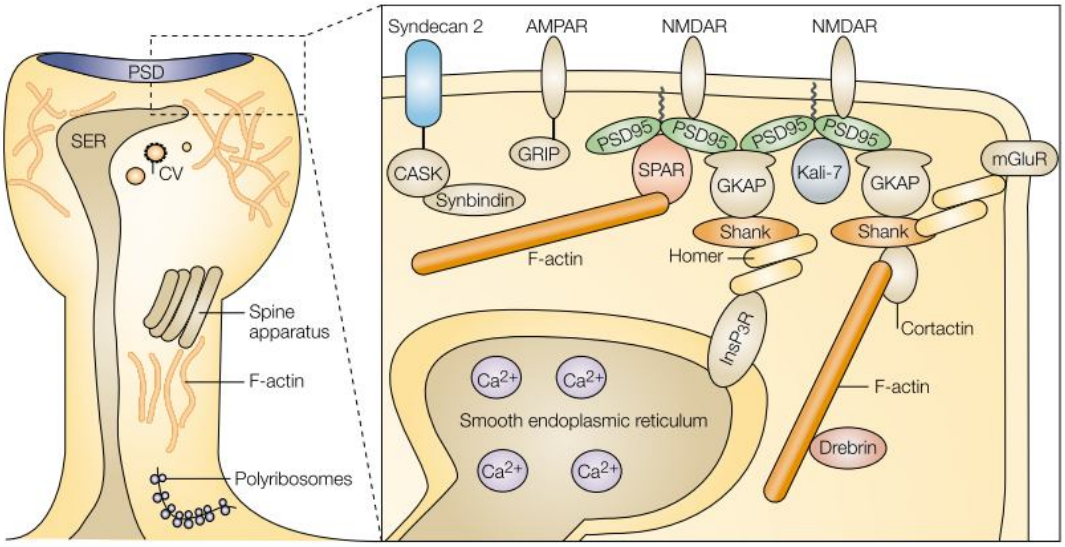

Figure 4. The structure of a mushroom spine.

The PSD is enriched in glutamate receptors, and many scaffolding, adapter and signalling proteins (enlarged box on the right) (Kennedy, 2000; Sala et al., 2008). Contacts between proteins indicate an established interaction between them. Spines are enriched in polymers of F-actin with many proteins interacting with the F-actin cytoskeleton. Many other proteins are not depicted in this diagram. As it is a large spine, it can contain many organelles: smooth endoplasmic reticulum (SER), coated vesicles (CV), and the spine apparatus, which is an organelle formed by stacks of SER membrane surrounded by densely staining material. All of these seem to be related to protein expression and trafficking to and from the synapse. Polyribosomes have been detected in dendritic shafts, occasionally extending into spines, providing an indication that protein translation might occur in the spine. GRIP, glutamate-receptor-interacting protein; GKAP, guanylate-kinase-associated protein; Kali-7, Kalirin-7; SPAR, spine-associated RapGAP; CASK, $Ca^{2+/}$calmodulin-dependent serine protein kinase; $InsP_3R$, inositol-1,4,5-trisphosphate receptor (Hering and Sheng, 2001).

Spines are formed in early postnatal life, shaped by experience, and maintained during adulthood, contributing to the formation and elimination of synapses (Tada and

Sheng, 2006). In the early stages of synaptogenesis, spines are rare, whereas dendrites are rich in filopodia that quickly extend and retract from the shaft (Hering and Sheng, 2001). Filopodia are very abundant in the brain during the first postnatal week *in vivo*, but its abundance and length change later during development (Hayashi and Majewska, 2005), with concomitant increase of thin and mushroom-shapes spines, the predominant forms in the adult rat brain (Hering and Sheng, 2001). Spine maturation requires increased spine density and stabilization, with a simultaneous decrease in the overall length and number of dendritic filopodia and spine motility (Dunaevsky et al., 2001), suggesting that filopodia are the precursors of stable spines (Dunaevsky and Mason, 2003a; Dunaevsky and Mason, 2003b).

1.5.2. Structure-function relationship

Besides being the first recognizing spines, Ramón y Cajal also speculated that spine's function would be to connect axons to dendrites and also might be involved in learning. The advent of EM allowed many studies on spines and synaptic structures and thus proved Ramón y Cajal correct (Parnass et al., 2000). Usually each spine only participates in a single synapse, which possibly indicates local synapse-specific compartmentalization instead of merely an expansion of the postsynaptic area. The main accepted idea about spine function is to sense glutamate release from presynaptic nerve terminals (Kasai et al., 2003) and provide a microcompartment for segregating postsynaptic chemical responses. Ionotropic glutamate receptors are the major excitatory neurotransmitter receptors in the CNS (Polleux and Gosh, 2008), responsible for the primary depolarization in glutamate-mediated neurotransmission and playing key roles in synaptic plasticity (Santos et al., 2009). AMPARs are permeable to sodium (Na^+) and

potassium (K^+), and their activation accounts for most of the inward current that generates the excitatory synaptic response when the cell is close to its resting membrane potential. Contrarily, NMDARs activation is voltage-dependent because of the block by extracellular magnesium (Mg^{2+}) at negative membrane potentials. However, with membrane depolarization Mg^{2+} dissociates from its binding site within the NMDAR channel, allowing Ca^{2+} and Na^+ to enter the cell (Citri and Malenka, 2008). In fact, NMDAR activation is the primary source of Ca^{2+} entry into the spine (Bloodgood and Sabatini, 2007; Hayashi and Majewska, 2005; Sabatini et al., 2002). AMPARs have an indirect effect on Ca^{2+} entry by inducing the membrane depolarization necessary to activate voltage-sensitive calcium channels (VSCCs) and relieve the Mg^{2+} block from NMDARs (Bloodgood and Sabatini, 2007). Metabotropic glutamate receptors (mGluRs) also influence intracellular Ca^{2+} concentration by regulating Ca^{2+} release from intracellular stores, such as the SER. Spine Ca^{2+} regulates enzymes that trigger rapid modifications of synaptic strength, and is also involved in short-term changes in membrane excitability and synaptic structural plasticity. Being so, spine Ca^{2+} signaling is critical for the induction of LTP and LTD (Polleux and Gosh, 2008; Sabatini et al., 2002) .

Spine neck geometry allows the compartmentalization of Ca^{2+} signals, acting as barrier to isolate the movement of small molecules and proteins (Majewska et al., 2000; Svoboda and Yasuda, 2006). Spines with narrower or longer necks retain more Ca^{2+} in their heads and have slower bidirectional diffusion with the parent dendrite after synaptic activation, in comparison with spines with small necks (Fig. 5) (Bourne and Harris, 2007). In addition, the degree of biochemical isolation of the spine head is regulated by activity, as chronic increases and decreases in global activity respectively shift the population of dendritic spines toward greater or lesser degrees of biochemical isolation (Bloodgood and

Sabatini, 2007). Spine geometry also allows them to operate as independent electrical compartments, as synaptic electrical currents at the spine will generate a spine voltage signal that is larger than that in the parent dendrite (Polleux and Gosh, 2008).

Ca^{2+} signals in spines are affected by the dynamics of spine morphology. The surface-to-volume ratio of a spine decreases with its size, which affects the $[Ca^{2+}]_i$ (Sabatini et al., 2002). The geometry of the neck might also be important in $[Ca^{2+}]_i$ clearance, and consequently in the control of kinetics and magnitude of postsynaptic Ca^{2+} responses. Besides diffusing to the dendrite shaft, $[Ca^{2+}]_i$ can be decreased by extrusion, and spines are classified as "diffusers" or "pumpers" according to the predominant pathway (Fig. 5). The relative contribution of each pathway to effective $[Ca^{2+}]_i$ clearance is still controversial, but it is believed that pumpers are predominantly thin spines due to their small neck conductance, relying on extrusion to clear Ca^{2+} from the spine cytoplasm. Since Ca^{2+} extrusion is a slow process, integrated Ca^{2+} signals in these spines are large. Conversely, larger spines have larger neck conductance, making them predominantly diffusers (Bloodgood and Sabatini, 2007; Sabatini et al., 2002). Changes in neck length during spine motility alter Ca^{2+} kinetics within the spine. In addition spine Ca^{2+} signals may elicit changes in spine morphology by altering the actin cytoskeleton. Even though the kinetics of Ca^{2+} signals needed to induce these morphological changes are unknown, these evidences prove that there is a correlation to Ca^{2+} accumulation and signaling with spine morphology (Hayashi and Majewska, 2005; Majewska et al., 2000; Yuste and Denk, 1995). Despite the fact that more studies are required to evaluate the relative contribution of Ca^{2+} flux and spine geometry, the initial evidence shows that there is a delimited regulation of Ca^{2+} signals in spines, enabling them to operate as complex and autonomous cellular

compartments controlling many aspects of postsynaptic signals (Hayashi and Majewska, 2005).

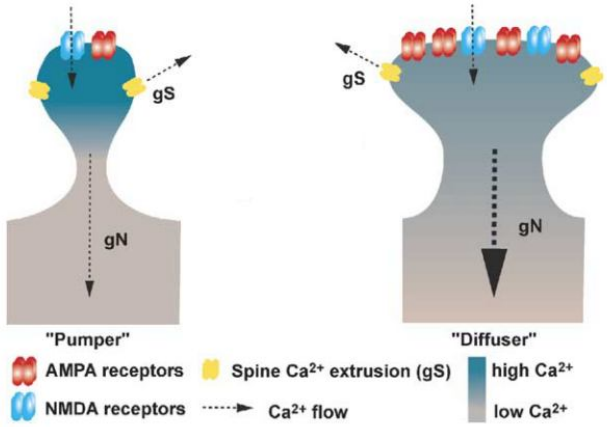

Figure 5. Spine neck geometry and Ca^{2+} compartmentalization in spines. After Ca^{2+} influx, small and large spines have different responses. Small spines (left) have narrow heads with low neck conductance (gN), limiting Ca^{2+} diffusion to the parent dendrite. Ca^{2+} is mainly expelled through extrusion pumps, head conductance (gS), in the spine head. The result is a large, prolonged Ca^{2+} signal in the spine and little Ca^{2+} increase in the dendritic shaft. Large spines (right) have proportionally larger AMPAR and NMDAR currents. Ca^{2+} efflux happens through Ca^{2+} extrusion in the spine head, and through diffusion along the neck to the dendritic shaft, given its large conductance. In these spines, Ca^{2+} increases are more moderate and transient. (Hayashi and Majewska, 2005).

1.5.3. Relationship with synaptic plasticity

A growing body of evidence points to changes in spine morphology correlated with events where the strength of synapses is affected, being it behavioural stimulation or neurological disorders:

1. Visual stimulation increases spine density in the rat visual cortex (Parnavelas et al., 1973);

2. Visual deprivation alters spine morphology and reduces spine numbers in the rabbit visual cortex (Globus and Scheibel, 1967);

3. Stress increases spine density in the hippocampus of male rats and reduces spine density in female rats (Shors et al., 2001);

4. Fragile X-syndrome is characterized by spines with abnormal morphology, and increased spine density in the cerebral cortex (Hinton et al., 1991; Irwin et al., 2001);

5. Down's syndrome and epilepsy are characterized by reduced spine density in the hippocampus and cortex (Ferrer and Gullotta, 1990; Swann et al., 2000);

Recent studies are opening the way to understand spine dynamics during LTP and LTD. High-frequency stimulation will cause a prolonged membrane depolarization in the spine membrane, activating NMDARs. The subsequent rise in $[Ca^{2+}]_i$ at spines is the trigger for LTP. As this only happens when there is a temporal correlation between presynaptic glutamate release and postsynaptic depolarization, NMDARs are often called "coincidence" detectors (LaMantia, 2004). Much remains unclear, but the role of Ca^{2+}/calmodulin kinase II (CaMKII) and protein kinase C (PKC) in LTP induction has been already described. These kinases participate in signalling cascades that involve targeting and insertion of AMPARs in the postsynaptic membrane (as happens in silent synapses) (Citri and Malenka, 2008; LaMantia, 2004). They also have a role in F-actin reorganization and increasing the F-actin/G-actin ratio (Hayashi and Majewska, 2005; Matsuzaki, 2007; Okamoto et al., 2004; Santos et al., 2009). This is most likely regulated by multiple actin-binding proteins such as the downstream effectors of small G-proteins of the Rho family and Rap (Kennedy, 2000; Tada and Sheng, 2006; Xie et al., 2005). The addition of AMPARs would be expected to increase the response of the postsynaptic cell to glutamate release, hence strengthening synaptic transmission as long as LTP is maintained (Fig. 6A).

The anchoring of AMPARs to the PSD seems to occur through interactions with immobile proteins in the PSD, also in dependence of F-actin dynamics (Frey and Morris, 1997). LTP also has effect in the presynaptic terminal, which can happen through a retrograde signaling, possibly involving the brain-derived neurotrophic factor (BDNF) (Citri and Malenka, 2008; LaMantia, 2004) (Carvalho et al., 2008).

Maintenance of LTP must also involve the structural remodeling of synapses as it is observed that the potentiation of AMPARs-mediated currents in the membrane induce spine enlargement (Fig. 6B). There is input-specificity of the synaptic plasticity because the morphology of neighbouring spines and their AMPARs content are unaltered (Citri and Malenka, 2008; Matsuzaki, 2007). In addition, spine enlargement is dependent on the size of the spine prior to stimulation: small spines tend to enlarge whereas large spines do not. This may be due to differences in the amplitude and regulation of $[Ca^{2+}]_i$ $^+$ signals (Noguchi et al., 2005). In spines with larger necks Ca^{2+} diffuses to the dendrite rapidly, which possibly prevents Ca^{2+} rising to surpass the necessary threshold for spine enlargement and LTP induction. Even strong stimuli do not induce persistent enlargement of large spines which may be evidence for the differences in the molecular machinery between large and small spines. Moreover, spine structure stabilization in large spines may involve molecular mechanisms that regulate the direction and length of F-actin (Matsuzaki, 2007). Spines in the adult visual cortex of mice are a good example of this situation. It has been demonstrated that these spines can survive for one year *in vivo* and that larger spines are more stable. This suggests that small spines are “learning spines” and large spines are “memory spines” (Bourne and Harris, 2007). Small spines that are strongly stimulated by learning may become larger and more stable. Spines for which activation is not necessary or disturbs the learning process will ultimately disappear. It is worth mentioning that other

studies show that spine structural changes do not correlate perfectly with LTP (Lang et al., 2004), but this may be due to different experimental setups or to the testing of different forms of LTP. It is possible that only longer-lasting forms of LTP are associated with spine enlargement (Matsuzaki, 2007).

Late-phase LTP (L-LTP) consists of a persistent potentiation for more than 2 hours after LTP induction, and requires additional mechanisms such as protein synthesis in the cell body, the dendrite, and possibly in the spine (Bourne and Harris, 2007; Citri and Malenka, 2008). LTP increases neck conductance, facilitating the entry of polyribosomes and mitochondria to the spine head (Noguchi et al., 2005). Polyribosomes may increase the levels of scaffolding proteins in the PSD, such as CaMKII and activity-regulated cytoskeletal protein (Arc) (Job and Eberwine, 2001), and mitochondria would supply the energy required to enlarge the spine. The increased neck conductance may facilitate the diffusion of Ca^{2+} to the dendrite and the soma, regulating the transcription of genes important to control the $[Ca^{2+}]_i$ in spine head and the enlargement of the spine (Cohen and Greenberg, 2008; Matsuzaki, 2007). Finally, larger spines have perisynaptic astroglial processes that can provide synaptic stabilization and regulate levels of glutamate and other substances. Taken together, these features suggest again that large, mushroom spines are more stable “memory spines”. On the contrary, thin spines have smaller PSDs that contain NMDARs and few AMPARs, making them ready for strengthening by addition of AMPARs. Thin spines maintain structural flexibility to enlarge and stabilize, or shrink and dismantle as a response to stimuli, making them candidate “learning spines” (Bourne and Harris, 2007).

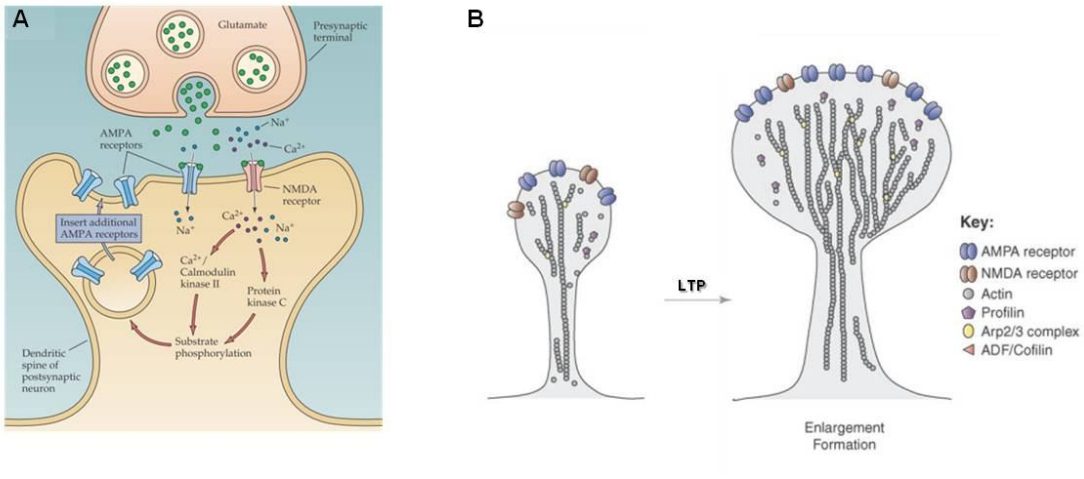

Figure 6. LTP in dendritic spines.

Molecular mechanisms underlying LTP **(**A). When glutamate is released, two events will take place: 1. NMDARs will open, but only if the postsynaptic membrane is depolarized in order to expel Mg^{2+} from the channel (not depicted in the diagram); 2. Ca^{2+} will enter the spine, activating protein kinases, such as CaMKII and PKC. The interaction of these kinases with proteins in the PSD, results in the insertion of AMPARs in the postsynaptic membrane, leading to increased spine sensitivity to glutamate release. Spine morphological changes in LTP (B). LTP shifts the actin equilibrium toward F-actin, inducing reorganization of the spine head, with recruitment of many actin-binding proteins that will promote AMPARs insertion in the membrane. Lipids and other components are also targeted to the membrane, resulting in spine enlargement. This is followed by an increase in the presynaptic active zone, matching the size of the spine. It is possible that this happens through protein interactions between both terminals (not depicted in the diagram). (LaMantia, 2004; Tada and Sheng, 2006)

LTD is also regulated by Ca^{2+} influx through NMDAR activation. The major determinant of LTP or LTD seems to be $[Ca^{2+}]_i$ in the postsynaptic cell. Small rises in $[Ca^{2+}]_i$ trigger LTD, whereas LTP requires an increase in $[Ca^{2+}]_i$ beyond some critical threshold (Citri and Malenka, 2008; LaMantia, 2004; Malenka and Nicoll, 1993). LTP

activates Ca^{2+}-dependent kinases, whereas LTD triggers the activation of the Ca^{2+}-dependent protein phosphatase cascades, which involves the Ca^{2+}/calmodulin-dependent phosphatase calcineurin (or protein phosphatase 2B) and protein phosphatase 1 (PP1) (Citri and Malenka, 2008; Lisman, 1989; Santos et al., 2009). This leads to the dissociation of AMPARs from their molecular scaffolds in the PSD and lateral diffusion to endocytic zones on the periphery of the PSD. Here, they are endocytosed and possibly degraded (Citri and Malenka, 2008) (Fig. 7A).

Internalization of AMPARs may cause spine shrinkage, frequently observed in LTD (Fig. 7B). Therefore, it is generally believed that the activity-dependent trafficking of AMPARs during LTP and LTD is the first critical step in the morphological growth or shrinkage of spines (Citri and Malenka, 2008; Matsuzaki, 2007). The size of individual synapses correlates closely with the content of AMPARs (Matsuzaki, 2007; Nusser et al., 1998; Takumi et al., 1999). These structural modifications are the mechanisms by which bidirectional changes in synaptic strength are maintained (Citri and Malenka, 2008)

Synaptic plasticity also affects spine dynamics, as new spines and filopodia are formed and eliminated both spontaneously or after stimulation. The increased level of spine elimination during postnatal development may be an indication of major reorganization of the neural circuits, and may be fundamental to brain maturation (Bhatt et al., 2009; Dunaevsky and Mason, 2003b) Despite many studies showing spine plasticity, it is still not clear to which degree dendritic spines undergo remodeling in a normal and healthy adult brain. Uncovering the degree of spine dynamics in the mature brain will provide important insights into how long-term information is stored or lost in neural circuits (Zito et al., 2009).

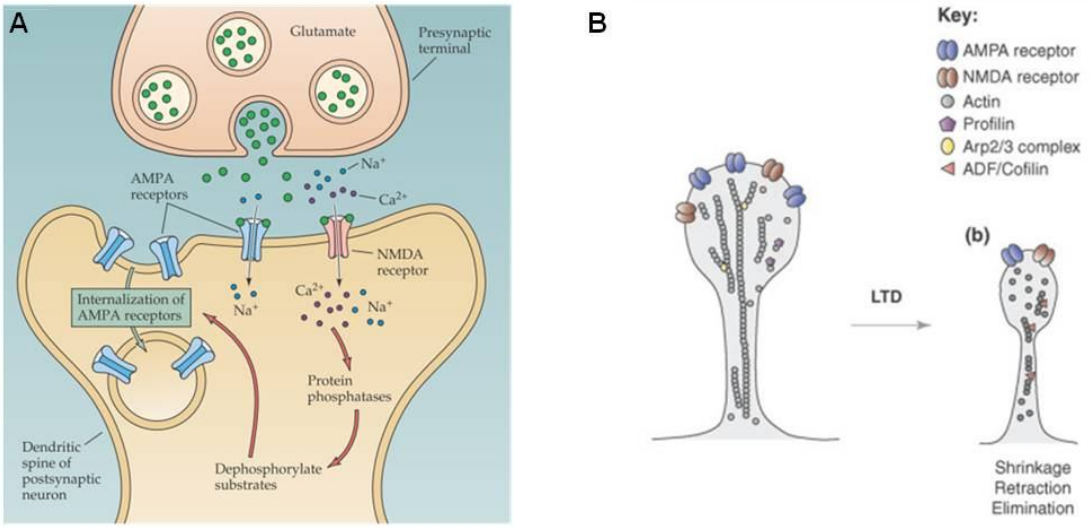

Figure 7. LTD in dendritic spines.

Molecular mechanisms underlying LTD (A). LTD induction is also triggered by Ca^{2+} influx by NMDARs activation. However, the increase in $[Ca^{2+}]_i$ is significantly lower. This activates protein phosphatases that induce internalization of AMPARs, and decreases the spine sensitivity to glutamate. Spine morphological changes in LTD (B). LTD stimulation will shift the actin equilibrium towards an increase in G-actin. Actin depolimerization will impair the organization of the spine, leading to shrinkage or reduction. (LaMantia, 2004; Tada and Sheng, 2006)

As spine size correlates with synaptic strength, changes in spine morphology indicate that synaptic strength can be modified without synapse turnover. This is important in the rapid changes occurring in LTP and LTD (Matsuzaki et al., 2004). Hence, spines' dynamic during changes in synaptic strength may underlie various forms of learning and plasticity in the mature brain (Bourne and Harris, 2007).

1.6. When things go wrong: synapse pathology

As described above, synapse development and plasticity are highly complex mechanisms critical for the correct maturation of neuronal circuits,. Thus, it is not surprising that perturbation in such refined architecture results in the disruption of neuronal circuits, impairment of brain functions and the onset of neurological disorders (Johnston, 2004). In fact, accumulating evidence points to the dysfunction of neuronal communication as the underlying cause of many psychiatric and neurological disorders, such as mental retardation (Pfeiffer and Huber, 2009), schizophrenia (Stephan et al., 2006), Parkinson's disease (Calabresi et al., 2006), autism (Selkoe, 2002; Südhof, 2008), Alzheimer's disease (Marcello et al., 2008; Selkoe, 2002), addiction (Russo et al., 2010), Down's syndrome (Galdzicki et al., 2001), and epilepsy (Müller et al., 1993; Thompson et al., 1996). Given the complexity of neural circuits, it is easy to foresee many possible causes for the onset of neurological disorders. In fact, synaptic pathology may occur due to abnormal density and/or morphology of dendritic spines (Fiala et al., 2002; Russo et al., 2010), synapse loss, aberrant synaptic signaling and plasticity (van Spronsen and Hoogenraad, 2010), or impairment of protein trafficking and gene expression (Cohen and Greenberg, 2008) (for reviews on the subject, see van Spronsen and Hoogenraad, 2010; Johnston, 2004; Fiala et al., 2002).

Neurological disorders are an illustration of the importance of synapse-specific molecules for the correct neural assembly and synapse plastictiy. Advances in understanding brain disorders are important not only to obtain efficient therapies but also to increase our understanding of the biochemical basis of synaptic function and plasticity (van

Spronsen and Hoogenraad, 2010). Novel functions for synaptic molecules may be unravelled and new therapeutic targets may be identified.

1.7. Dissociated cell cultures to study synaptic plasticity: when less is much more

The previous sections highlighted the importance of correct neural formation and connectivity for normal development and adaptation to the external environment. Not surprisingly, the study of network properties and synaptic plasticity is of major importance for contemporary neuroscience. In order to see the 'entire picture', different levels of complexity must be assessed, going from behavioural to molecular changes.

It is not always easy to correlate the data obtained from different approaches. Additionally, given the complexity of the developing nervous system, it has been difficult to obtain new insight on the molecular detail of synaptic plasticity (Fletcher et al., 1994). *In vivo* studies are usually performed with mammals, such as mice or rat, which is a limited system if one wants to evaluate what happens in a cell-by-cell basis (da Silva and Dotti, 2002). The highly ordered arrangement of neurons in regions such as the hippocampus, the olfactory bulb, or the visual cortex has facilitated *in vivo* studies on cellular physiology (Hubel and Wiesel, 1977). However, they have not proven to be useful for probing collective properties of neuronal network *in vivo*, as the three-dimensional structure of cells hinders the simultaneous recording of electrical activity (Kleinfeld et al., 1988). Given the difficulty in visualizing and manipulate individual neurons, it is very difficult to obtain clear results in synaptogenesis using intact brains. The use of organotypical brain slices is of great interest to overcome such limitations. Synaptic plasticity can be studied using electrophysiological techniques, and the hippocampal slice is the most commonly used

preparation (Bortolotto et al., 2001). Nevertheless, sometimes a lower level of complexity is required.

The use of transgenic mouse models for neurological disorders is a common practice to study disease aetiology and the screening of potential targets. However, it usually takes months for the animals to develop the pathology, as in the case of transgenic mice models for Alzheimer's disease (Trinchese et al., 2004). All the referred limitations triggered the establishment of dissociated neuronal cultures as a model system for the study of basic molecular and cellular mechanisms involved in neural circuit development and synaptic plasticity (Banker and Goslin, 1998).

Dissociated primary neuronal cultures are simplified neural tissue preparations. They can be grown in a highly controlled environment and still form synapses and develop into interconnected networks retaining physiological activity and plasticity (Soussou et al., 2007). Dissociated cultures from hippocampal origin are one of the most extensively used model systems in the field of molecular and cellular neurobiology (Grabrucker et al., 2009). The hippocampus has been a major experimental system for studies of synaptic plasticity in the context of putative information storage mechanisms in the brain (Neves et al., 2008), given its precisely organized anatomical structure, the relatively homogeneous pyramidal cell population, and the increasing links between this brain region and both episodic and long-term memory storage (Kotaleski and Blackwell, 2010; Neves et al., 2008). Dissociated cultures from rat or mice hippocampus are usually prepared from late embryonic or early postnatal periods, as it is defined that at this stage the generation of pyramidal cells is complete and the tissue is still easy to dissociate, with very few glial cells (Banker and Goslin, 1998). There are many different protocols to culture and manipulate dissociated hippocampal cell according to the experimental goals and demands

Primary neuronal cultures have been successfully applied for decades. They represent a great simplification of the *in vivo* situation, allowing the access to individual neurons for electrophysiological recording and stimulation, pharmacological manipulations and high-resolution microscopic analysis (Grabrucker et al., 2009). Primary cultures can live for several weeks, contrarily to live material in brain slices, whose use is limited to a few hours. This allows for long-term follow-up. In addition, less biological material is necessary for the preparation of the primary cultures, thus avoiding the sacrifice of animals (Banker and Goslin, 1998; Potter and DeMarse, 2001).

Through the use of immunocytochemical techniques, pre- and postsynaptic players can be visualised and monitored during synaptic development and plasticity (Bartlett and Banker, 1984a, b). The electrical activity can also be evaluated in a single-cell basis. Using fluorescent probes sensitive to $[Ca^{2+}]_i$ levels, analysis of spontaneous and experience-induced activity may be evaluated (Craig et al., 1994; Fletcher et al., 1994). This model also has advantages in the study of compounds with potential effect in disease therapy. It facilitates the administration of drugs selectively to the pre- or post-synaptic terminals, and allows for the testing of drug efficacy briefly after birth of animal models of disease (Trinchese et al., 2004).

There is however the risk that the phenomena observed in culture do not resemble the situation *in situ*, as intact brains are much more than neurons communicating. Primary cultures are usually developed with the purpose of resembling as much as possible the situation *in situ*, trying to study phenomena in culture that are also present in intact brains. However, that is not always easy since the cells are growing in a constrained, two-dimensional space with great differences in the surrounding environment and neighbouring cells (Banker and Goslin, 1998). Nonetheless, in many different situations dissociated

cultures have proven to be remarkably similar to the *in situ* situation, and many important data on neuronal development, synaptic plasticity and neurological disorders have been obtained using this system. It is known that cultured hippocampal neurons pass through defined stages of maturation (Dotti et al., 1988), interconnect with each other (Bartlett and Banker, 1984b; Fletcher et al., 1994), exhibit particular morphological features and have expression and distribution patterns of neuronal proteins that are essentially similar to those of neurons developing in the intact brain (Garner et al., 2006; Ziv and Garner, 2001).

All of the above potentiate the use of primary neuronal cultures as an attractive model system for the easier testing, diagnosing, and a potential application for high-content screening of compounds with potential therapeutic effect.

1.8. Objectives of the study

The following work is integrated in the PhD project of Peter Verstraelen, from a collaboration between the Laboratory of Cell Biology and Histology of the Department of Veterinary Sciences at the University of Antwerp and the Department of Neurosciences at Janssen Pharmaceutica N.V., initiated in October of 2009. The project focuses on the setup and full characterization of primary neuronal cultures with special attention on synaptic plasticity, both in healthy and pathological conditions. Recent research suggests impairment of synaptic plasticity and connectivity in widespread neurological diseases like Alzheimer's disease or schizophrenia. The ultimate goal is the development of neuronal cell cultures to be used as efficient biosensors for the testing of novel compounds targeting neurological disorders. Wild type and transgenic animal will be used, the former to validate data from behavioural and brains slices studies, and the latter to have a system that is used as model

for neurological disorders. These cultures will ultimately allow the follow-up of phenotypic changes in these diseases and the high-content screening of pharmacological compounds with therapeutic potential. To do so, morphological and functional features of the developing neuronal network can be evaluated.

As the project is now in its first phase, optimization of the technical and methodological setup was necessary. Therefore, the work presented here shows the first data on the establishment and characterization of primary hippocampal cultures from wild type animals. Sensitive tools and procedures to study neuronal dynamics will be highlighted. The results will allow the selection of important parameters that can be used in the future. It will be possible to design a protocol for the rapid and efficient characterization of primary neuronal cultures of different origin, and for the testing of pharmacological compounds.

CHAPTER 2 Materials & Methods

2.1. Media

Plating medium: Minimum Essential Medium (MEM) supplemented with 10% horse serum and 0.6% D-glucose (Merck, Germany). N2 medium: MEM with 1x N2 supplement, 0.6% D-glucose and 1mM sodium pyruvate. C6 glioma cells conditioned N2 medium: rat C6 glioma cells were grown in Dulbecco's modified Eagle's Medium (DMEM) supplemented with 10% of fetal calf serum (FCS), 2mM L-glutamine, 100U/ml penicillin, 100ug/ml streptomycin, 1% non-essential amino acids and 1x N2 supplement. After 2 days of conditioning, this medium was collected, centrifuged at high speed for 20 minutes and the supernatant was stored at -20ºC. C6-CM: 1:1 mix of N2 medium and C6 glioma conditioned N2 medium. All reagents are from Invitrogen, USA (except when mentioned otherwise).

2.2. Cell culture

Primary cultures of embryonic Wistar Crl-Wl rat hippocampal neurons (Charles River, Germany) and C57/BL6 YFP-transgenic mice (Jackson Labs, USA) were prepared as previously described (Banker and Goslin, 1998), with some modifications. After sacrificing a pregnant animal, embryonic (E17-18 for rat and E16 for mice) hippocampi were isolated and dissociated with 0.05% trypsin (Invitrogen, USA) in HEPES-buffered Ca^{2+}- and Mg^{2+}-free Hank's balanced salt solution (HBSS, Invitrogen) for 10 minutes at 37°C. To stop trypsinization, hippocampi were rinsed three times with plating medium. Mechanical dissociation was performed by using two fire-polished glass Pasteur pipettes of different diameters. After centrifugation at 1000 rpm for 5 minutes, the supernatant was discarded and the pellet was ressuspended in plating medium. Finally, cells were counted using trypan blue in the ViCell XR Viability Cell Analyzer and ViCell software package

(Beckman Coulter, CA, USA). Cells were plated at a density of 10.000 cells per well (100µl of suspension, approximately 30.000 cells per cm^2) in 96-well microplates. Four to six hours after plating, medium was replaced with 200µl of C6-CM medium.

To expose the primary cultures to different concentrations of NGF and JNJ#X, stock solutions were dissolved in C6-CM medium and added to the cells when replacing the plating medium; controls were incubated with 0.1% dimethylsulfoxide (DMSO, Merck). All cultures were grown in a humidified incubator with 5% CO_2 at 37ºC. Where referred to, medium was replaced once a week, by removal of 75µl and addition of 100µl of N2 medium to each well.

2.3. Microplates

Primary cultures prepared as described were plated in Poly-D-Lysine (PDL) pre-coated 96-well microplates (either BD BioCoat™ 96-well Black/Clear microplates or Greiner BioOne PS µclear® 96-well microplates). These microplates have a working area of $0.34cm^2$. The bottom is flat and made of polystyrene, which provides a uniform growing surface and allows for high resolution imaging. Cultures were always plated in the inner wells (maximum 60 wells per plate), and the outer wells were filled with miliQ water, in order to minimize medium evaporation.

Figure 8. BD BioCoat™ 96-well Black/Clear microplates (adapted from www.bdbiosciences.com).

2.4. Viral transfection

Rat primary hippocampal cultures at 7DIV were transfected either with lentiviral particles tagged with yellow fluorescent protein (Lentivirus-YFP) (Sigma Aldrich, MO, USA) at a multiplicity of infection (MOI) of 5; or adeno-associated virus, serotype 6, tagged with enhanced green fluorescent protein (AAV-6-eGFP) (a gift from Dr. Sebastian Kügler), at a MOI of 100.

2.5. Plate coating

In order to test alternative substrates for cell culture, collagen coated 96-well microplates (BD BioCoat™) and additional coatings on PDL microplates were tested. For the latter, 96-well microplates were incubated with 0.01, 0.1, 0.5 and 1 mg/ml polyethylenimine (PEI, Sigma Aldrich), for 1 hour at 37˚C, followed by rinsing with miliQ water. All wells were filled with miliQ water and microplates remained in a humidified incubator with 5% CO_2 at 37ºC until plating.

2.6. Immunocytochemistry

Cells were fixed at 1, 4, 7 and 11 days *in vitro* (DIV) in 4% paraformaldehyde / 4% sucrose, for 10 minutes at room temperature, and permeabilized with 0.25% Triton X-100 (Sigma Aldrich) for 5 minutes. Non specific binding was blocked with 10% bovine serum albumin (BSA, Sigma Aldrich) in phosphate buffered saline (PBS, Invitrogen) for 30 minutes at 37ºC. Cells were incubated overnight at 4ºC with primary antibodies diluted in 3% BSA in PBS. Secondary antibodies were incubated for 1 hour in the dark at 37ºC. In between each of the steps, cells were rinsed in PBS, 3 times for 5 minutes each.

2.6.1. Antibodies

The following antibodies were used: rabbit polyclonal antibody to neuronal class III β-tubulin (βIII-tubulin, 1:4000, Covance, NJ, USA), Synaptic Ras-GTPase Activating Protein (SynGAP; 1:1000, Thermo Scientific, IL, USA), and vesicular GABA transporter (VGAT; 1:750, Synaptic Systems, Göttingen, Germany); mouse monoclonal antibody to Glial Fibrillary Acidic Protein (GFAP, 1:1000, Merck,) and synaptophysin (1:1000, Millipore, MA, USA); guinea-pig polyclonal anti-Vesicular Glutamate Transporter 1 (VGLUT1, 1:5000, Millipore), and chicken polyclonal anti-Microtubule Associated Protein-2 (MAP2, 1:5000, Abcam, CA, UK). Goat secondary antibodies were used as follows: anti-rabbit, chicken and mouse Alexa Fluor 488, anti-mouse Alexa Fluor 555, anti-guinea-pig Alexa Fluor 568 (1:500, Molecular probes, USA) and anti-chicken AMCA (1:200, Jackson Immuno Research, PA, USA). The Neurotox-1 kit (Millipore, USA) was also used, following manufacturer's instructions.

2.7. Cytochemistry

Fixed cells, either with or without permeabilization were labeled with phalloidin FITC (1:20, Molecular Probes, USA) for 1 hour at room temperature, protected from light. 1,1'-dioctadecyl-3,3,3',3'-tetramethylindocarbocyanine perchlorate (CM-DiI, 1:500, Invitrogen), was also used to label fixed cells for 15 minutes at room temperature. When mentioned, fixed cells were permeabilized with 0.1% Triton X-100 for 5 minutes, 10 or 100 µg/ml digitonin for 30 minutes (Sigma Aldrich), or in a glycerol gradient - 50% glycerol (20min); 80% glycerol (20min); 100% glycerol (50min) (Sigma Aldrich). Whenever

mentioned, nuclei were labeled with 4',6-diamidino-2-phenylindole (DAPI, 1:5000, Thermo Scientific) for 5 minutes, protected from light

2.8. Live-Cell Imaging

Cultures were loaded with 2µM Fluo3 acetoxymethylester (Fluo3-AM; Invitrogen) in PBS supplemented with Ca^{2+}, Mg^{2+} (Invitrogen) and 1g/l D-glucose for 30 minutes at 37ºC. After loading, the cultures were incubated for an additional 10 minutes in the same solution, in the absence of Fluo3-AM (100µl/well). The cultures were observed on a Zeiss LSM 510 laser scanning microscope (Thornwood, NY, USA) with a Plan NeoFluar 20x N.A. 0.5 objective. An argon laser was used for excitation at 488nm; emission was detected at 530nm . Time lapse images were collected at intervals of 0.398 seconds, and 1250 images per experiment were acquired. After acquiring 1000 images, 30µM glutamate (Merck, Germany) was added until the end of the experiment.

2.9. Image acquisition and analysis

Phase contrast images of the developing cultures were acquired at with an Olympus IX70 Microscope and Cell^{B} imaging software (Olympus Europe, Hamburg, Germany). For assessment of cell populations and analysis of neurite outgrowth images were obtained using MIAS-2 high content multimode microscopy reader and eaZYX Image Analyzer (DigiLab, MA, USA). Discrimination between cell types was performed using Apoptosis Assay 6.0.2 software and total neurite length was measured with the Neurite Outgrowth Assay 6.0.0 software (both from DCILabs, Belgium). Images of the synaptic markers and dendritic spines were obtained in a Zeiss LM510 META microscope coupled with an

Axiocam HR CCD camera. Acquisition was performed with LSM 510 v4.2 software (CarlZeiss Imaging, Germany). Analysis was carried out using ImageJ software (NIH, USA). In live cell imaging experiments, 10 to 20 fluorescent cell bodies per field were manually selected as region of interest (ROI) and the mean fluorescence intensity of ROIs was measured using LSM510 v4.2 software. An additional ROI over an area lacking cells was also measured to be used as background for subtraction of fluorescence intensity. Data from these experiments were analyzed using AxoGraph X (AxoGraph Scientific, Australia). Whenever mentioned, statistics was performed using unpaired t-test or one-way analysis of variance (ANOVA) using Tukey's Multiple Comparison Test.

CHAPTER 3 Results

3.1. Establishing primary hippocampal cultures in 96-well microplates

Given the novelty of this approach, cultures were monitored over time and different conditions have been tested to optimize culture quality.

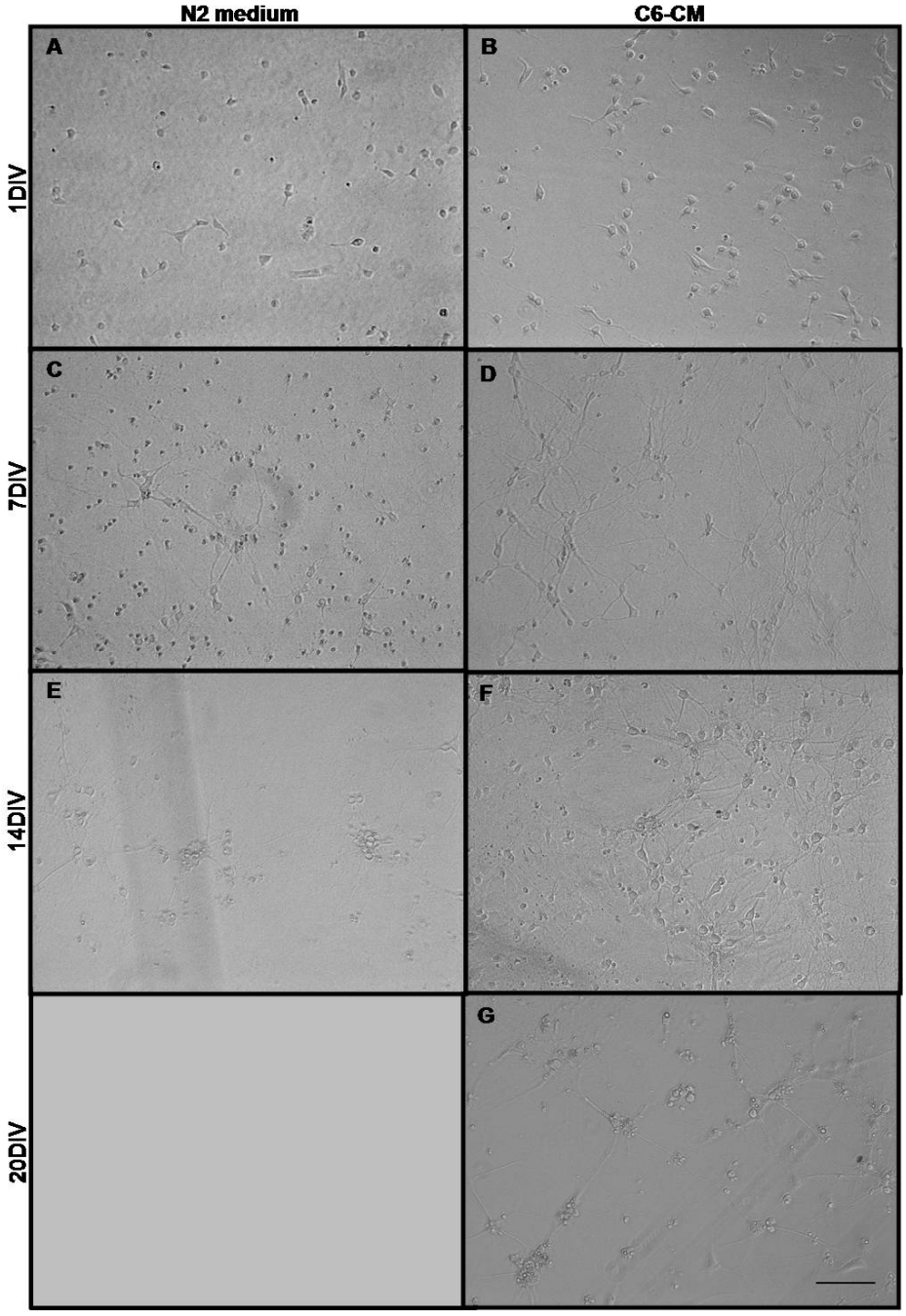

Figure 9. Phase-contrast images of primary hippocampal cultures growing in N2 medium (A, C, E) and in C6-CM (B, D, F, G). Scale bar, 100µm.

Cultures at 1DIV look similar. Most of the cells are spherical, and some cells have early extensions. There is not many debris, indicating that cell death is low (Fig. 9A, B). At 7DIV, there is a lot of debris in cultures growing in N2 medium, and only few cells with extending processes (Fig. 9C). Cultures growing in C6-CM have less dead cells and many cells with extending processes, resembling pyramidal neurons (Fig. 9D). After 14DIV, virtually all cells in N2 medium are dead (FIG. 9E). In contrast, cell death in C6-CM medium is much lower. In this case, some cell bodies are very close together, forming clusters (Fig. 9F). At 20DIV, cells growing in C6-CM medium are dead (Fig. 9G).

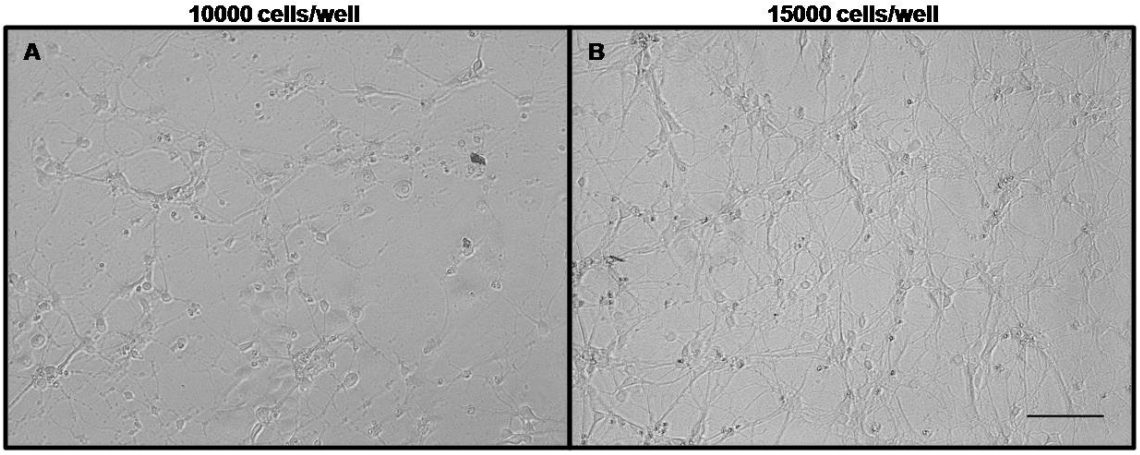

Figure 10. Phase contrast micrograph of 5DIV primary hippocampal cultures plated with an initial density of 10000 cells per well (A) or 15000 cells per well (B) in C6-CM. Scale bar, 100µm.

Primary cultures plated with an initial density of 10000 cells per well have less cell clustering (Fig. 10A). Cultures in B seem to have more clusters, and each cluster seems to have a higher number of cell bodies. In addition, there is more debris (Fig. 10B).

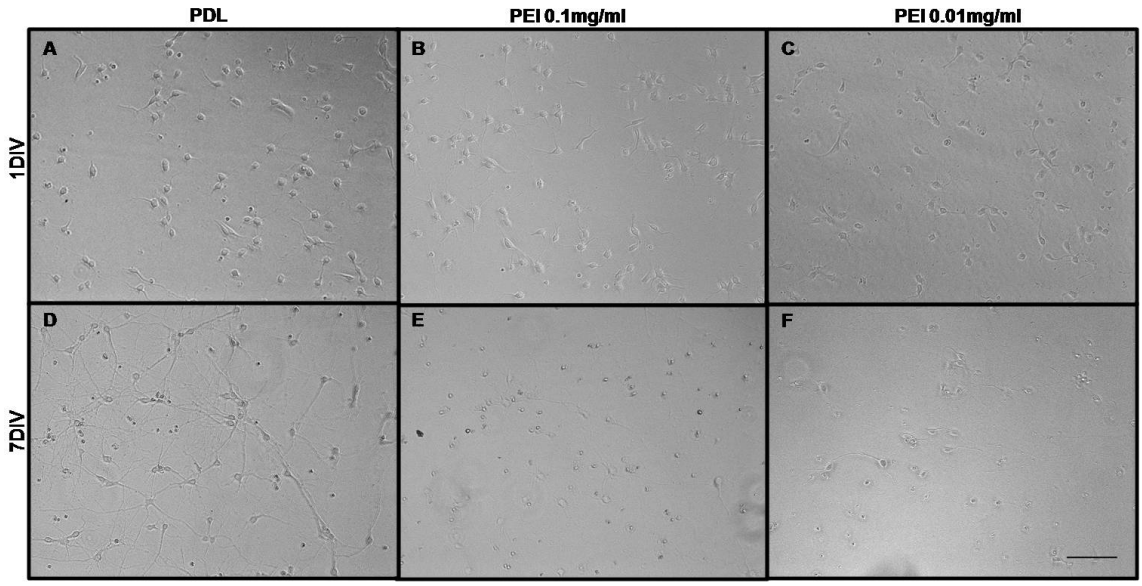

Figure 11. Phase contrast micrograph of primary hippocampal cultures growing in PDL (A, D), 0.1 mg/ml PEI (B, E) or 0.01 mg/ml PEI (C, F). Scale bar, 100µm.

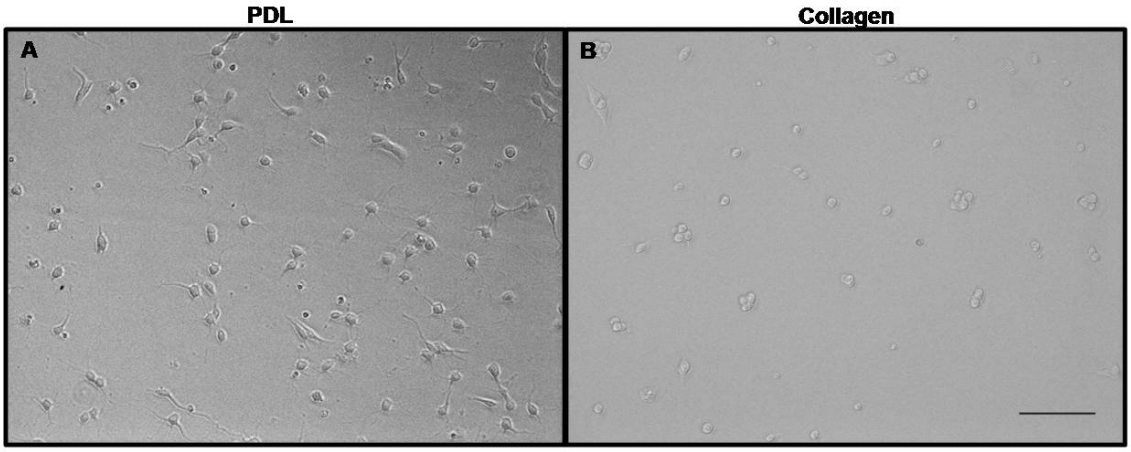

Figure 12. Phase contrast micrograph of 1 DIV primary hippocampal cultures growing in PDL (A) or collagen (B). Scale bar, 100µm.

At 1DIV, cultures growing on PDL- and PEI-coated wells look similar (Fig.11A, B, C). Cultures in collagen-coated plates are dead at this timepoint, evidence by bright and round nuclei (Fig. 12B). At 7DIV, most of the cells in PEI-coated wells are dead (Fig. 11E, F), contrary to cultures growing in PDL-coated wells (FIG. 11D).

Given the suboptimal development and maturation of the cultures, optimization of the methods applied in this setup is still mandatory. Cultures prepared and maintained as described in the previous chapter represent the most favourable conditions so far. For the characterization of these cultures, different approaches were performed. The results will provide the first insight in understanding neuronal dynamics in this setup. All the subsequent results are from primary hippocampal cultures growing in C6-CM medium regarding timepoints that go as far as 11 days *in vitro*. The development of neurons and the maturation of the neural circuit will be monitored.

3.2. Characterization of the cultures

The final goal is to obtain a reliable and reproducible model that can work as a biosensor in the testing of novel compounds. The characterization of the culture will focus several aspects of neuronal development, with the use of different methodologies. As it is a new setup, most techniques required adaptation of standard used protocols.

3.2.1. Discrimination of cell types

Cultures fixed at different timepoints were labelled using antibodies against specific cell-type markers: βIII-tubulin for neurons, and GFAP for type 1 and 2 astrocytes. Nuclei were stained with DAPI.

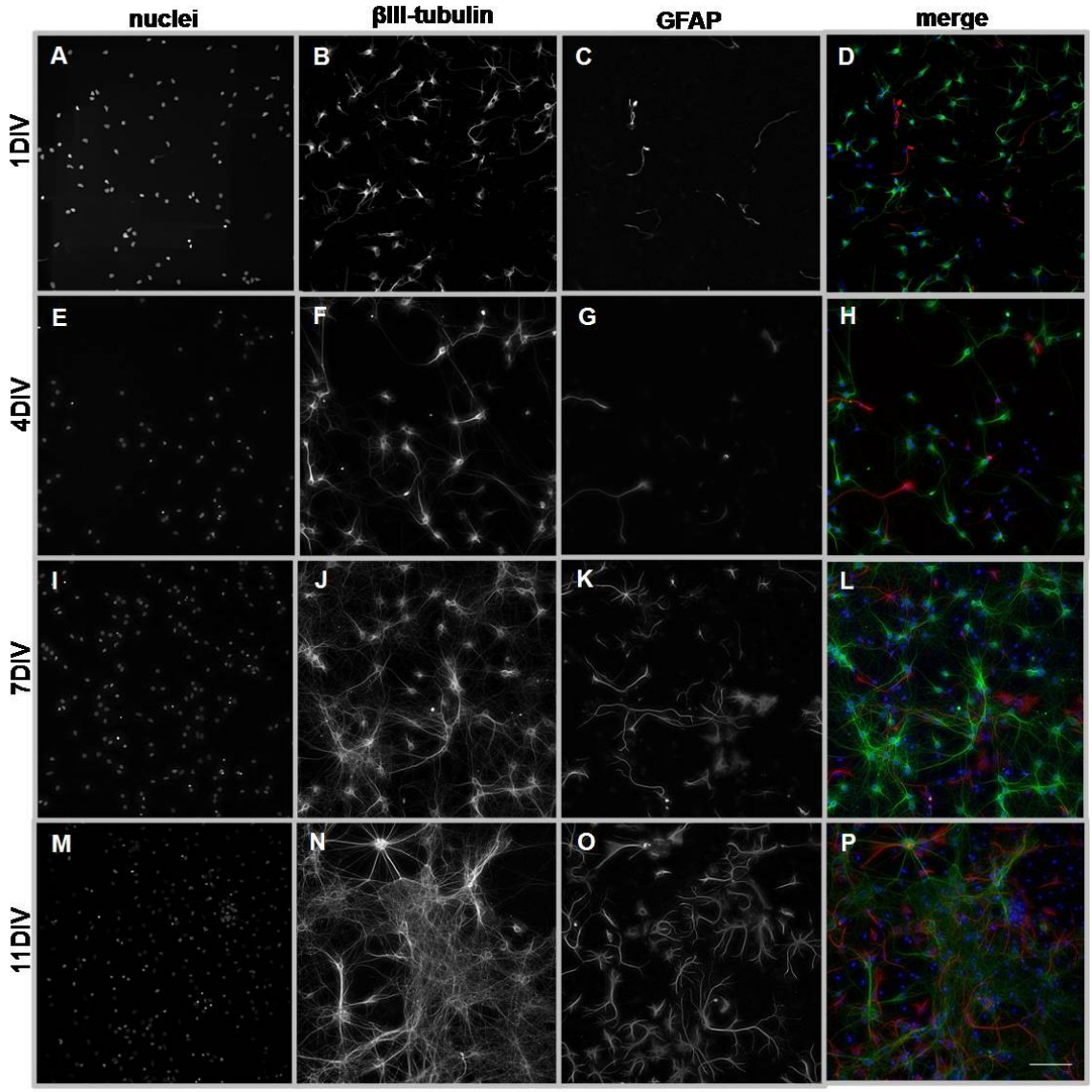

Figure 13. Discrimination of cell populations in primary hippocampal cultures. Nuclei of fixed cultures were labelled with DAPI (A, E, I, M), neurons were labelled with an antibody against βIII-tubulin (B, F, J, N), and astrocytes with an antibody against GFAP (C, G, K, O). D, H, L, and P are merged images of the three stainings. There is a clear difference in morphology between cell populations and with time. Scale bar, 100μm.

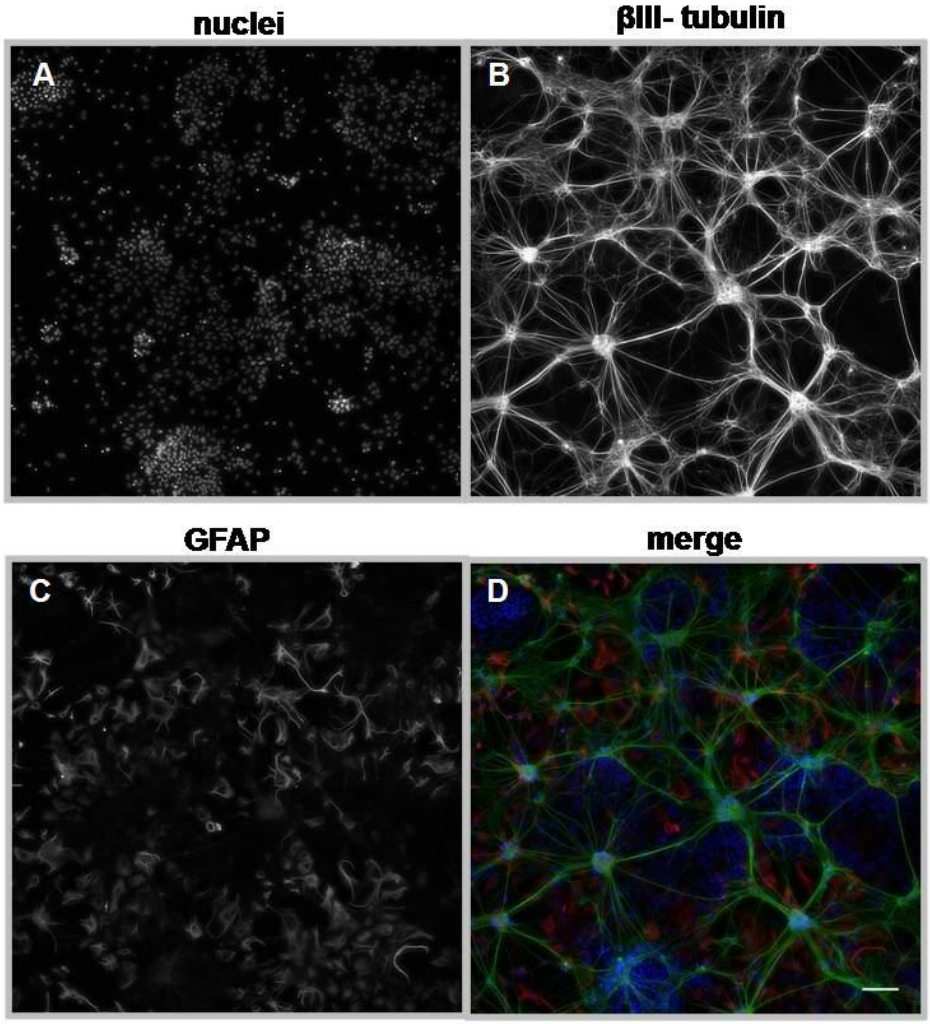

Figure 14. Primary hippocampal cultures at 11DIV.
The cultures have many nuclei stained (A). Neuronal cell bodies are clustered together and the processes are fasciculated with very intense βIII-tubulin signal (B). Astrocytes occupy a considerable area of the visual field and exhibit variable morphology (C). Other nuclei are present and form big groups in the visual field (D). Note that the clustering of cells observed in previous brightfield images corresponds to the neural population. Scale bar, 100μm.

A visual analysis of the images obtained for each timepoint allows for the identification of different populations, neurons labelled with βIII-tubulin, and astrocytes labelled with GFAP. There are no βIII-tubulin(+)/ GFAP(+) cells. Additionally, the cell-

type specific markers do not stain all the cells present, as there are βIII-tubulin(-)/GFAP(-) nuclei (Fig. 13).

Each of the markers used is distributed throughout the entire respective cells, which allows the morphological observation of each population. Neurons and astrocytes have different morphologies since the initial timepoints in culture. At each timepoint, all neurons have similar morphology (Fig. 13B, F, J, N), while the morphology of astrocytes is heterogeneous (Fig. 13C, G, K, O). The number of cells also changes with time. Astrocytes and βIII-tubulin(-)/GFAP(-) cells increase from 4 to 7DIV and from 7 to 11DIV. Differences in the number of neurons are not evident, even though neurite growth with time is very obvious. At 11DIV, neuronal clustering was often observed (Fig. 13N and Fig. 14B). At the same time, astrocytes are distributed through large areas of the visual field, forming a dense network (Fig. 14C, D), and extended regions with many βIII-tubulin(-)/GFAP(-) nuclei close together were frequently observed (Fig. 14A, D). Simultaneously, it was common to see neurons apart from these areas clustered together (Fig. 14B, D).

For a more accurate analysis, countings of each of the groups were made computationally. Each group was normalized to the total number of nuclei at 1DIV and an unpaired t-test was performed to compare populations.

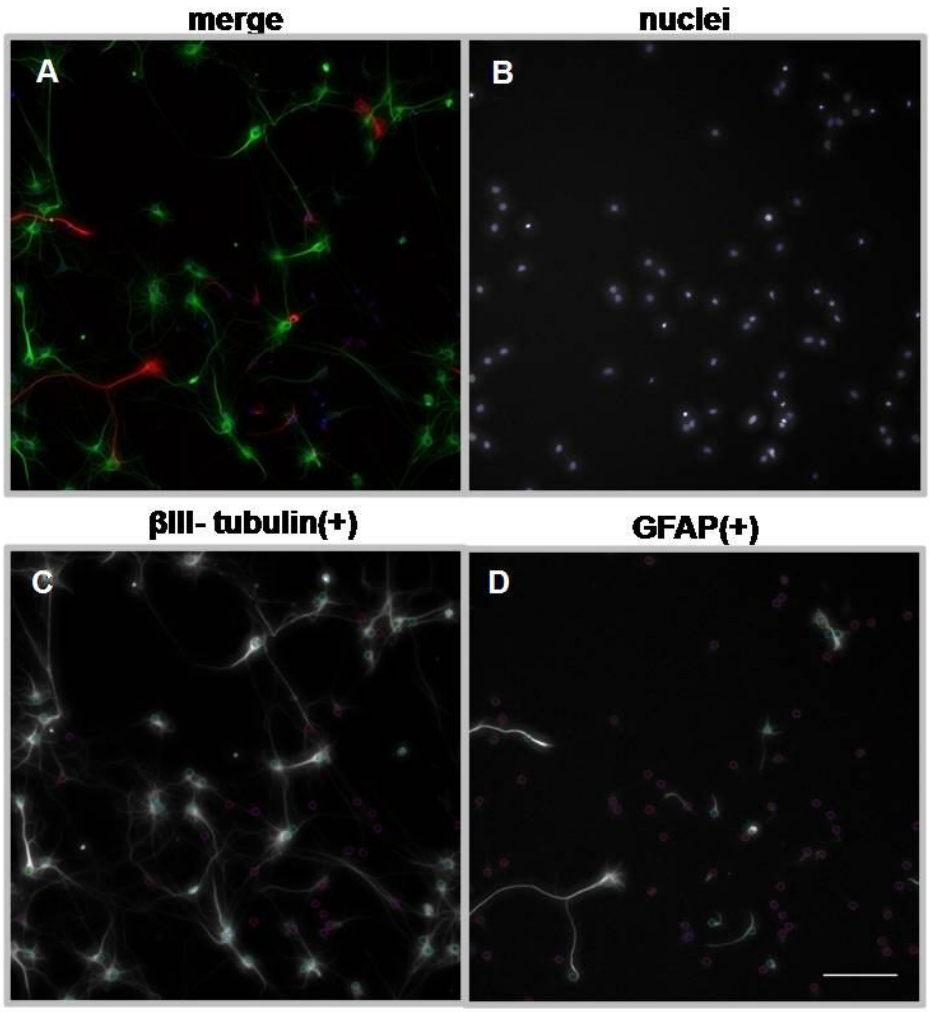

Figure 15. Counting of neurons and astrocytes in a 4DIV primary culture. Overlay of βIII-tubulin (green), GFAP (red) and DAPI (blue) staining (A). Images were analyzed using Apoptosis Assay software, that uses the DAPI staining to detect the total number of nuclei (B), and the specific cell-type marker to classify cells based on a combination of cell morphology and intensity (C and D). Neurons are then referred as 'βIII-tubulin(+) cells' (nuclei with green circles in C) and astrocytes as 'GFAP(+) cells' (nuclei with green cicles in D). Nuclei that did not score as neurons or astrocytes are delimited with pink circles in C and D. Scale bar, 100μm.

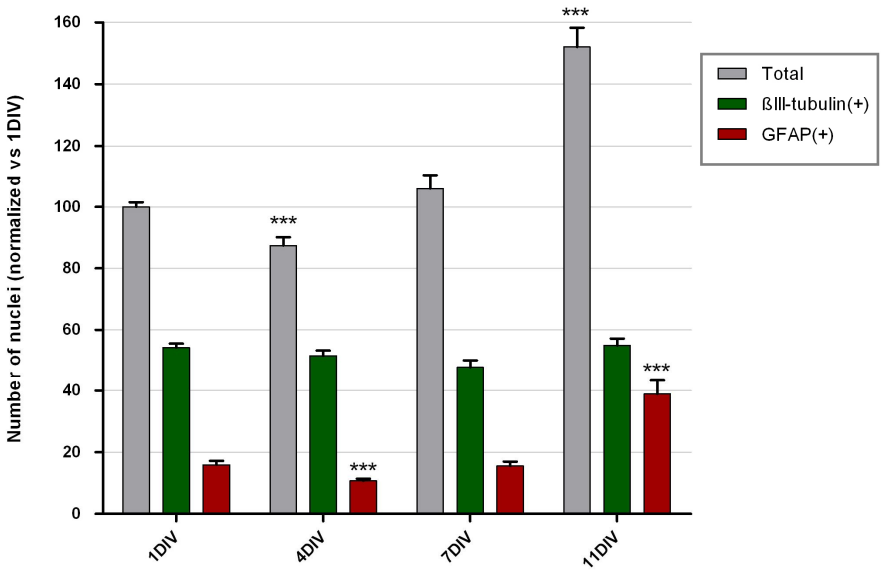

Figure 16. Changes in cell populations in primary cultures over time.
All values were normalized to the total number of nuclei at 1DIV. Plotted are mean values and error bars are standard error of the mean (SEM); *** $p<0.001$ vs. 1DIV; $n>50$.

There is an overall decrease in the number of cells from 1 to 4DIV. From 4DIV on, the total number of nuclei increases, and is very evident at 11DIV. The number of neurons is maintained at all the timepoints considered: as expected, there is no increase in the number of neurons (given their postmitotic character, not prone to cell division) but it is interesting to observe that the number is also not decreasing over time, which may be an indication of minimal neuronal death in the timeframe considered. It should be noted however that this approach also indicates that the neuronal population is approximately 50%, which is considerably low when compared with previous reports. The number of astrocytes is low in the initial timepoints (less than 20%), and increases from 4 to 11 DIV, clearly indicating astrocytic proliferation. Other cells in culture may be inferred by subtracting the number of neurons and astrocytes to the total number of nuclei. Even

though this group is not very representative in the early timepoints, its increase is significant over time, correlating with the extended areas of βIII-tubulin(-)/ GFAP(-) cells described above.

3.2.2. Neuronal development

Neuronal morphology was evaluated in the developing culture. For that, βIII-tubulin(+) cells were compared with previous studies on the development of neuronal cells in culture (Dotti et al., 1988).

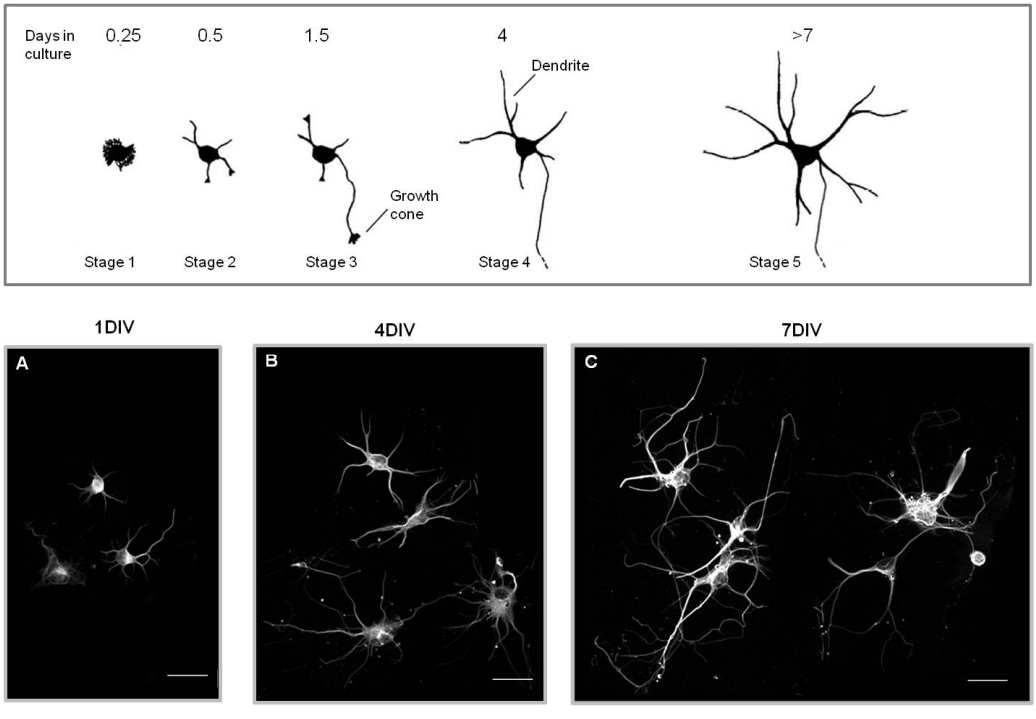

Figure 17. Neuronal development in the primary hippocampal culture.
Top panel: Representative scheme of developmental stages of embryonic hippocampal neurons in culture (adapted from Dotti et al., 1988). Bottom panel: Neurons stained for βIII-tubulin at 1DIV (A), 4DIV (B) and 7DIV (C). Scale bar, 50 μm

Firstly, it is clear that not all cells are in the same developmental stage: at 1DIV and 4DIV is possible to observe neurons resembling stage 1 to stage 4 (Fig. 17 top panel, A). At 1 DIV, most neurons have a morphology that resembles stage 2 and 3, with the former having short processes extending from the cell bodies and the latter with one longer and thinner process, most likely to be the axon precursor, and several minor processes per cell. Some neurons have more than 1 long process. At 4DIV also the minor processes are elongating and acquiring the typical dendritic branching, matching stage 4 defined by Dotti et al. (Fig. 17 top panel, B). From 7DIV on it becomes very complicated to find individual neurons and it is possible that individual cells do not resemble the morphology of neurons that are more close together. There seems to be an increase in the cell body area, and neurites are longer and branched (Fig. 17 top panel, C). Also evident is the formation of the neuronal clusters and fasciculation of the processes from 7 to 11DIV, as seen in Fig. 14.

3.2.3. Neurite outgrowth

The images obtained with the βIII-tubulin marker were further used to study neurite outgrowth in the culture. For that purpose, neurite length per neuron was considered. For each image, measurements of the total neurite length were performed using Neurite Outgrowth Assay 6.0.2 software (DCILabs, Belgium), and divided by the number of βIII-tubulin(+) cells obtained from the previous task. All values were normalized to the 1DIV situation. Comparisons between the timepoints were performed by one-way ANOVA using Tukey's Multiple Comparison Test.

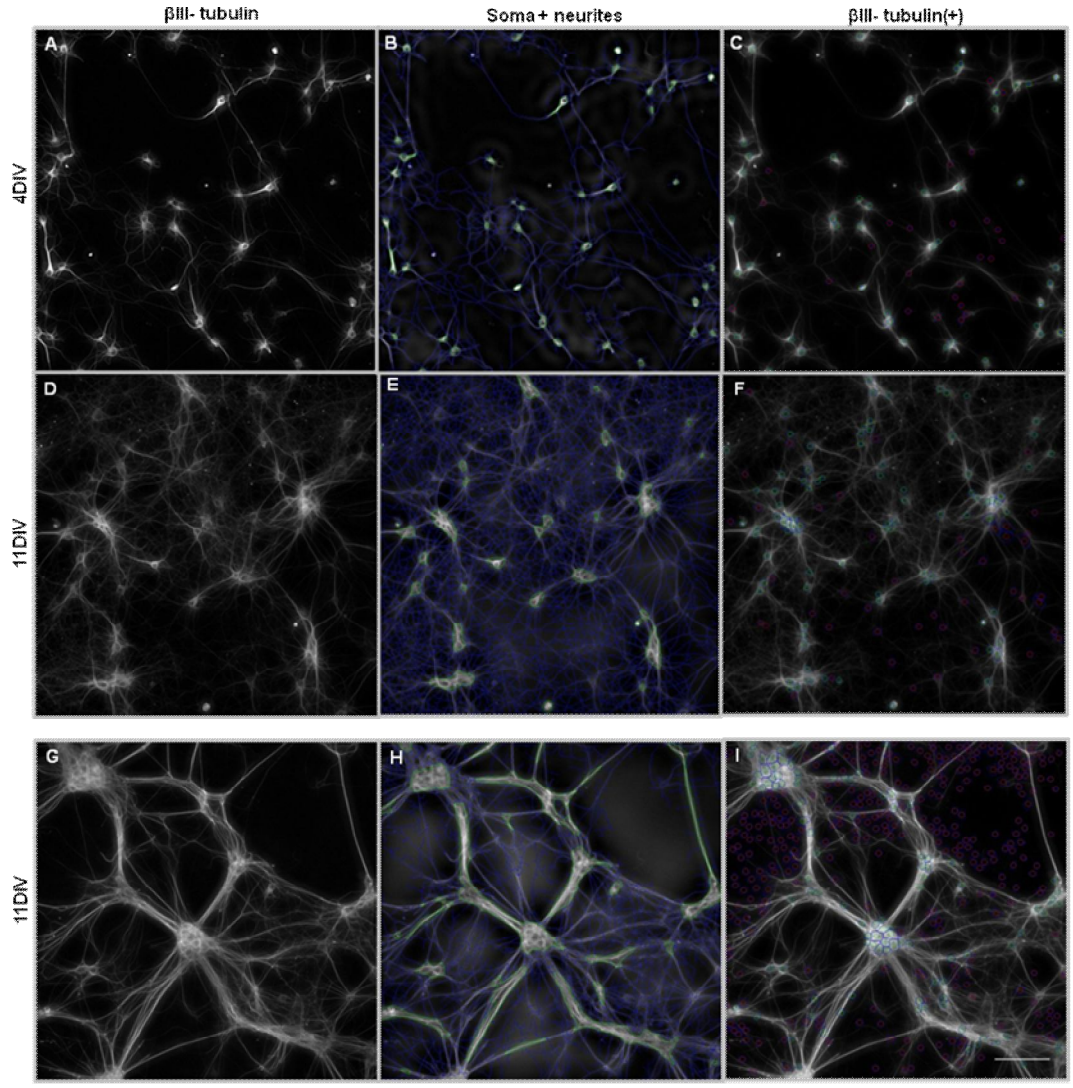

Figure 18. Assessment of neurite outgrowth.

Top panel: Images of neurons stained for βIII-tubulin were acquired at different timepoints (A, D). Using Neurite Outgrowth Assay software the total neurite length of each image was measured. This software is based on a algorithm sensitive to intensity and cell morphology, that can discriminate between cell bodies (green) and neurites (blue) (B, E, H). The number of neuronal nuclei was assessed as described above (C, F, I). The analysis is sensitive when cells are sparse (B, C, E, F). Bottom panel: When neuronal clusters are imaged (G) the neurite measurement is not accurate, as many fasciculated processes are considered as cell bodies and not measured as neurites (H). Also neuronal nuclei are not accurately counted (I). Regions with large clusters where not considered in the analysis. Scale bar, 100 μm.

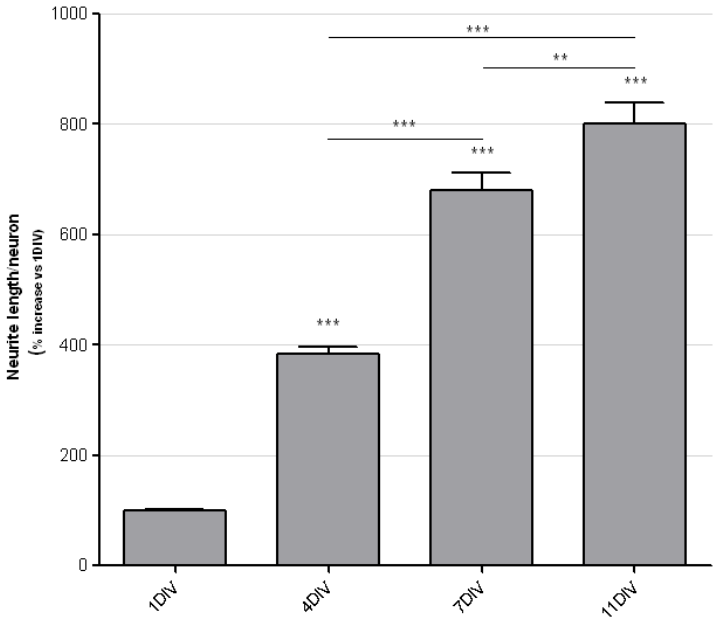

Figure 19. Neurite length per neuron at different timepoints.
The values were obtained by dividing total neurite length with the number of neuronal cells for each image. Plotted are the mean values normalized to 1DIV values, and error bars are SEM. ** $p<0.01$; ***$p<0.001$ (one-way ANOVA using Tukey's Multiple Comparison Test); $n>60$.

Visual analysis of βIII-tubulin staining and the values obtained from the software analysis show the increase in neurite length over the timepoints considered, very evident between each of the timepoints. The increasing neurite complexity from 7DIV to 11DIV complicates this analysis. In fact, even though the results obtained from the analysis software show an increase on the neurite length per neuron at 11DIV, the sensitivity of the software to neurite measurement is now much lower, and the associated error might be amplified (Fig. 18H, I).

3.2.4. The effect of NGF and JNJ#X in neural population and neurite outgrowth in the developing primary hippocampal culture

In order to validate the sensitivity of the described techniques, primary hippocampal cultures were exposed to NGF and JNJ#X from the day of plating. Phenotypical changes were monitored as changes in neural population and neurite outgrowth were evaluated.

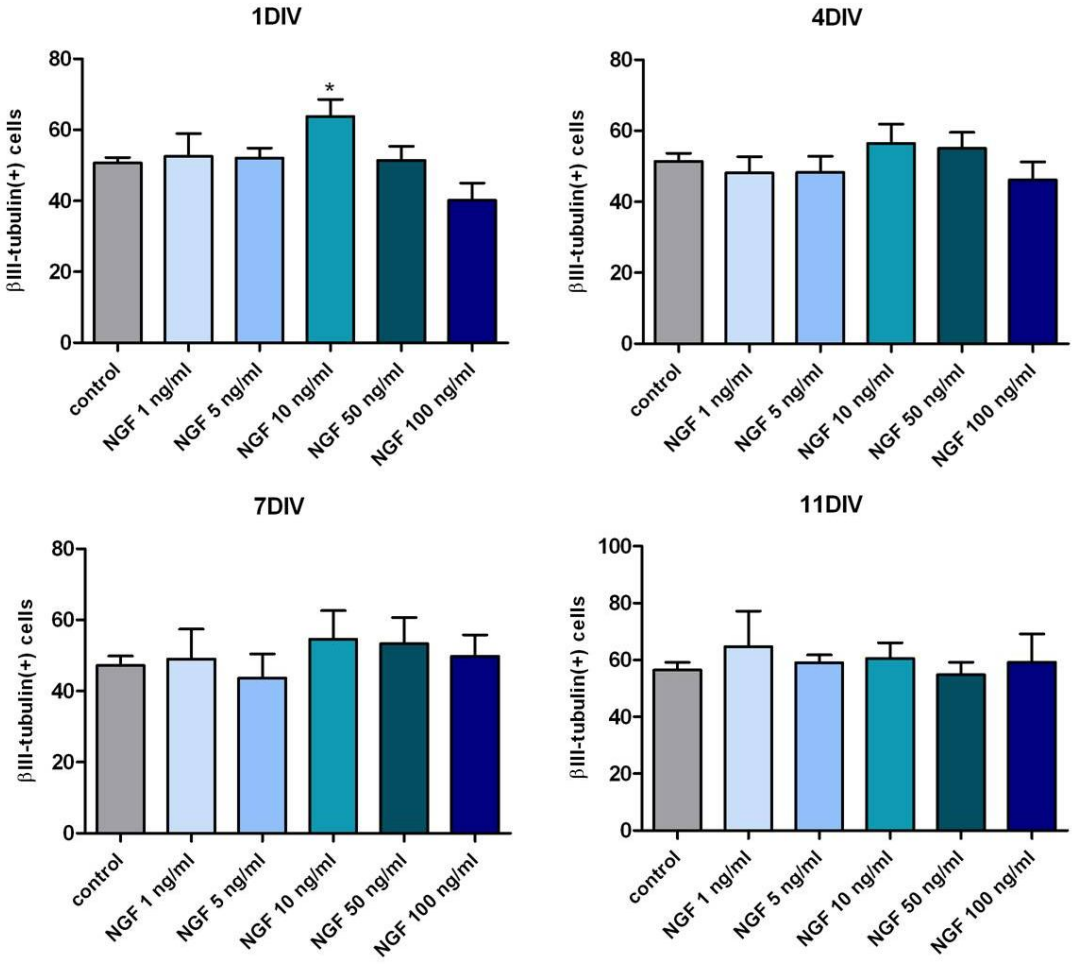

Figure 20. The effect of NGF in the neuronal population.
All values were normalized to the total number of nuclei at 1DIV. Plotted are mean values, and error bars are SEM. Unpaired t-test was performed to compare NGF stimulation to control situation at each timepoint. * $p<0.05$: $n>4$

The results show that the tested NGF concentrations do not seem to affect the neuronal population in culture. Only 10ng/ml NGF has shown a higher number of neurons after 1DIV, which may be an indication of protection against cell death related with the isolation procedure.

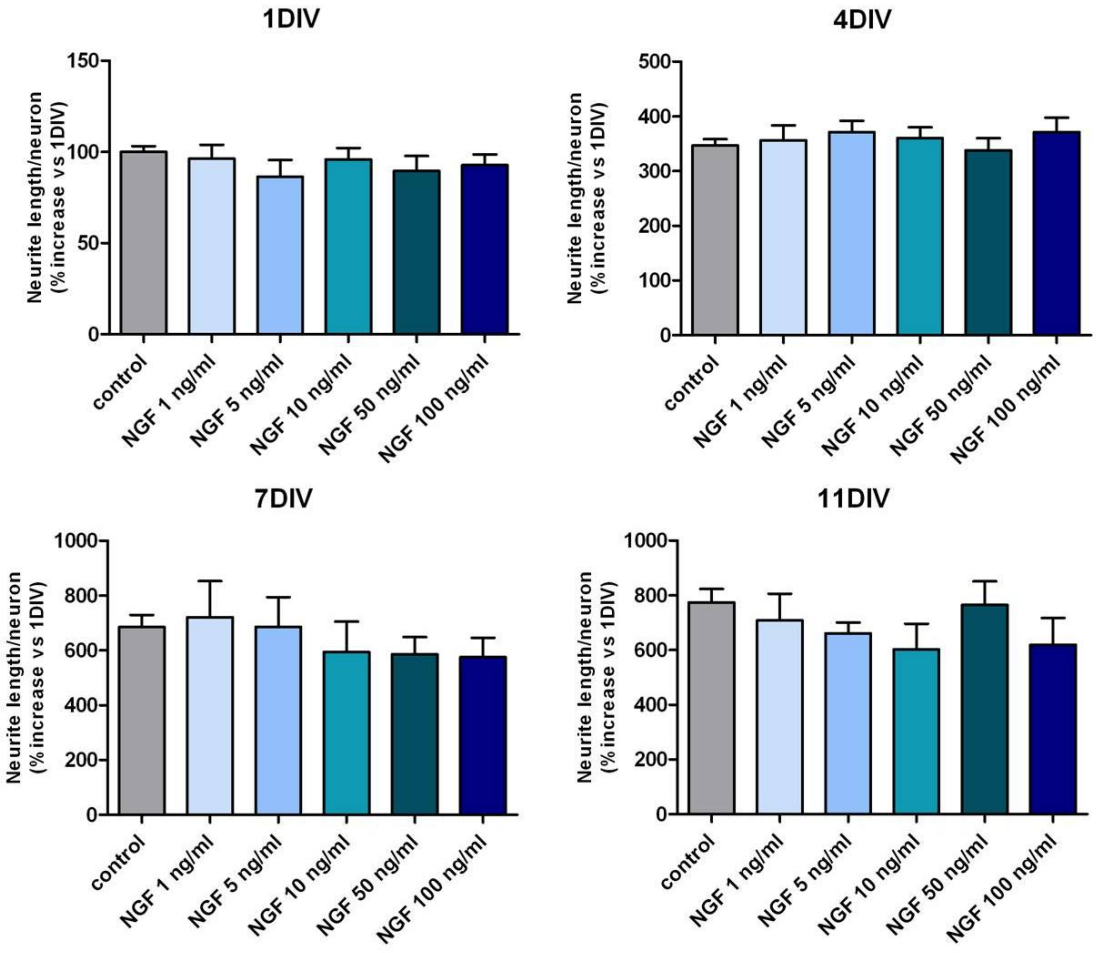

Figure 21. Effect of NGF on neurite outgrowth.
All values were normalized to control at 1DIV. Plotted are mean values, and error bars are SEM. Unpaired t-test was performed to compare NGF stimulation to control situation at each timepoint. * $p<0.05$: $n>4$

The results show that none of the tested NGF concentrations induces changes in neurite outgrowth at any of the timepoints considered.

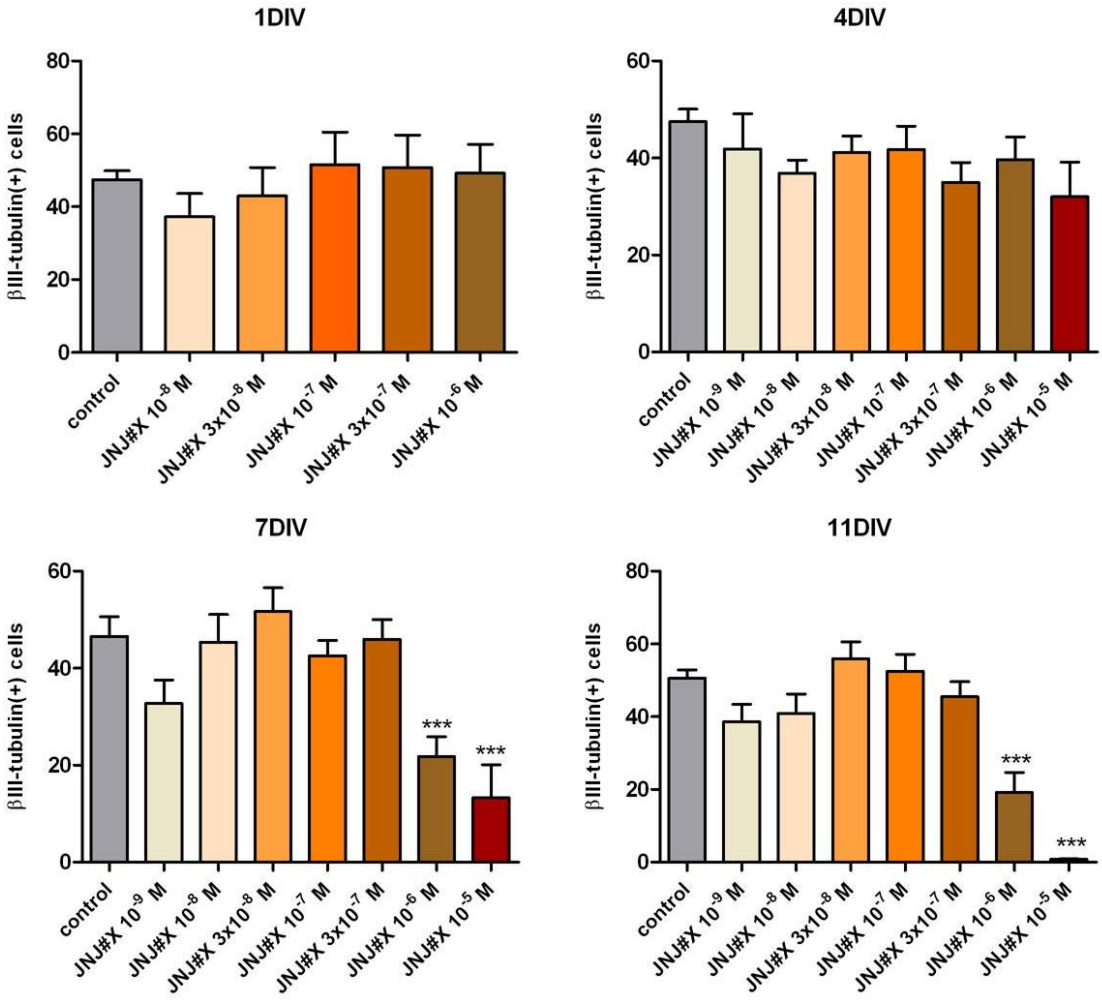

Figure 22. The effect of JNJ#X on neuronal population.
All values were normalized to the total number of nuclei at 1DIV. Plotted are mean values, and error bars are SEM. Unpaired t-test was performed to compare JNJ#X stimulation to control situation at each timepoint. *** $p<0.001$; $n>4$

Lower concentrations of JNJ#X do not seem to affect neural population with time of exposure. However, prolonged exposure of JNJ#X in high concentrations (10^{-5} M and 10^{-6} M) causes neuronal death. Visual analysis of the stainings evidenced the overall death of cells in cultures (data not shown). However, concentrations lower than 10^{-6} M do not seem to affect cell death in any of the timepoints considered.

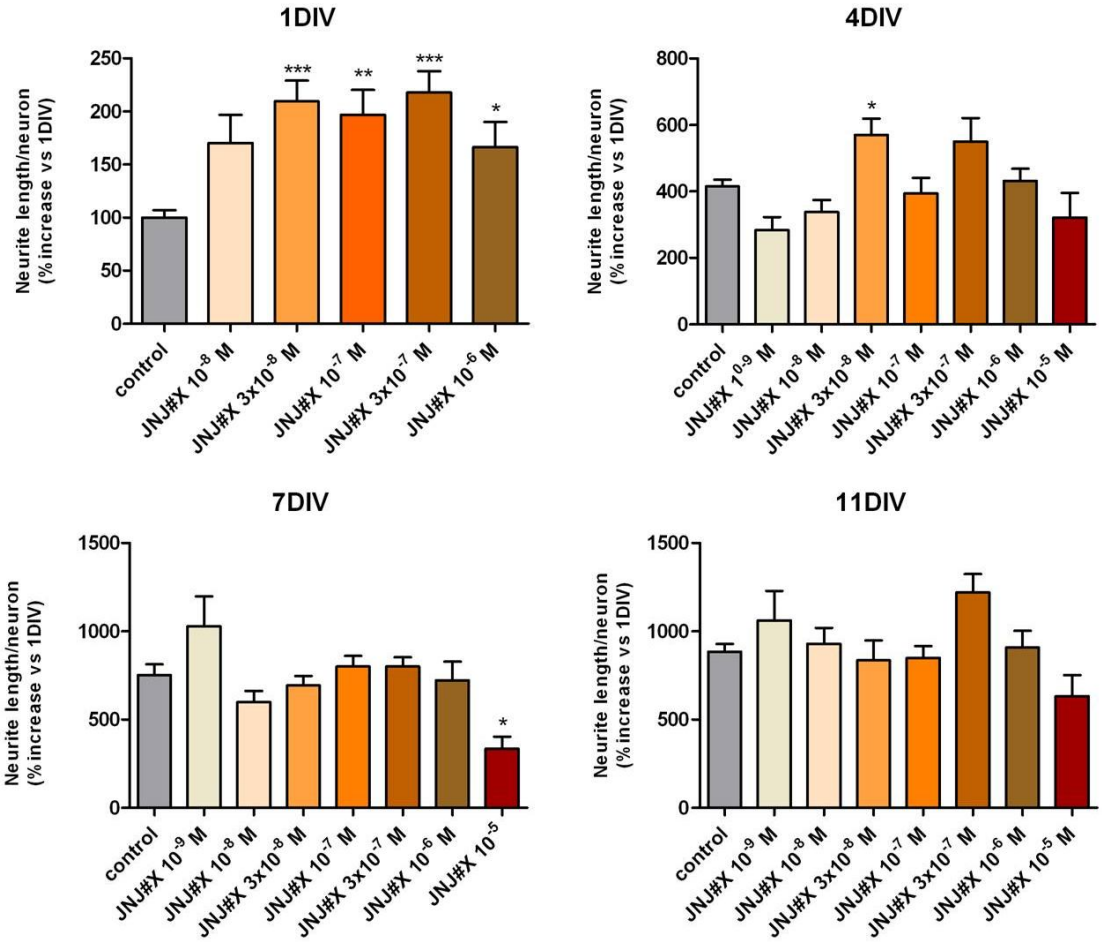

Figure 23. The effect of JNJ#X on neurite outgrowth.

All values were normalized to control at 1DIV. Plotted are mean values, and error bars are SEM. Unpaired t-test was performed to compare JNJ#X stimulation to control situation at each timepoint. * $p<0.05$; ** $p< 0.01$; *** $p<0.001$; $n>4$

There is an increase in neurite length per neuron at 1DIV with JNJ#X doses from $3x10^{-8}$ M to 10^{-6} M. The enhanced growth is only detected until 4DIV for doses of $3x10^{-8}$ M of JNJ#X. Higher concentrations (10^{-5} M) cause an evident decrease in neurite length per neuron at 7DIV, related to the significant neuronal loss (Fig. 22, 7DIV).

3.2.5. Distribution of synaptic markers

Other aspects of neuronal dynamics were evaluated. The formation and maturations of synapses was monitored through immunocytochemistry, by analyzing the expression patterns of synaptic components. Initially, the Neurotox-1 kit was tested, where neurons were stained for βIII-tubulin and synaptophysin.

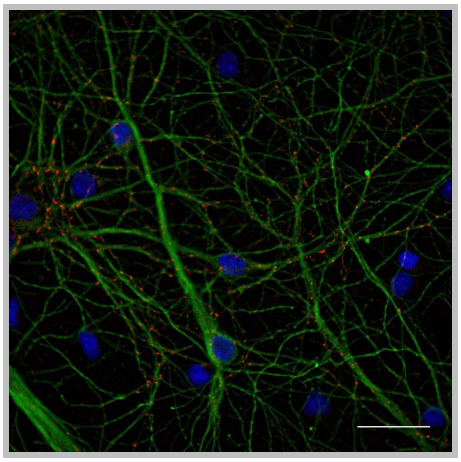

Figure 24. Immunocytochemistry of the neuronal population at 7DIV.
A kit was used to stain βIII-tubulin (green), synaptophysin (red) and nuclei (blue). Scale bar, 100 μm.

Clusters of synaptophysin are clear along neurites. However, as βIII-tubulin stains all neuritic processes, the discrimination between axons and dendrites is not clear. In addition, as a more refined analysis of the synaptic components was intended, other presynaptic markers (VGLUT1 and VGAT) and the postsynaptic marker SynGAP were used. MAP2 was also labeled to trace the somatodendritic regions of neurons.

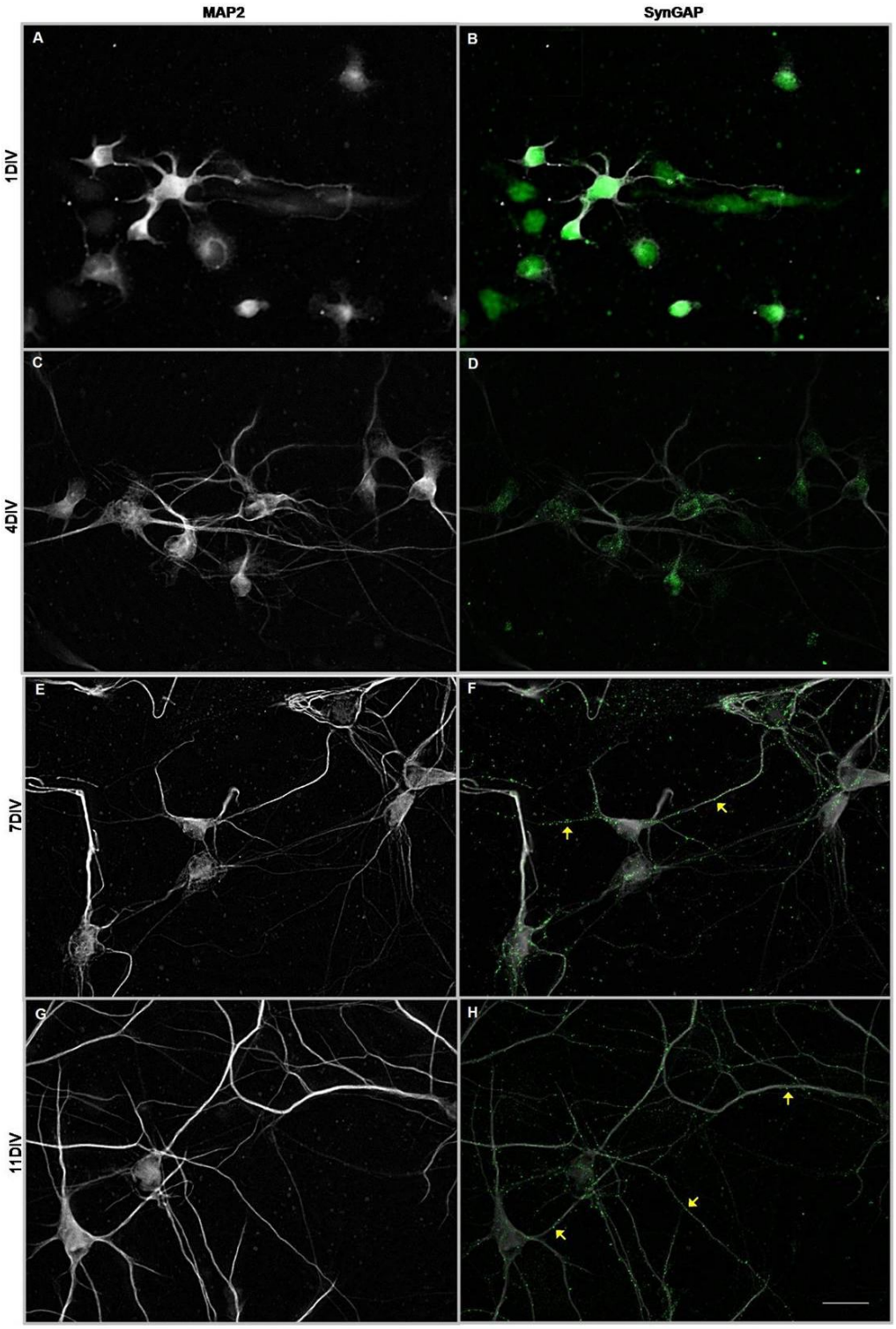

Figure 25. Distribution of MAP2 (A, C, E, G) and SynGAP (B, D, F, H) in developing primary hippocampal cultures. MAP2 traces (grey) were added to SynGAP (green) images to facilitate visualization of neurites. Scale bar, 50 µm.

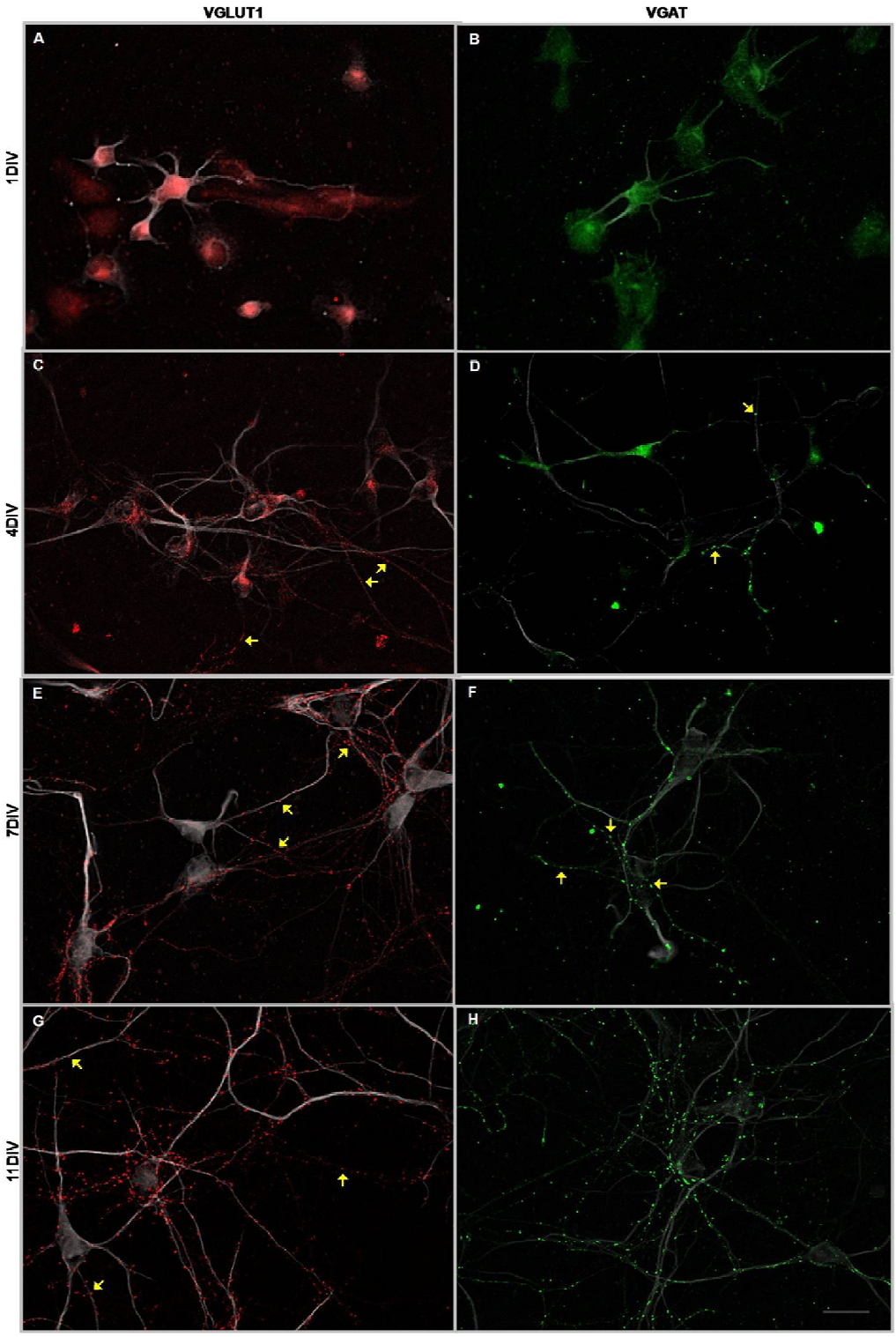

Figure 26. Distribution of VGLUT1 (A, C, E, G) and VGAT (B, D, F, H) in developing primary hippocampal cultures. MAP2 traces (grey) are also included to facilitate visualization of neurites Scale bar, 50 µm.

Visual analysis of the immunostainings reveals that the distribution of the markers changes over time. At 1 DIV, MAP2 is present in all developing processes (Fig. 25A) , even though from 4DIV on is selectively detected at the somatodendritic region in most neurons, as a very weak signal is located in thin processes, most likely to be axons (Fig. 25C, E, G). At 1DIV, none of the markers tested has a clear distribution, as there is only a bright staining in the soma and proximal processes (Fig. 25B, and Fig. 26A, B). At 4DIV, SynGAP is still restricted to soma and initial segments of proximal dendrites (Fig. 25D). At 7DIV, SynGAP puncta are evident (clusters are evidenced with yellow arrows). They are mainly located at the soma and proximal dendrites, with some clusters detected in distal dendrites (Fig. 25F). At 11 DIV, SynGAP puncta are distributed throughout all the dendritic length and less in the soma (Fig. 25G). VGLUT1 and VGAT clusters are distributed to the processes early. At 4DIV, it is possible to detect intense clusters of VGLUT1 and VGAT along thin and longer neurites (Fig. 26C, D yellow arrows). This pattern is refined for both markers at 7DIV (Fig. 26E, F) and 11DIV (Fig. 26G, H). There is an apparent increase in cluster size and distribution along the neurites accompanied by lesser signal in the cell bodies. Clusters of VGLUT1 and VGAT are also detected surrounding the cell bodies and along dendrites.

In order to monitor changes in the expression of components of excitatory synapses, combined images from stainings of VGLUT1 and SynGAP were analysed.

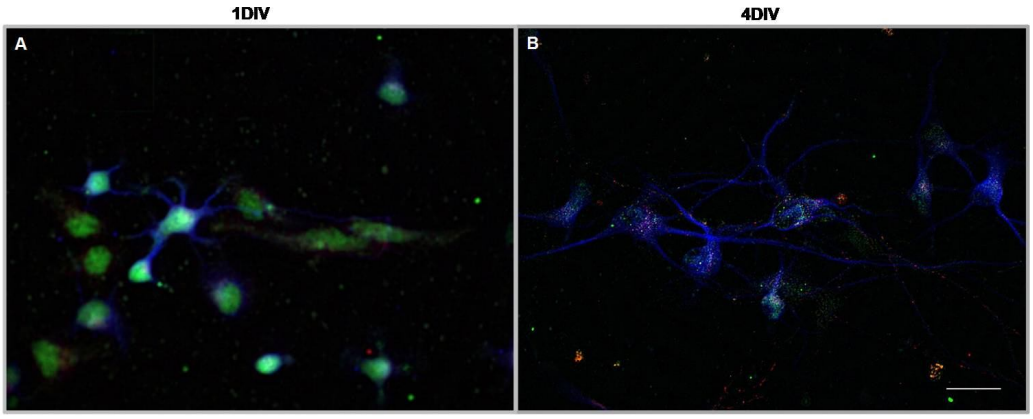

Figure 27. Distribution of components of excitatory synapses in developing primary hippocampal cultures. Overlayed images of MAP2 (blue), VGLUT1 (red) and SynGAP (green) at 1DIV (A), and 4DIV (B). Scale bar, 50 µm.

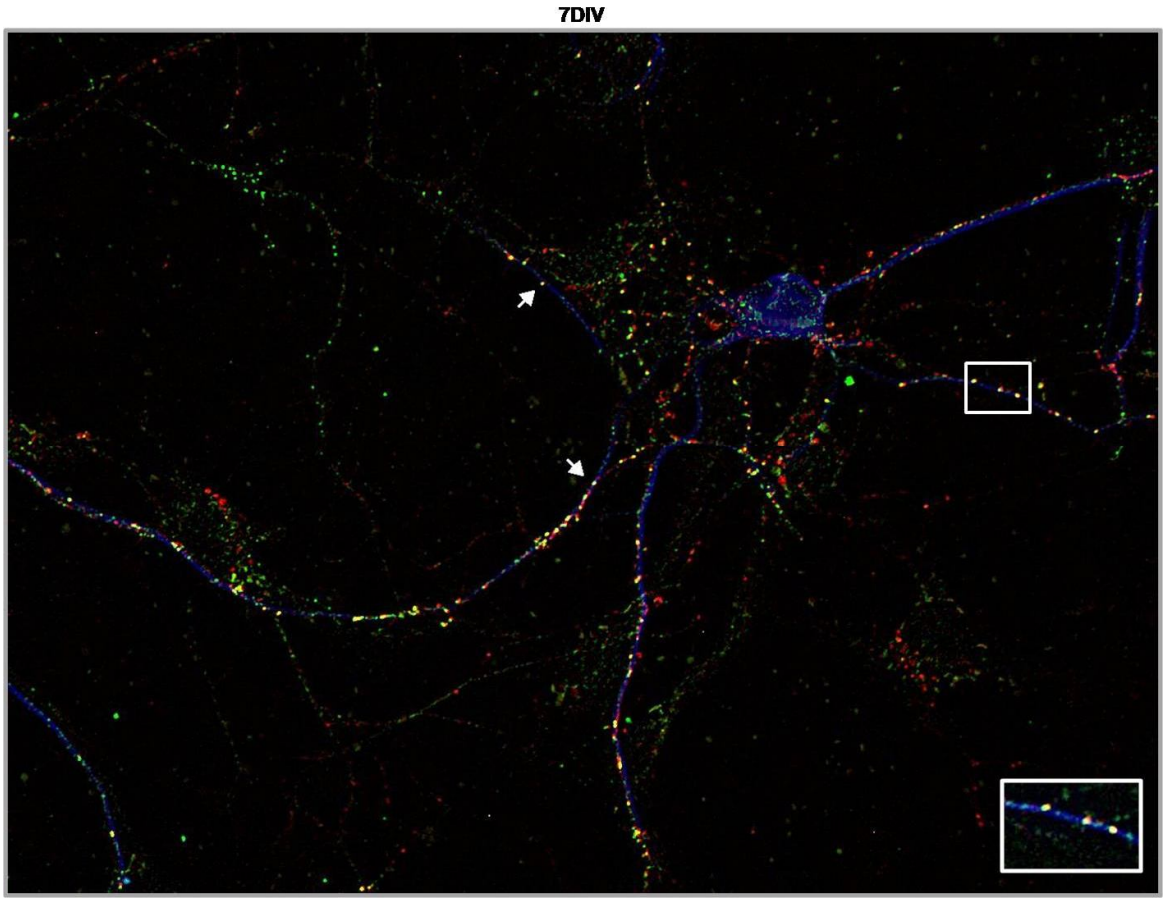

Figure 28. Distribution of components of excitatory synapses in 7DIV primary hippocampal cultures. Overlayed images of MAP2 (blue), VGLUT1 (red) and SynGAP (green). Colocalizations of VGLUT1 and SynGAP are evidenced as yellow particles (white arrows). Scale bar, 50 µm.

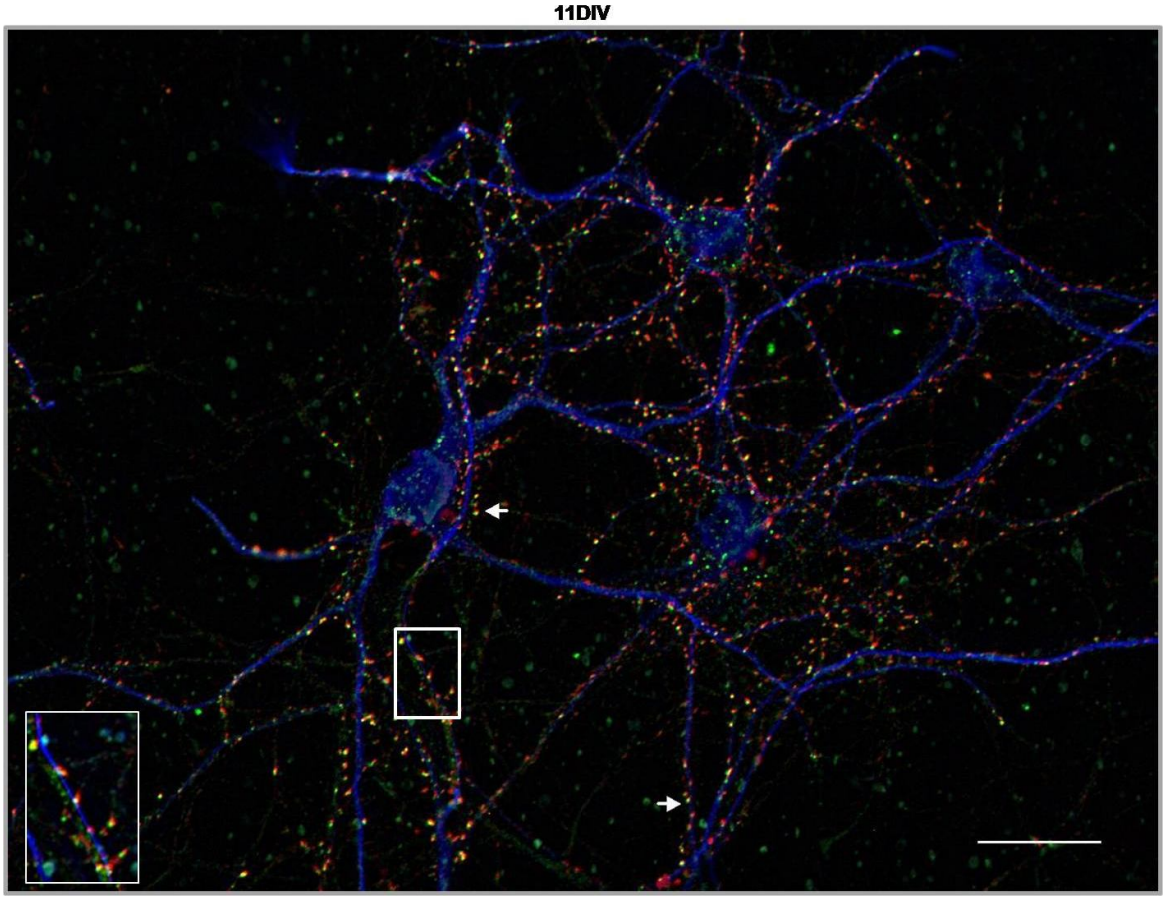

Figure 29. Distribution of components of excitatory synapses in 11DIV primary hippocampal cultures. Overlayed images of MAP2 (blue), VGLUT1 (red) and SynGAP (green). Colocalizations of VGLUT1 and SynGAP are evidenced as yellow particles (white arrows). Scale bar, 50 µm.

Overlayed images of both markers and MAP2 show the distribution of each markers along neurites. As previously described, at 1DIV the markers are confined to the somatic region, and no puncta are detected (Fig. 27A). At 4DIV, some clusters of VGLUT1 are detected but not any of SynGAP (Fig. 27B). From 7DIV on, it is possible to see that some clusters of VGLUT1 are present along dendrites, most likely corresponding to axonal contacts with the postsynaptic dendrite. SynGAP clusters are also detected in dendrites (Fig. 28). Additionally, it is possible to see colocalization of both markers along the

dendritic length, as yellow particles in the overlay (Fig. 28, white arrows). The same is also evident at 11DIV (Fig. 29). There seems to be a difference in the number and size of the particles from 7DIV to 11DIV, even though a visual analysis is insufficient to draw conclusions. In addition, at 7DIV the individual or colocalized clusters are located in the dendritic shaft (enlarged square in Fig. 28), whereas at 11DIV it seems that some clusters are located slightly away from the dendritic shaft, (enlarged square in Fig. 29), possibly in spine heads (although we did not test this further).

Using ImageJ software, MAP2 images were used to define a region to count the number of puncta of each marker. Grains of the markers were measured both individually and colocalized. Only images from 7 and 11DIV were included in this analysis. Results are expressed as the number of particles per length of neurite and also as the mean area of particles. Comparisons were performed with unpaired t-test.

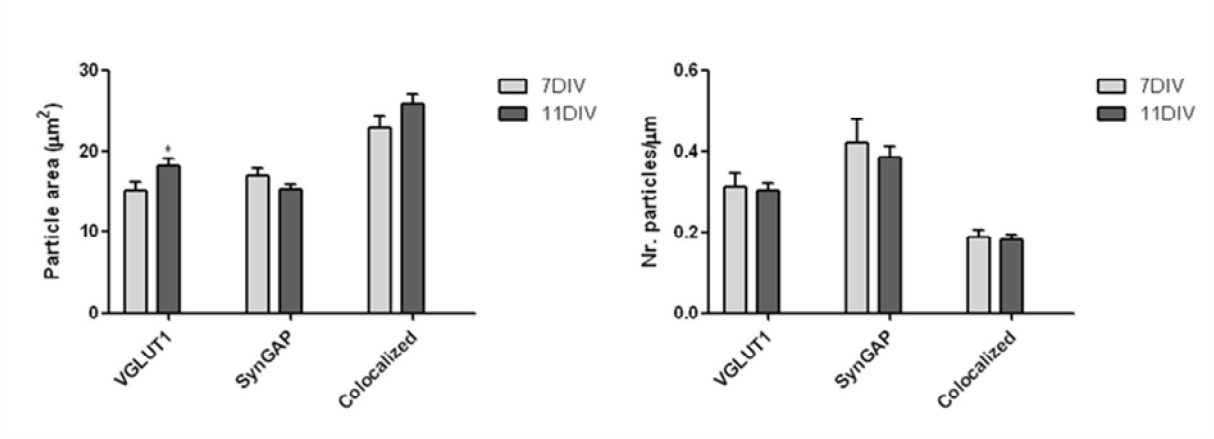

Figure 30. Distribution of excitatory synaptic markers along dendrites at 7DIV and 11DIV. Plottted means and error bars are SEM. *;p<0.05 vs 7DIV; n=9

The number of particles per length is less for VGLUT1 than for SynGAP. However, as the regions were selected using MAP2 labeling, the VGLUT1 particles analysed would correspond to axonal contacts, and as such it is expected that the value is lower than the

particles of the postsynaptic marker. The number of particles per micrometer does not change from 7 to 11DIV for each marker, neither do the colocalizations. At each of the timepoints, approximately 60% of VGLUT1 and 45% of SynGAP grains are colocalized. Changes in particle area were only detected in VGLUT1, with an increase in cluster area from 7 to 11DIV, confirming the visual observation.

3.2.6. Visualization of spines

For the identification of dendritic spines, different methodologies were tested:

1) Live YFP-transgenic cultures were scanned to check for YFP expression. In the timepoints considered, YFP expression was sparse. It was clearly detected in neurons only after several days *in vitro* and so it was not possible to obtain satisfactory results for the timepoints of interest (Fig. 31A);

2) Primary hippocampal cultures transfected with viral vectors tagged with fluorescent proteins. The viral vectors tested were lentivirus-YFP or AAV-6-GFP. Live cells were monitored in a similar way as the YFP-transgenic neurons (Fig. 30B, C). After 5DIV, the transfection efficiency is very different for each of the viral particles. Lentivirus-YFP label few cells in culture and a morphological observation does not clarify if the labelled cells are neurons (Fig. 31B). AAV-6-GFP is much more efficient, as pyramidal neurons in culture are clearly detected (Fig. 31C).

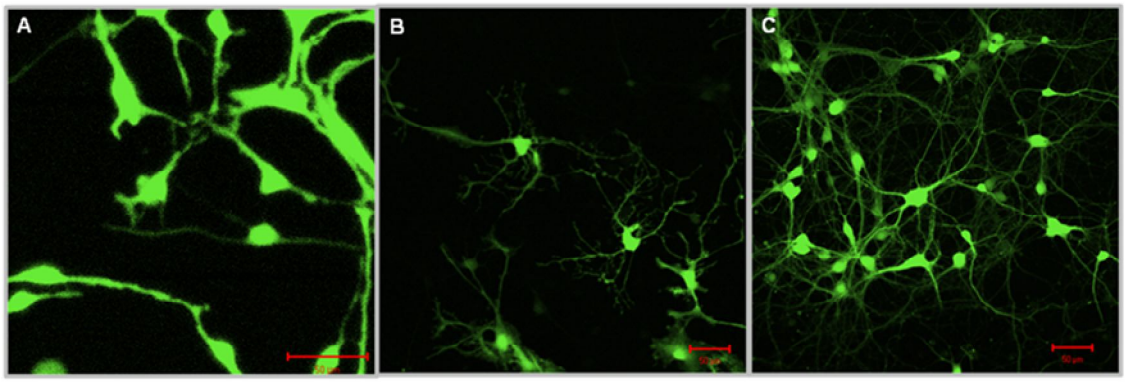

Figure 31. YFP expression at 6 DIV primary cultures of YFP transgenic mice (A). Fluorescent signal of 5DIV primary cultures, transfected with lentivirus-YFP (B), or AAV-6-GFP (C). Scale bar, 50 µm

3) As spines are enriched in F-actin, phalloidin coupled with a fluorophore was used to stain the cultures.

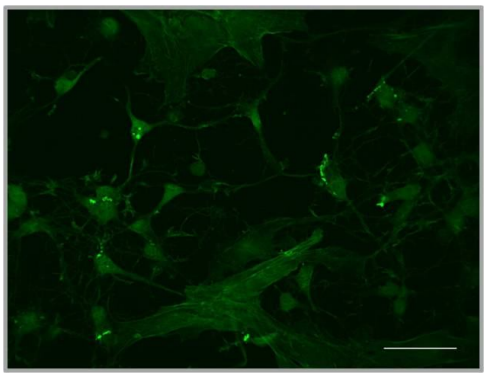

Figure 32. Primary cultures (3DIV) labeled with phalloidin. Scale bar , 50 µm.

Although at times it was possible to detect spines along the dendritic shaft, we could rarely obtain good images since phalloidin stains all the cells in culture.

4) CM-DiI, a hydrophobic dye that spreads throughout the cell membrane, was used to label fixed cultures. It was possible to identify many protrusions along neurites labelled with CM-DiI.

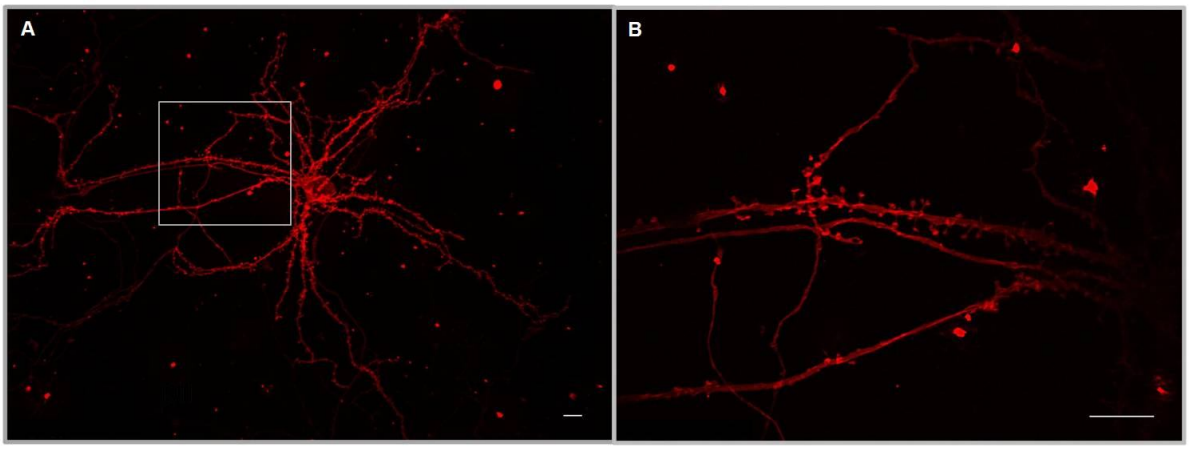

Figure 33. Primary cultures (13DIV) labeled with CM-DiI. Neuron labeled with CM-DiI (A). Enlarged image of the same cell allows the visualization of protrusions of different morphologies along neurites (B). Scale bar, 10 µm

As CM-DiI labelled many neuritic protrusions, additional stainings were combined with this dye.

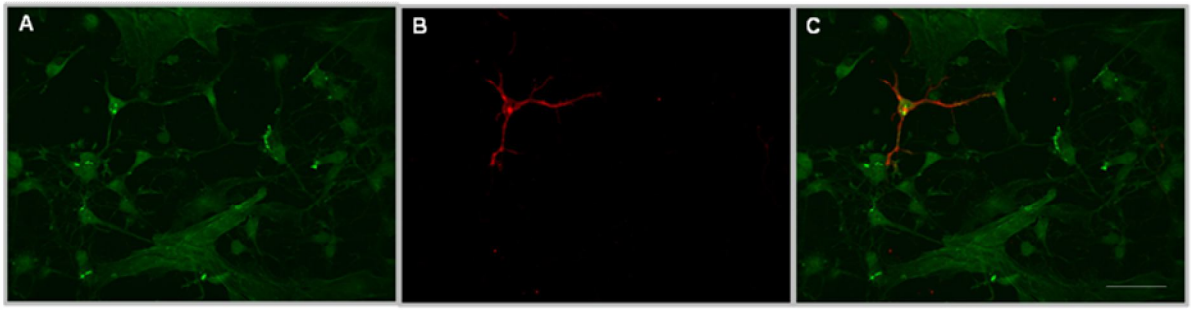

Figure 34. Primary cultures (3DIV) labelled with phalloidin (A) and CM-DiI (B). Overlay of both stainings in C. Scale bar, 50 µm

CM-DiI only stains a few cells in culture (Fig. 34B), which facilitates the visualization of individual cells. When used in combination with phalloidin, it may be easier to discriminate dendritic spines (Fig. 34C).

CM-DiI labelling was combined with immunocytochemistry staining. However, as permeabilization with TritonX-100 caused the extraction of CM-DiI incorporated in the membrane (not shown), it was necessary to optimize the standard procedure. By using digitonin, a more sensitive detergent for permeabilization, CM-DiI labelling was preserved but additional stainings were not successful. Finally, permeabilization with glycerol simultaneously prevented CM-DiI loss from cells and immunocytochemical staining (Fig. 35).

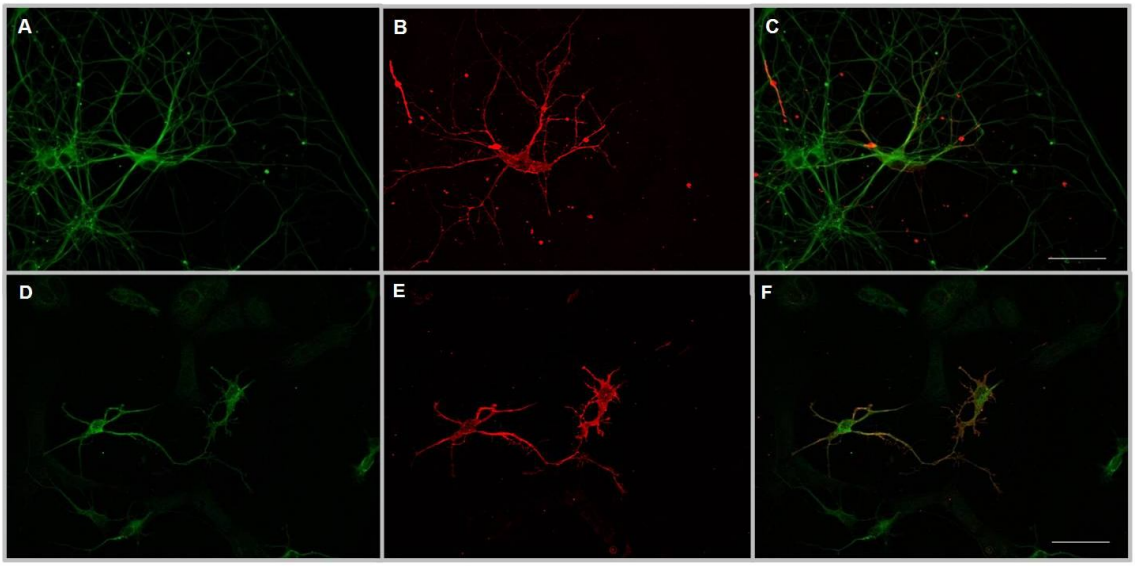

Figure 35. Combined CM-DiI labelling with immunocytochemical staining. Primary cultures fixed at 11DIV were labelled with βIII-tubulin (A) and CM-DiI (B). Cultures at 3DIV were labelled with MAP2 (D) and CM-DiI (E). C and F are the overlayed images. Scale bar, 50 µm

Combined stainings of CM-DiI with βIII-tubulin and MAP2 show that CM-DiI is a neuronal tracer. However, it does not label all neurons in culture. In addition, it is clear that CM-DiI is evenly distributed in neurons, as the staining overlays completely the other markers.

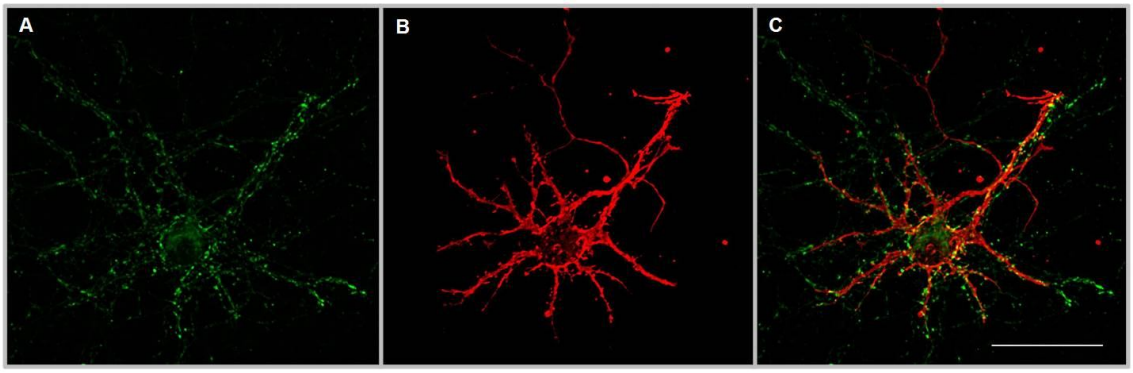

Figure 36. Primary cultures (11DIV) labeled with synaptophysin (A) and CM-DiI (B). Synaptophysin is located in cultures along processes, frequently colocalizing with protrusions labeled with CM-DiI (C). Scale bar, 50 µm

CM-DiI labeling shows that many protrusions at dendrites (Fig. 36B) are colocalized with synaptophysin puncta (Fig. 36C), possibly an indication of synaptic sites. Additional work with other synaptic markers is currently ongoing.

3.2.7. Monitoring spontaneous activity

To evaluate spontaneous electric activity in the developing culture, live cells were loaded with Fluo3-AM. The microplates were transferred to a confocal microscope and a time-lapse sequence was recorded. The mean fluorescence intensity for each ROI was measured over time. In the final minutes of each experiment, glutamate was added at a final concentration of 30µM, in order to discriminate cell populations, based on the response to glutamate stimulus, as described by Pickering and colleagues (Pickering et al., 2008). These authors showed that the pattern of Ca^{2+} influx after a stimulus with 30µM glutamate for 50s allows for discrimination between neurons and non-neuronal cells.

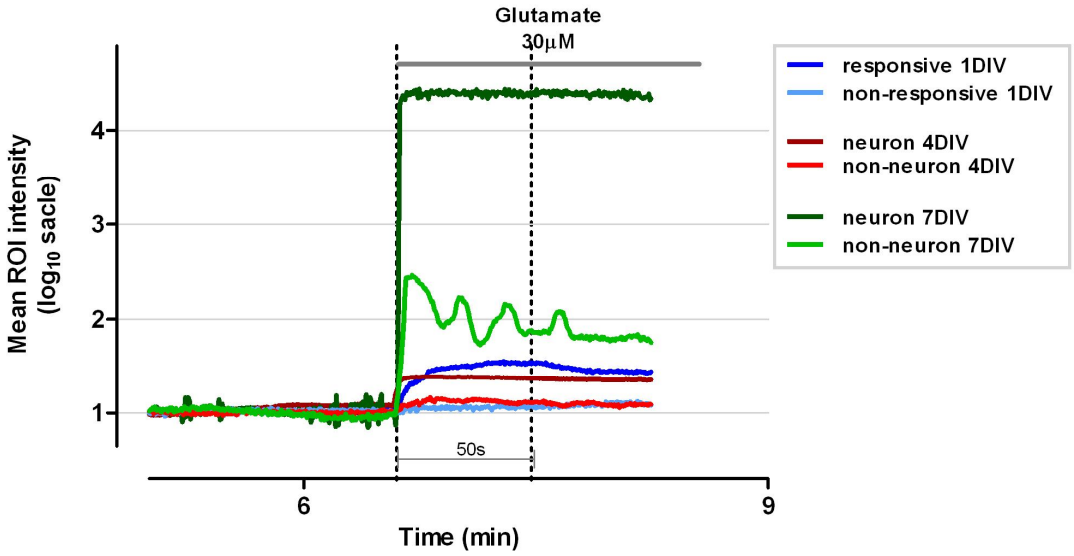

Figure 37. Administration of 30µM of glutamate in the end of the experiment allows for discrimination between neuronal and non neuronal cells, according to the pattern of calcium influx, traceable by the fluorescent changes using Fluo3-AM probe.

The effect of the glutamate stimulus is very weak for cultures at 1DIV. Therefore, for this timepoint cells were classified as responsive or non-responsive to glutamate, and not by the pattern of Ca^{2+} dynamics after glutamate stimulus (Fig. 37). From 4DIV on, the pattern of Ca^{2+} influx is similar to the results of Pickering et al. There are obvious differences in the time course of calcium influx, with neurons having a steep and persistent rise and the non-neuronal population having a sharp (even though frequently smaller) rise followed by a gradual decay. Commonly these episodes are recurring until the end of the recording. Thus, measurement of the intracellular Ca^{2+} flux following a 30µM glutamate stimulus allows for the accurate discrimination of the neuronal cell populations in primary hippocampal cultures. This has importance in the analysis of spontaneous neuronal activity.

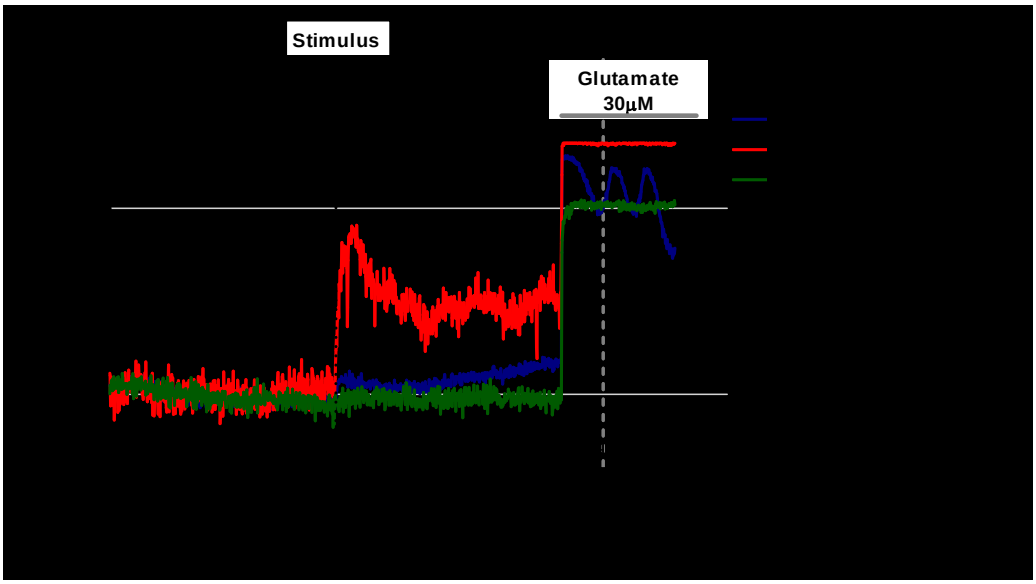

Figure 38. Schematic diagram of live-cell imaging experiments. Each experiment lasts approximately 8 minutes and 1250 images are acquired; 500 images are recorded prior to stimulation of the culture ; after that a stimulus is added to the culture with a pipette and another 500 images are recorded, followed by addition of 30µM glutamate until the end of the experiment. The plotted traces are an adapted representation from a 7DIV culture.

To assess spontaneous activity, bursts of Ca^{2+} flux in unstimulated cultures were measured for approximately 3 minutes (Fig. 38). After this period, different stimuli should have been administered to test the effect on the ongoing spontaneous activity. Some recordings showed synchronized Ca^{2+} transients in neuronal cells after 7DIV (Fig. 39A). However, traces of fast Ca^{2+} flux were rarely detected, in any of the timepoints considered (Fig. 40A). Hence, it was not worth to do stimulations, given that the effect of the added compounds is not evident if the basal culture does not have significant firing. Additionally, it was not possible to analyze the refinement or synchronicity of firing between cells along time. A more thoroughly examination of the analysed fields evidenced that this situation varied with the distance between cells. If the selected field had cells close together (Fig.

39B), spontaneous activity was more pronounced than in distant cells (Fig. 34B). Current tests of spontaneous activity in cultures with different densities confirms this: cultures with higher plating densities have more overall spontaneous activity than lower densities do.

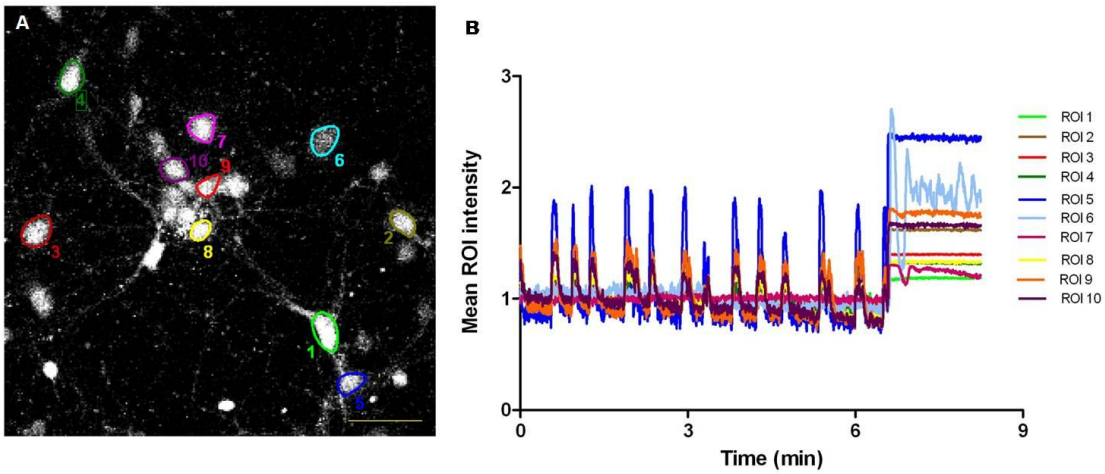

Figure 39. Recorded field of a primary culture with 7DIV (A) where cells are close to each other. Almost all the selected cells exhibit synchronized Ca^{2+} transients (B). ROI 6 does not exhibit changes in Ca^{2+} levels but the final addition of glutamate show that it does not respond as a neuronal cell. Scale bar, 50 µm

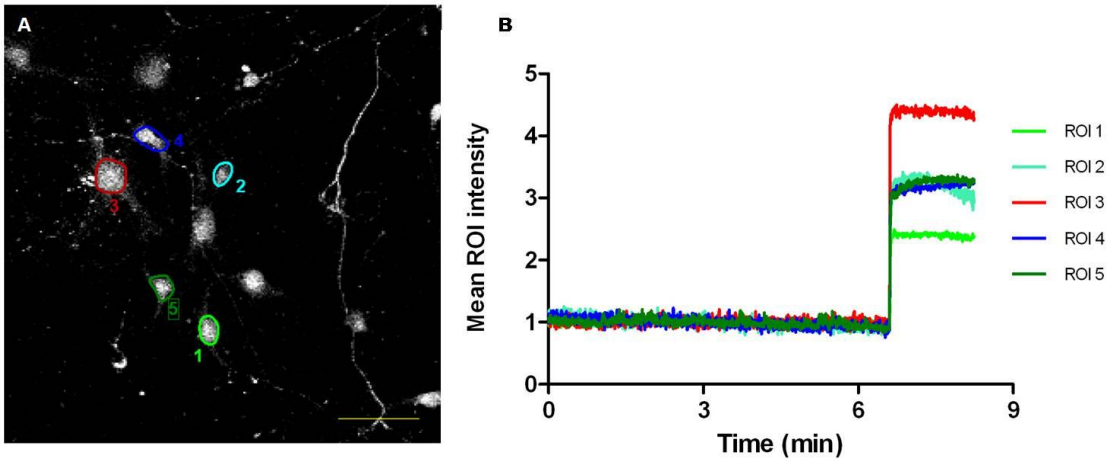

Figure 40. Recorded field of a primary culture with 7DIV where cells are dispersed. There are no detectable traces for any of the selected cells (B). Scale bar, 50 µm.

CHAPTER 4 Discussion

With the purpose of attaining a reliable system for high content studies using hippocampal neurons, cultures were prepared in 96-well microplates. Janssen Pharmaceutica has the necessary tools and expertise for setting up primary neuronal cultures of different anatomical region. The use of 96-well microplates will allow for the simultaneous screening of several medicinal compounds, as well as the possibility of applying different techniques in the same plate, thus saving in time, resources, and number of animals. However, growing primary neuronal cultures in 96-well microplates is not a widespread procedure, with very few publications (Yu and An, 2002). Literature on using 96-well microplates for the growth of primary hippocampal cultures is very sparse. This setup is currently being used with successful results to perform Enzyme-Linked Immunosorbent Assay (ELISA), to measure the levels of factors released by neurons to the medium in cultures up to 1 week (Michaki, V., unpublished data), etc. However, as the purpose of this work requires imaging techniques and long-lasting cultures several problems have surfaced that will now be briefly discussed.

4.1. Establishing primary hippocampal cultures in 96-well microplates

4.1.1. Sustaining media

The use of the N2 medium alone was not sufficient for neuronal survival and development. This was easily seen by visualization of the cultures under a contrast-phase microscope. Most of the wells in N2 medium had a lot of dead cells in the first days of culture (Fig. 9). Different approaches for long-term culturing of hippocampal neurons are used by several groups from lab to lab, depending on the final objective. Many of them include the use of additional factors that influence the survival and growth of hippocampal

cells. This can be either the use of an astroglial feeder layer, releasing trophic factors into the medium, or the addition of a sterilized glass coverslip on top of the cells; this coverslip is not in direct contact with the cells, as it is supported by paraffin drops, thereby creating a microenvironment favorable for neuronal growth. At the moment, such application is not available for the 96-well microplate setup and the lack of this conditioning step may cause the inefficiency of N2 medium to sustain growth and viability of these cultures. Additional supplements, such as the popular neuronal media supplement B27 (Invitrogen), were not considered as its use has been avoided in the lab given the variability between batches (Chen et al., 2008) and previous problems in cultures verified in this lab. Trying to overcome this limitation, C6-CM was used as an alternative. Rat C6 glioma cells represent a well-characterized, homogeneous population of CNS glial tumor cells that can be grown in large amounts and resemble astroglial cells in the expression pattern of GFAP and glutamine synthetase (Westermann et al., 1988). Also, previous evidence shows that C6-CM with 10% FCS (as prepared in this work) supported neuronal survival and promote neurite outgrowth in embryonic rat hippocampal neurons (Okuda et al., 1994), due to the presence of neurotrophic factors released from C6 glioma cells (Westermann et al., 1988) that include glia-derived nexin, cilliary neurotrophic factor (CNTF)-like factor, S100β proteins, and nerve-growth factor (NGF) (Okuda et al., 1994). Our results show an evident difference using C6-CM instead of N2 medium (Fig. 9).

Another problem arose by the fact that the cultures do not survive for long periods of time, even in the C6-CM medium (Fig. 9G). Primary hippocampal cultures prepared using previously established protocols are reported to survive and remain healthy for 4 to 6 weeks, with a slight degree of cell death and process degeneration after 2 to 3 weeks (Banker and Goslin, 1998; Vicario-Abejón, 2004). In our cultures, there is a high degree of

debris in the cultures and many dead cells are observed after 14 to 20DIV. Fixation procedures result in a high loss of cells (probably death *a priori* and detached from the substrate, which causes its clearance in the washing steps of the procedure), and process fragmentation. Additionally, between 7 and 11 DIV, many of the neuronal cell bodies are very close together (neuronal clustering) and there is an apparent thickness of the neurites (process fasciculation). Cell bodies of embryonic neurons naturally tend to aggregate but an exaggerated clustering may trigger faster neuronal cell death (Banker and Goslin, 1998). Some protocols suggest that this may be avoided by controlling the cell density, making sure that it is not higher than 2.5×10^5 cells/cm^2, and also by inhibiting glial proliferation (Vicario-Abejón, 2004). There is an ongoing debate regarding clustering of neurons in culture, and what constitutes a healthy situation (Banker and Goslin, 1998; Doré et al., 1997; Soussou et al., 2007). However, given the fact that this setup should be established for the study of synaptic plasticity in a mature neuronal network through imaging techniques, it is detrimental to improve culture conditions. The goal is to obtain reproducible and healthy neuronal cultures that are viable for extended periods of time. Therefore, several conditions were tested.

4.1.2. Cell density

Cells were plated at a density of 10000 cells/well (approximately 30000 cells/cm^2). This was determined by preliminary tests where a series of cell densities were tested (data not shown). Cultures with lower cell density had higher and earlier cell death. In higher densities cells seemed to be closer to each other and the neuronal clustering occurs earlier

than in a low density culture, most probably given the available space for cells to migrate (Fig. 10).

4.1.3. Well coating

The microplates used are coated by the manufacturer with poly-D-Lysine (PDL), a polycationic molecule that allow cells – with an overall negative surface charge – to attach to similarly charged substrates. Inversely to its enantiomer Poly-L-Lysine, PDL does not interfere with cell physiology, as it is not cleaved by extracellular proteases (Soussou et al., 2007). Many studies with neuronal primary cultures have been successfully developed with this coating (Dotti et al., 1988; Gerrow et al., 2006; Rao et al., 1998). However, as explained above, our cultures were clustering and dying prematurely. Trying to overcome the formation of neuronal clusters, alternative coatings were tested. Different substrates were used for additional well coating, such as polyethyleneimine (PEI), used in some reported studies (Liu et al., 2008; Liu et al., 2006). PEI lacks the slightly negatively charged carbonyl moiety of PDL, and is therefore a more positively charged polycationic organic molecule, on which neurons reportedly mature faster (Lelong et al., 1992). In addition, 96-wells microplates coated with collagen were also tested. Collagen is a natural component of the extracellular matrix, commonly used for plate coating (Rao and Winter, 2009; Winter et al., 2009). Cells were plated and cultured in previously described conditions. None of the substrates tested yielded better results than the initial PDL coating (Figs. 11 and 12). Ongoing experiments with laminin coating (other molecule of the extracellular matrix) are not satisfactory so far (data not shown).

4.1.4. Medium change

As these are the first steps in the establishment of primary hippocampal cultures using the 96-well microplate setup, the medium was not changed in the first cultures plated. To assess if the increasing clustering and cell death was due to a nutrient deficit in the medium after one week, medium was replaced after 7DIV. However, as mature neurons require conditioned medium to survive and are more vulnerable to the effects of changing medium than less differentiated neurons (Vicario-Abejón, 2004), only a fraction was replaced by fresh N2 medium. Unfortunately, this did not seem to have improved the quality of the cultures, as clustering remained and a high number of cells died after this timepoint.

4.1.5. Inhibition of proliferation

One of the reasons for neuronal clustering may be the presence of other cells in the culture. Even though it is proved that the presence of glial cells is important for the growth of neuronal cultures (Ray et al., 1993), the presence and proliferation of this and other cell types may exert a negative effect on the neuronal population. To control the proliferation of other cell types in the culture, cytosine arabinoside, a mitotic inhibitor, can be added to the cultures. These experiments are currently ongoing.

4.1.6. Creating a microenvironment in the wells

Attempts at mimicking the microenvironment of the glass coverslip of the 6- and 12-well plate setup were tried. For that an ‘insert’ to be introduced in the wells was designed. Cultures were prepared with N2 medium and the insert was added. Preliminary

results were not satisfactory and most likely further optimization of the insert design will be required.

In summary, at the moment there are limitations regarding the further use of these systems for imaging-based studies of synaptic plasticity, given that the overall aspect of the cultures does not resemble previously established approaches. Therefore, it is still necessary to further optimize the methods for establishment and maintenance of the cultures in this setup. Cultures prepared with the most favorable conditions so far were subjected to different techniques for characterization. For the reliable use in imaging and functional approaches to study synaptic plasticity, it is necessary characterize the growing cultures along time. For that, several parameters were tested.

4.2. Characterization of the cultures

4.2.1. Discrimination of cell types

Cultures obtained from embryonic hippocampi are mainly consisting of pyramidal neurons. However, it is virtually impossible to obtain a pure neuronal culture from a hippocampal dissection (Banker and Cowan, 1977; Banker and Goslin, 1998). It is important to monitor the presence different cell types in culture over time. Hence, characterization was performed through immunocytochemical stainings using cell-type specific markers from 1DIV onwards. Class III β-tubulin, a neuron specific tubulin isoform and GFAP, an intermediate filament protein specific of astrocytes were used cell type identification. Both markers are adequate for this type of study, given that they are cell type specific, stain proteins that are expressed early in development and have high expression levels, and are distributed throughout the entire cell (Banker and Goslin, 1998).

Images of the stained cells showed that neurons and astrocytes have different morphologies, evident from the initial moments after plating (Fig. 13). Neurons have a homogeneous morphology: even though not all neurons in the field are in the same developmental stage, there is correspondence to previous descriptions of developmental neuronal changes *in vitro*, namely a large nucleus and many cylindrical processes that extend and branch with time (Fig. 13B, F, J, N) (Cáceres et al., 1986). Astrocytes have different morphologies, ranging from flattened and polygonal to highly branched with radial symmetric processes (Fig. 13C, G, K, O). Staining the nuclei with DAPI showed that additional cell types are present in these cultures (Fig. 13D, H, L, P). However, other cell types were not studied. The results obtained by image analysis were very consistent for all the cell cultures considered (Fig, 16): the number of neuronal cells did not vary throughout the timepoints considered, even though it is considerably less than what is referred in the literature for primary hippocampal neuronal cultures (Banker and Cowan, 1977). This may be an indication of suboptimal conditions for neuronal growth in this setup, affecting the neuronal yield since the moment of plating. It does not seem valid to discuss the isolation process, as it is done in the same way as for 6- or 12-well plates. The number of astrocytes and total number of nuclei increased significantly at 7DIV and 11DIV. The initial reduction (from 1DIV to 4DIV) may be due to the death of cells that did not recover from the dissociation and plating process. It does not seem to be a chronic condition affecting the culture, as there is considerable increase on each cell population at later timepoints, and most importantly, it does not seem to affect the neuronal population. The astrocytic population in culture represents 10 to 20% of the total number of cells at 1DIV, decreases at 4DIV (as the total number of nuclei), and then grows after that with a pronounced increase at 11DIV. The results are in agreement with the previous visual

analysis and represent an expected result, as astrocytes tend to proliferate at high rates, possibly even more in this setup given the conditioning of medium by C6 glioma cells (Kato et al., 1981), and as there was no treatment with mitotic inhibitors. It should be noted that the high number of astrocytes (Fig. 14C) in the images sometimes compromised the correct analysis by the software used, especially in the later timepoints, as the software could not discriminate effectively nuclei from neurons or astrocytes. Given that the increase in the total number of nuclei was more pronounced than the number of astrocytes, it is possible to say that non neuronal, non astrocytic cells are also present in culture and proliferated in this time frame. Visual analysis of the images obtained from the immunocytochemical procedures also confirms this, as a high number of βIII-tubulin(-)/ GFAP(-) nuclei was present (Fig 14. A, D). The most common nonneuronal cells present in culture are astrocytes and fibroblasts (Banker and Goslin, 1998) and so it is very likely that these nuclei correspond to the latter cell type. However, this hypothesis was not tested. Nevertheless, it may be detrimental to control the proliferation of non-neuronal cells, given that it was frequent to observe extended areas occupied by βIII-tubulin (-)/ GFAP(-) nuclei, as neurons were apart from these regions, many times with the cell bodies clustered and many fasciculated processes (Fig. 14D). Hence, the addition of mitotic inhibitors, such as cytosine arabinoside (AraC) should be evaluated. The results here presented are also useful in understanding the timeframe into which AraC should be included. AraC should be avoided at the time of plating, to allow the presence of some astrocytes in culture but it should be added before massive proliferation of astrocytes and other cells ensues (as it is done in standard protocols). This work is at the moment ongoing.

4.2.2. Neuronal development

The morphological analysis of neuronal development represents a powerful tool to evaluate neuronal growth and polarization in primary hippocampal cultures. It has been previously demonstrated that hippocampal neurons growing in culture have a characteristic pattern of differentiation (Dotti et al., 1988; Ray et al., 1993). As aforementioned, staining neurons with βIII-tubulin allows for morphological analysis of these cells. Individual neurons were analyzed at different timepoints and the morphology was compared with previous data from the work of Dotti and colleagues (Dotti et al., 1988) (Fig. 17). At the initial timepoints there is a high resemblance between literature data and the data from the cultures used in the present study probably reflecting similar health and functionality. Even though it is relatively easy to visualize individual neurons at the early timepoints considered (1DIV and 4DIV, Fig. 17A and B), this analysis is much harder for 7DIV and 11DIV, as individual neurons are rarely observed, particularly the neuritic processes. Even though Fig. 17C shows individual neurons at 7DIV, this is not a common situation in the cultures and there is no certainty that neurons growing close together show the same characteristic branching as the ones presented. Neurons at 11 DIV were not analyzed as it was not possible to find individualized neurons. Additionally, clusters of neurons and process fasciculation, starting around 7DIV may compromise this analysis. This limitation could be overcome by decreasing cell density – in fact, the quoted studies were performed in low-density cultures (500-2500 cells/cm^2) (Dotti et al., 1988), which allows for easier visualization of individual cells. However, this has been challenging in the 96-well microplates setup. An alternative approach could be transfection with viral vectors expressing fluorescent proteins, as it is possible to transfect only a portion of cells in culture. Then it could be possible to analyze individual neurons regardless of cell density.

Additionally, the use of CM-DiI could be considered. CM-DiI is a long-chain carbocyanine dye that is rapidly incorporated into membranes (Honig and Hume, 1989a). As it labels neurons retrogradely and anterogradely, it is distributed throughout the entire cell, allowing for the evaluation of neuronal development (Honig and Hume, 1989b). In addition, it has been previously reported that CM-DiI can be added to living, growing cells and can be used to monitor neurite outgrowth along time (Honig and Hume, 1986). Our most recent results, where cells were labeled with CM-DiI and βIII-tubulin (Fig. 35A, B, C), clearly show the potential of this dye for the visualization of individual neurons in culture.

4.2.3. Neurite outgrowth

The formation and growth of the neuronal network in culture was assessed. For that, neurite length per neuron was evaluated. The increase in neurite length per neuron is evident through visualization of neurons stained with βIII-tubulin (Fig. 18A, D), which is confirmed with computational analysis. The measurements were very accurate for the initial timepoints (1DIV and 4DIV, Fig. 18 B, C) but had an increasing associated error in the later timepoints, due to the density and complexity of the neuronal network. From 7DIV on, the complexity is such that it becomes complicated to properly measure neurite length (Fig. 18D, E, F). In addition, the formation of the neuronal clusters and process fasciculation increase the intensity of βIII-tubulin signal along the neurites (Fig. 18G), thus processed by the analysis algorithm as a cell body (Fig. 18H). As so, the measured area of neurites is probably an underestimate of the real situation.

The measurements are expressed as the ratio between neurite length per neuron (Fig. 19) given the fact that the areas scanned by the automated microscope varied significantly in the number of cells. As such, a simple measure of the total neurite length in

the considered fields might be erroneous and the adopted strategy minimizes the associated error. The results clearly show that neurites are growing with time, and even though it is harder to measure neurite length at 11DIV, there is a significant increase from 7 to 11DIV. However, the software is not able to effectively measure neurites in the later timepoints, which complicates the analysis of the neurite growth at the 11DIV situation. Once again, this is a consequence of a high cell density that does not allow the analysis of individual cells. Again, this may be overcome by the same alternatives presented in the previous topic. As CM-DiI is evenly distributed through neurons and stains only a few cells in cultures it could be successful in the assessment of neurite outgrowth at later timepoints (Fig. 34A, B, C).

4.2.4. The effect of NGF and JNJ#X in neural population and neurite outgrowth in the developing primary hippocampal culture

Primary neuronal cultures are extensively used for testing compounds that may exert trophic, protective and even toxic effects in neurons, as well as inducing or inhibiting plasticity (Chang et al., 2001). Activity-dependent mechanisms have been demonstrated in many brain areas during early postnatal life when immature circuits are first driven by sensory experience. During this period, experimental manipulations that perturb normal firing of sensory afferents result in marked changes in neural circuits (Feller, 1999). As such, in order to obtain a reliable sensor for the future screening of compounds affecting synaptic plasticity, it is necessary to validate our model by demonstrating the sensitivity of the approaches to detect changes in the neuronal network upon external stimuli. As the

previously described techniques were successful applied in the described setup, further studies on their validation were carried out.

Primary cultures were grown either in the presence of a neurotrophin and a test compound (JNJ#X), since the moment of plating. Nerve growth factor (NGF), the first neurotrophin to be characterized, was first discovered while searching for neuronal survival growth factors (Levi-Montalcini, 1987) in the development of sympathetic and sensory ganglia. NGF promotes differentiation and neuronal growth in the developing brain, and supports neuronal survival in the adult brain (Hetman and Xia, 2000; Levi-Montalcini, 1987; Lewin and Barde, 1996). NGF exerts its effects in different neuronal cells by two distinct types of receptors, the high affinity neurotrophin receptor tyrosine kinase A (TrkA) and the common low affinity neurotrophin receptor p75 (p75NTR). It has been previously shown that endogenous and exogenous neurotrophins contribute to regulation of dendrite morphology and play a major role in the structural adjustment and maturation of neuronal circuits (McAllister et al., 1999; McAllister et al., 1995), even though the signaling pathways underlying neurotrophin effects on neurite outgrowth are not completely elucidated (Salama-Cohen et al., 2005). Previous studies of the effect of NGF in hippocampal neuronal cultures indicate that exogenous NGF promotes neurite survival (Culmsee et al., 2002) and dendrite elongation of pyramidal cells (Salama-Cohen et al., 2005). In our results, only 10ng/ml of NGF seems to exert a protective effect in the neurons in the cultures at 1DIV, an effect that is not traceable at the other timepoints (Fig. 20). Additionally, there is no significant effect of NGF in neurite outgrowth in our culture (Fig. 21). As it has been reported that the culture supernatant of hippocampal neurons from embryonic day 17 is virtually devoid of NGF (Houlgatte et al., 1989), an effect of NGF on neuronal survival and neurite outgrowth was expected. The outcome is most likely

attributable to the use of C6-CM medium, since it has been demonstrated that C6-CM is effective in supporting neuronal survival and enhancing neurite elongation (Okuda et al., 1994). In addition, it was reported that it contains NGF synthesized by C6 glioma cells and released to the culture system (Murphy et al., 1977). Hence, it is normal that the addition of NGF to the medium does not induce significant changes to the culture system, already conditioned with an unknown amount of NGF. With time, the NGF initially present in the medium should be cleared by the cell. However, as astrocytes *in vitro* are able to synthesize and secrete NGF (Furukawa et al., 1986), the net concentration of NGF in the medium may be maintained. Finally, there is the possibility that differences were not detected due to limitations in the techniques.

JNJ#X is an antipsychotic drug currently under investigation at Janssen Pharmaceutica. The addition of JNJ#X to the primary cultures did not induce immediate effects on neuronal survival. However, at later timepoints there was a significant decrease in the neural population with 10^{-5}M and 10^{-6}M JNJ#X (Fig. 22). JNJ#X did affect neurite outgrowth: there is an increase of neurite length per neuron at 1DIV for any of the concentrations analyzed, that is significant for a concentration range from $3x10^{-8}$M to 10^{-6}M (Fig. 23). This effect is also detectable at 4DIV for $3x10^{-8}$ M of JNJ#X. Additionally, it is possible to see that 10^{-5} M also induces an evident degeneration of neurites at 7DIV. These results provide evidence for the rapid effect of JNJ#X on neurite outgrowth of the described culture. It is not known what the mechanisms are through which JNJ#X induces neurite outgrowth in the hippocampal neurons but most likely they are different from signaling by NGF. It should be noted that both NGF and JNJ#X were added only one time to the culture and it is not known what the clearance rate is for each of the compounds. This

could justify the lack of effect of JNJ#X for more extended periods – possibly additional exposures would induce different outcomes.

Even though these are preliminary data, they are still very useful for validation of the approaches tested, as it was possible to discriminate the effect of JNJ#X in the culture populations and morphology.

4.2.5 Distribution of synaptic markers

With the development of the neural circuitry in these cultures, synapse formation is expected. There is a great interest in trying to understand the assembly of the synaptic components and important timeframes. However, at the moment few data are available describing the exact time frame of synaptogenesis during neuronal maturation in culture (Grabrucker et al., 2009). Trying to investigate synaptogenesis and synapse maturation in our culture, immunocytochemistry was used to trace the distribution of pre- and postsynaptic markers over time. Initially, the Neurotox-1 kit was used (Fig. 24) to analyse synaptophysin distribution. Synaptophysin is a membrane glycoprotein of synaptic vesicles, ubiquitously expressed in neurons and a popular presynaptic marker. At 7DIV, it was possible to see puncta of synaptophysin along neurites. However, the labeling of βIII-tubulin is not helpful to visualize individual neurites in our setup, given the intricate neuritic network. In addition, our interest was to perform triple stainings, with a pre- and postsynaptic marker and a neuritic tracer.

Additional antibodies were tested: VGLUT1 and VGAT are presynaptic vesicular transporters for glutamate and GABA, respectively. SynGAP is a Ras-GTPase activating protein highly enriched at excitatory synapses. MAP2, a microtubule-stabilizing protein was used to visualize the dendritic trees. Even though MAP2 is initially distributed

throughout the cell (Fig. 25A), it becomes restricted to the dendrites around 4DIV (Fig. 25C) (Cáceres et al., 1986). At 1DIV, all of the markers stain very weakly and show an even distribution in the cell cytoplasm and the neurites, and no puncta were detected (Fig 25B and Fig. 26A, B). At 4DIV, the presynaptic markers formed little clusters that were seen along thin processes with weak MAP2 signals, most likely to be axons (Fig. 26C, D). Clusters of these markers were rarely observed along dendrites, which is an indication that synapses are not formed yet. At this timepoint, the distribution of SynGAP did not differ much from 1DIV (Fig. 25 D). Such observations are in agreement with previous studies, showing that presynaptic vesicle cluster in hippocampal neurons in culture soon after the axon emerged, but that there is a delay in the aggregation of postsynaptic markers in dendrites (Fletcher et al., 1994) and in synapse formation. At 7DIV, all MAP2 positive processes were outlined by SynGAP (Fig. 25F). VGLUT1 and VGAT clusters were detected surrounding the cells bodies, and neurites, indicating synaptogenesis in culture (Fig. 26E, F), in agreement with the study from Fletcher and colleagues. The same was detected at 11DIV (Fig. 26G, H). At this timepoint, SynGAP is weakly detected in the cell body and more selectively distributed to the dentrites (Fig. 25H). Studies where other components of the PSD machinery were tested in combination with EM looking at PSD thickening also revealed that detection of these proteins was only possible after 7DIV (Grabrucker et al., 2009; Rao et al., 1998). This provides evidence for the normal development of the neurons used in this study.

Given that the majority of hippocampal neurotransmission is excitatory, glutamatergic synapses were visualized by triple staining with VGLUT1, SynGAP and MAP2 (Figs. 27-29). VGLUT1 is a vesicular transporter involved in the uptake and storage of glutamate and is currently one of the most popular markers for glutamatergic nerve

terminals (Zander et al., 2010). SynGAP interacts with PDZ domains of PSD 95 and SAP102 and is enriched at excitatory synapses, forming a large macrocomplex with PSD95 and NMDARs, where it may play an important role in modulation of synaptic activity by regulating Ras activity (Kim et al., 1998). Analysis was performed at 7 and 11DIV (Fig. 30). There was not a clear change in the number of particles per length for any of the markers, but an increase in the size of VGLUT1 positive clusters was detected. Also, the number of colocalizations did not differ between the two timepoints. This was not in agreement with the study from Grabrucker and colleagues, as it was shown that the number excitatory synapses in primary hippocampal neurons increases in the timeframe considered, until 21DIV (Grabrucker et al., 2009). Many reasons may account for this difference: the optical resolution may limit the accurate counting of clusters, as there is the possibility that the increase in cluster size from 7 to 11DIV represents close adjacent puncta that could not be resolved, leading to an underestimation of synaptic number. New synapses with only a few vesicles may have been lost during analysis. Culture density may also be affecting the results, as it has been previously documented that higher density cultures have more synapses formed by 7DIV than low-density cultures (Fletcher et al., 1994). This is expected since the probability of afferent axons contacting postsynaptic dendrites is decreased in low-density cultures. It should be noted that cell density may also greatly affect the data acquisition, as it was very difficult to identify individual neurites. Even though the results do not show a difference in excitatory synapses from 7 to 11DIV, visual analysis shows a difference in the localization of the clusters (Fig. 28 and 29, enlarged boxes)): at 11DIV clusters seem to be slightly distant from the dendritic shaft stained by MAP2, which may be an indication of trafficking to dendritic spines, known to be specialized microdomains where most excitatory synapses are known to be located (Rao et al., 1998).

4.2.6. Visualization of spines

The formation and maturation of dendritic spines is another important landmark of neuronal maturation. To define an efficient approach for spine visualization and quantification, different methods were tested.

For live cell visualization, transgenic mice-derived YFP neurons and neuronal transfection of YFP using viral vectors were used. It has been previously demonstrated that transgenic YFP-expressing neurons allow for spine visualization (Feng et al., 2000; Pan and Gan, 2008). However, that was not possible in the described setup, as YFP expression was very sparse in the considered timepoints, and neuritic protrusions were not visualized (Fig. 31A). The YFP sequence is regulated by the Thy-1 promotor, which proved to become active only around day 11 after birth, and it has been shown that high levels of YFP expression in the hippocampus of these animals is detected from the second postnatal week (Niu et al., 2008). Transfection of fluorescent proteins has also been extensively used for different neurobiological studies (Young and Feng, 2004), including spine visualization (Hasbani et al., 2001; Malinow et al., 2010). Cultures transfected with lentivirus-YFP yielded low transfection efficiency, with low neuronal specificity (Fig. 31B). Transfection with AAV-6-eGFP was more efficient and more neuronal specific (Fig. 31C). However, their use was not continued, because parallel, *in vivo* studies are difficult to perform, due to the need for stereotactic injection in the brain of the animals; the cost of AAV-6-eGFP is also a limitation.

For spine visualization in fixed cultures, a staining with phalloidin coupled to a fluorophore was tested. Phalloidin is a toxin extracted from the poisonous fungus *Amanita phalloides* that binds to F-actin, which is enriched in dendritic spines. Phalloidin has been extensively used for the identification of dendritic spines (Fujisawa et al., 2006; Schubert et

al., 2006). Different timepoints were tested, and spines (or spine precursors) were at times detected, but it was impossible to acquire any image for analysis, as phalloidin will bind to F-actin in all cells in culture, severely impairing image analysis (Fig. 32).

Successful visualization of spines was obtained with the use of CM-DiI. Preliminary tests showed that CM-DiI is capable of labeling live or fixed cultures (Honig and Hume, 1986; Papa et al., 1995). However, for still unknown reasons there is a high variability in the labeling efficiency for each of the experiments (data not shown). In each of the cases, it was possible to see protrusions of the neuritic processes that resemble spines or its precursors (Fig. 33).

Performing a double staining with CM-DiI and phalloidin allows for more selectivity in the visualization of protrusion along dendrites. However, Fig. 33 is from a primary culture of 3DIV, and very few protrusions were evidenced. This may be due to the fact that spines are initially detected in cultures after one week (Papa et al., 1995). To evaluate cell specificity of CM-DiI, several double stainings were performed. Preliminary tests show that CM-DiI does not label cells after our standard immunocytochemical procedure, probably due to the permeabilization procedure, in which the plasma membrane is extracted (data not shown). In addition, it is washed away after permeabilization with 0.1% Triton X-100. Permeabilizing with 10 or 100ng/ml digitonin preserves CM-DiI (Matsubayashi et al., 2008) in the membrane but it was not possible to double stain the culture, possibly because digitonin did not promote sufficient membrane permeabilization for the effective penetration of the antibodies. Finally, permeabilization with glycerol allowed for additional immunocytochemical staining after CM-DiI incubation. As so, MAP2 and βIII-tubulin staining were combined with CM-DiI (Fig. 35). The results show that CM-DiI is distributed throughout the neuron, and some protrusions along neurites are

detected. These are very optimistic results that open the possibility to perform double stainings with CM-DiI and pre- and postsynaptic markers for the full confirmation of spines. In fact, that was recently achieved, with the combined staining with CM-DiI and synaptophysin (Fig. 36). Additional stainings are now under investigation. As obvious, after optimization of these procedures, it will be interesting to evaluate spinogenesis and spine morphology and dynamics in the primary hippocampal neurons growing in this setup. An algorithm allowing for spine counting and classification is now being finalized (unpublished data).

As preformed for the assessment of cell populations and neurite outgrowth, the sensitivity of the presented approaches should be evaluated. Additional studies where the effects of NGF and JNJ#X in the synaptic markers clustering, formation and maintenance of spines were investigated but nothing could be concluded due to time restraints.

4.2.7. Monitoring spontaneous activity

Accumulating evidence shows that electrical activity is essential for the development of neural circuits in many brain regions (Zhang and Poo, 2001). Observations of spontaneous electrical activity at early stages of development before the onset of synaptogenesis predict its potential role in the assembly of the nervous system (Spitzer, 2006). Evaluation of spontaneous electrical activity is an interesting tool to assess functionality and maturation of the neuronal network forming in the microwells.

Spontaneous activity consists of rhythmic bursts of action potentials that last for tens to hundreds of milliseconds with intervals of a few minutes, involving correlated firing of large populations of neurons (Feller, 1999; Zhang and Poo, 2001). In the developing

hippocampus, these events correspond to the increase in $[Ca^{2+}]_i$ in pyramidal cells and interneurons in the CA1 region due to the presence of voltage-gated calcium channels in neuronal membranes (Feller, 1999; Göbel and Helmchen, 2007; Spitzer, 2006).

Changes in the $[Ca^{2+}]_i$ levels were measured using the fluorescent probe Fluo3-AM. The acetoxymethyl (AM) ester group coupled to a Fluo3 probe results in an uncharged molecule that can permeate cellular membranes. Once inside the cell, ester groups are cleaved by nonspecific cytosolic esterases, resulting in a trapped, membrane impermeable form of Fluo3 (Göbel and Helmchen, 2007). Fluo3 binds to free Ca^{2+} ions in the cytoplasm and emits fluorescence when excited at 488nm, thus allowing for the visualization of Ca^{2+} transients. Given that the culture is not homogeneous, it was necessary to discriminate between cells in order to assure that neuronal activity was evaluated. It has been reported that Ca^{2+} oscillations are different among brain cells: for instance, astrocytes usually have slow, wave-like calcium signals. Nevertheless, at times it may be difficult to distinguish between cells only through calcium influx. A recently published approach for discrimination between cell types in live cell imaging experiments of cortical cultures showed that a 30uM glutamate stimulus causes a Ca^{2+} transient that can be used for cell discrimination (Pickering et al., 2008). The same was tested in our rat hippocampal cultures (as in mice cultures) and similar traces were identified (Fig. 37). At 1 DIV, there was no clear difference in the response pattern. However, by 4DIV some cells in culture exhibited a pattern of calcium influx very similar to the results published by Pickering et al, most likely to be neurons. Other traces were detected after glutamate stimulus. This pattern is detectable in the older cultures, with an evident increase in the magnitude of response. Additionally, it was detected that cells exhibiting spontaneous and synchronous activity, similar to published data (Cohen et al., 2008), also had the same response to glutamate,

which is an indication that the glutamate stimulus is also useful as a marker for cell populations of primary hippocampal cultures. All live-cell imaging experiments were then performed with glutamate added in the final minutes to allow for neuronal discrimination.

Unstimulated cells were imaged to assess spontaneous activity, supposedly followed by a stimulus and another series of image acquisition to evaluate the effect of stimulation in the electrical activity of the network (Fig. 38). However, it was very rare to obtain records of cells firing spontaneously in any of the timepoints considered. Studies on spontaneous activity in primary hippocampal cultures revealed that sporadic and unsynchronized firing occurs soon after attachment of cells, with synchronized events first detected at 3DIV, and that more neuronal cells are recruited along the first two weeks to result in a fully synchronized activity of neurons, likely to span across the entire culture plate and last for long periods of time (Cohen et al., 2008). This is evidence for dramatic changes in the culture network burst in the first 2 weeks, resulting in higher magnitudes, coherence, rate and time course of individual bursts. The lack of spontaneous activity in our cultures thus represented an unexpected outcome.

The most likely reason for this outcome is the density of cells in culture. It has been documented that the number of neurons in a network is determining the expression of spontaneous activity, such that small networks consisting of few neurons do not have traceable bursting events, whereas larger networks produce higher rates of activity (Chang et al., 2001; Cohen et al., 2008). A study on the effect of different substrates on network morphology and spontaneous electrophysiological activity of dissociated hippocampal neuron indicates that neuronal networks where clustering and process fasciculation are more frequent show more synchronized firing and faster bursting, even though its mean firing rate dropped; inversely, neural networks with many individual cells and thin

branching were negatively correlated with synchronous activity and bursting (Soussou et al., 2007). With this in mind, the fields where spontaneous and synchronized activity was detected were compared to others where no activity was detected. It became clear that the spontaneously active events occurred when cells were closer together (Fig. 39). Fields where cells were dispersed and the contact was not evident, rarely exhibit any traceable change in Ca^{2+} flux (Fig. 40). In addition, parallel ongoing studies on mice cultures with different cell densities reveal that lower densities have less spontaneous activity than higher density cultures (Peter Verstraelen, unpublished data). So, the absence of spontaneous activity in this setup may be due to a spatial effect and not to cell functionality. It should also be noted that this lack of electrical activity may have effects on the development of the neural circuit, given that it is detrimental for communication amongst cells and synaptic development and maintenance (Ham et al., 2008). The influence of cell distance in the onset of spontaneous activity should be further evaluated, in order to understand what the appropriate cell density for these experiments is.

CHAPTER 5 Concluding remarks

The results depicted in this work evidence the successful application of the techniques, as well as the first data on the formation of neuronal circuitry in our setup. The described approach allows for the discrimination of cell populations in culture as well as the developmental, morphological and functional characterization of the primary hippocampal neurons growing in the 96-well microplate setup. The ensemble of techniques focuses important aspects to consider in developing in the primary neuronal culture. Validation of the discrimination of cell types and neurite outgrowth was successfully preformed. As the images are obtained in an automated fluorescence microscope, a great amount of data is collected in a short period of time. In addition, there are available algorithms for the computational analysis of such data. These are also optimistic results for the future high-content application. When validation is complete, it will provide an effective set of tools to discriminate changes in the culture along time, both in control conditions and in pharmacologically stimulated cultures.

When fully optimized, the use of 96-well microplates will be of great value for three main reasons: 1. it will allow for the rapid screening of pharmacological compounds; 2. it will be possible to obtain a great amount of data in short time; and 3. it will save biological material. However, before its use in high-content screening applications it is necessary to optimize culture conditions, as for now it is not possible to maintain healthy cultures for long-term studies. This may require modifications in culturing and maintenance procedures, such as changing the substrate, and/or the medium used. Of great interest in the lab is the implementation of an insert in the wells that will allow for the creation of a microenvironment that limits contact with the external environment, as is successfully achieved with the use of a coverslip in the 6-well setup. The presence and proliferation of

non neuronal cells should also be evaluated: as it is known that non neuronal cells, such as astrocytes, are important for the healthy development of neurons in culture, the results clearly showed that there is an extensive proliferation of these and other non-neuronal cells in the culture. These cells may be a problem in culture due to nutrient consumption. Additionally, it is evident that cell density could be a problem for the neural circuit development and the analytical approaches: the number of neurons seems to be too high for immunocytochemical studies, especially for the visualization of individual processes, spines and synaptic markers. In agreement with this are many studies where the same techniques were used, with very low density cultures (Deitch and Banker, 1993; Mandell and Banker, 1995). On the other hand, long term cultures require high cell survival for appropriate development and maturation of phenotypical and functional properties. Decreasing the cell density may impair the adequate development of the neural network, as nerve terminals require the afferent contact for adequate directionality of the growing processes and trafficking of synaptic components, as well as for the establishment of the adequate electrical circuit. A compromise between all of these considerations must be achieved in order to obtain a reliable and sensitive system that can be used as a biosensor for the high-content screening of pharmacological compounds targeting neurological disorders.

CHAPTER 6 References

Aguado, F., Espinosa-Parrilla, J., Carmona, M., and Soriano, E. (2002). Neuronal activity regulates correlated network properties of spontaneous calcium transients in astrocytes in situ. J Neurosci *22*, 9430-9444.

Banker, G., and Cowan, W. (1977). Rat hippocampal neurons in dispersed cell culture. Brain Res *126*, 397-342.

Banker, G., and Goslin, K. (1998). Culturing nerve cells, 2nd edn (Cambridge, Mass., MIT Press).

Bartlett, W., and Banker, G. (1984a). An electron microscopic study of the development of axons and dendrites by hippocampal neurons in culture. I. Cells which develop without intercellular contacts. J Neurosci *4*, 1944-1953.

Bartlett, W., and Banker, G. (1984b). An electron microscopic study of the development of axons and dendrites by hippocampal neurons in culture. II. Synaptic relationships. J Neurosci *4*, 1954-1965.

Ben-Ari, Y. (2002). Excitatory actions of gaba during development: the nature of the nurture. Nat Rev Neurosci *3*, 728-739.

Bhatt, D.H., Zhang, S.X., and Gan, W.B. (2009). Dendritic Spine Dynamics. Annual Review of Physiology *71*, 261-282.

Blankenship, A., and Feller, M. (2010). Mechanisms underlying spontaneous patterned activity in developing neural circuits. Nat Rev Neurosci *11*, 18-29.

Bliss, T., and Gardner-Medwin, A. (1973). Long-lasting potentiation of synaptic transmission in the dentate area of the unanaestetized rabbit following stimulation of the perforant path. J Physiol *232*, 357-374.

Bliss, T., and Lomo, T. (1973). Long-lasting potentiation of synaptic transmission in the dentate area of the anaesthetized rabbit following stimulation of the perforant path. J Physiol *232*, 331-356.

Bloodgood, B.L., and Sabatini, B.L. (2007). Ca2+ signaling in dendritic spines. Current Opinion in Neurobiology *17*, 345-351.

Bortolotto, Z., Anderson, W., Isaac, J., and Collingridge, G. (2001). Synaptic plasticity in the hippocampal slice preparation. Curr Protoc Neurosci *Chapter 6*, Unit 6.13.

Bourne, J., and Harris, K. (2007). Do thin spines learn to be mushroom spines that remember? Curr Opin Neurobiol *17*, 381-386.

Bourne, J.N., and Harris, K.M. (2008). Balancing structure and function at hippocampal dendritic spines. Annual Review of Neuroscience *31*, 47-67.

Calabresi, P., Picconi, B., Parnetti, L., and Di Filippo, M. (2006). A convergent model for cognitive dysfunctions in Parkinson's disease: the critical dopamine-acetylcholine synaptic balance. Lancet Neurol *5*, 974-983.

Carlisle, H., and Kennedy, M. (2005). Spine architecture and synaptic plasticity. Trends Neurosci *28*, 182-187.

Carter, A., and Sabatini, B. (2008). Spine calcium signaling. In Dendrites, G. Stuart, N. Spruston, and M. Häusser, eds. (New York, Oxford University Press), pp. 287-308.

Carvalho, A., Caldeira, M., Santos, S., and Duarte, C. (2008). Role of the brain-derived neurotrophic factor at glutamatergic synapses. Br J Pharmacol *153 Suppl 1*, S310-324.

Chang, J., Brewer, G., and Wheeler, B. (2001). Modulation of neural network activity by patterning. Biosens Bioelectron *16*, 527-533.

Chen, Y., Stevens, B., Chang, J., Milbrandt, J., Barres, B., and Hell, J. (2008). NS21: re-defined and modified supplement B27 for neuronal cultures. J Neurosci Methods *171*, 239-247.

Citri, A., and Malenka, R. (2008). Synaptic plasticity: multiple forms, functions, and mechanisms. Neuropsychopharmacology *33*, 18-41.

Cohen, E., Ivenshitz, M., Amor-Baroukh, V., Greenberger, V., and Segal, M. (2008). Determinants of spontaneous activity in networks of cultured hippocampus. Brain Research *1235*, 21-30.

Cohen, S., and Greenberg, M. (2008). Communication between the synapse and the nucleus in neuronal development, plasticity, and disease. Annu Rev Cell Dev Biol *24*, 183-209.

Craig, A., Blackstone, C., Huganir, R., and Banker, G. (1994). Selective clustering of glutamate and gamma-aminobutyric acid receptors opposite terminals releasing the corresponding neurotransmitters. Proc Natl Acad Sci U S A *91*, 12373-12377.

Culmsee, C., Gerling, N., Lehmann, M., Nikolova-Karakashian, M., Prehn, J., Mattson, M., and Krieglstein, J. (2002). Nerve growth factor survival signaling in cultured hippocampal neurons is mediated through TrkA and requires the common neurotrophin receptor P75. Neuroscience *115*, 1089-1108.

Cáceres, A., Banker, G., and Binder, L. (1986). Immunocytochemical localization of tubulin and microtubule-associated protein 2 during the development of hippocampal neurons in culture. J Neurosci *6*, 714-722.

da Silva, J., and Dotti, C. (2002). Breaking the neuronal sphere: regulation of the actin cytoskeleton in neuritogenesis. Nat Rev Neurosci *3*, 694-704.

Dailey, M., and Smith, S. (1996). The dynamics of dendritic structure in developing hippocampal slices. J Neurosci *16*, 2983-2994.

Deitch, J., and Banker, G. (1993). An electron microscopic analysis of hippocampal neurons developing in culture: early stages in the emergence of polarity. J Neurosci *13*, 4301-4315.

Dent, E., and Gertler, F. (2003). Cytoskeletal dynamics and transport in growth cone motility and axon guidance. Neuron *40*, 209-227.

Doré, S., Kar, S., and Quirion, R. (1997). Insulin-like growth factor I protects and rescues hippocampal neurons against beta-amyloid- and human amylin-induced toxicity. Proc Natl Acad Sci U S A *94*, 4772-4777.

Dotti, C., Sullivan, C., and Banker, G. (1988). The establishment of polarity by hippocampal neurons in culture. J Neurosci *8*, 1454-1468.

Dunaevsky, A., Blaszeski, R., Yuste, R., and Mason, C. (2001). Spine motility with synaptic contact. Nature Neuroscience *4*, 685-686.

Dunaevsky, A., and Mason, C. (2003a). Spine motility: a means towards an end? Trends Neurosci *26*, 155-160.

Dunaevsky, A., and Mason, C.A. (2003b). Spine motility: a means towards an end? Trends in Neurosciences *26*, 155-160.

Dunaevsky, A., Tashiro, A., Majewska, A., Mason, C., and Yuste, R. (1999). Developmental regulation of spine motility in the mammalian central nervous system. Proc Natl Acad Sci U S A *96*, 13438-13443.

Feller, M. (1999). Spontaneous correlated activity in developing neural circuits. Neuron *22*, 653-656.

Feng, G., Mellor, R., Bernstein, M., Keller-Peck, C., Nguyen, Q., Wallace, M., Nerbonne, J., Lichtman, J., and Sanes, J. (2000). Imaging neuronal subsets in transgenic mice expressing multiple spectral variants of GFP. Neuron *28*, 41-51.

Ferrer, I., and Gullotta, F. (1990). Down's syndrome and Alzheimer's disease: dendritic spine counts in the hippocampus. Acta Neuropathol *79*, 680-685.

Fiala, J., Spacek, J., and Harris, K. (2002). Dendritic spine pathology: cause or consequence of neurological disorders? Brain Res Brain Res Rev *39*, 29-54.

Fiala, J.C., Spacek, J., and Harris, K.M. (2008). Dendrite structure. In Dendrites, G. Stuart, n. Spruston, and M. Häusser, eds. (New York, Oxford University Press), pp. 1-42.

Fischer, M., Kaech, S., Knutti, D., and Matus, A. (1998). Rapid actin-based plasticity in dendritic spines. Neuron *20*, 847-854.

Fiszman, M., Borodinsky, L., and Neale, J. (1999). GABA induces proliferation of immature cerebellar granule cells grown in vitro. Brain Res Dev Brain Res *115*, 1-8.

Fletcher, T., De Camilli, P., and Banker, G. (1994). Synaptogenesis in hippocampal cultures: evidence indicating that axons and dendrites become competent to form synapses at different stages of neuronal development. J Neurosci *14*, 6695-6706.

Frey, U., and Morris, R. (1997). Synaptic tagging and long-term potentiation. Nature *385*, 533-536.

Fujisawa, S., Shirao, T., and Aoki, C. (2006). In vivo, competitive blockade of N-methyl-D-aspartate receptors induces rapid changes in filamentous actin and drebrin A distributions within dendritic spines of adult rat cortex. Neuroscience *140*, 1177-1187.

Furukawa, S., Furukawa, Y., Satoyoshi, E., and Hayashi, K. (1986). Synthesis and secretion of nerve growth factor by mouse astroglial cells in culture. Biochem Biophys Res Commun *136*, 57-63.

Galdzicki, Z., Siarey, R., Pearce, R., Stoll, J., and Rapoport, S. (2001). On the cause of mental retardation in Down syndrome: extrapolation from full and segmental trisomy 16 mouse models. Brain Res Brain Res Rev *35*, 115-145.

Garcia-Lopez, P., Garcia-Marin, V., and Freire, M. (2007). The discovery of dendritic spines by Cajal in 1888 and its relevance in the present neuroscience. Progress in Neurobiology *83*, 110-130.

Garner, C., Waites, C., and Ziv, N. (2006). Synapse development: still looking for the forest, still lost in the trees. Cell Tissue Res *326*, 249-262.

Gerrow, K., Romorini, S., Nabi, S., Colicos, M., Sala, C., and El-Husseini, A. (2006). A preformed complex of postsynaptic proteins is involved in excitatory synapse development. Neuron *49*, 547-562.

Globus, A., and Scheibel, A. (1967). The effect of visual deprivation on cortical neurons: a Golgi study. Exp Neurol *19*, 331-345.

Grabrucker, A., Vaida, B., Bockmann, J., and Boeckers, T. (2009). Synaptogenesis of hippocampal neurons in primary cell culture. Cell Tissue Res *338*, 333-341.

Göbel, W., and Helmchen, F. (2007). In vivo calcium imaging of neural network function. Physiology (Bethesda) *22*, 358-365.

Ham, M., Bettencourt, L., McDaniel, F., and Gross, G. (2008). Spontaneous coordinated activity in cultured networks: analysis of multiple ignition sites, primary circuits, and burst phase delay distributions. J Comput Neurosci *24*, 346-357.

Hamdache, K., and Labadie, M. (2009). On a reaction-diffusion model for calcium dynamics in dendritic spines. Nonlynear Analysis: Real World Applications *10*, 2478-2492.

Harms, K.J., and Dunaeusky, A. (2007). Dendritic spine plasticity: Looking beyond development. Brain Research *1184*, 65-71.

Harris, K. (1999). Structure, development, and plasticity of dendritic spines. Curr Opin Neurobiol *9*, 343-348.

Hasbani, M., Schlief, M., Fisher, D., and Goldberg, M. (2001). Dendritic spines lost during glutamate receptor activation reemerge at original sites of synaptic contact. J Neurosci *21*, 2393-2403.

Hayashi, Y., and Majewska, A.K. (2005). Dendritic spine geometry: Functional implication and regulation. Neuron *46*, 529-532.

Hering, H., and Sheng, M. (2001). Dendritic spines: Structure, dynamics and regulation. Nature Reviews Neuroscience *2*, 880-888.

Hetman, M., and Xia, Z. (2000). Signaling pathways mediating anti-apoptotic action of neurotrophins. Acta Neurobiol Exp (Wars) *60*, 531-545.

Hinton, V., Brown, W., Wisniewski, K., and Rudelli, R. (1991). Analysis of neocortex in three males with the fragile X syndrome. Am J Med Genet *41*, 289-294.

Honig, M., and Hume, R. (1986). Fluorescent carbocyanine dyes allow living neurons of identified origin to be studied in long-term cultures. J Cell Biol *103*, 171-187.

Honig, M., and Hume, R. (1989a). Carbocyanine dyes. Novel markers for labelling neurons. Trends Neurosci *12*, 336-338.

Honig, M., and Hume, R. (1989b). Dil and diO: versatile fluorescent dyes for neuronal labelling and pathway tracing. Trends Neurosci *12*, 333-335, 340-331.

Houlgatte, R., Mallat, M., Brachet, P., and Prochiantz, A. (1989). Secretion of nerve growth factor in cultures of glial cells and neurons derived from different regions of the mouse brain. J Neurosci Res *24*, 143-152.

Hubel, D., and Wiesel, T. (1977). Ferrier lecture. Functional architecture of macaque monkey visual cortex. Proc R Soc Lond B Biol Sci *198*, 1-59.

Irwin, S., Patel, B., Idupulapati, M., Harris, J., Crisostomo, R., Larsen, B., Kooy, F., Willems, P., Cras, P., Kozlowski, P., *et al.* (2001). Abnormal dendritic spine characteristics in the temporal and visual cortices of patients with fragile-X syndrome: a quantitative examination. Am J Med Genet *98*, 161-167.

Job, C., and Eberwine, J. (2001). Localization and translation of mRNA in dendrites and axons. Nat Rev Neurosci *2*, 889-898.

Johnston, M. (2004). Clinical disorders of brain plasticity. Brain Dev *26*, 73-80.

Kasai, H., Matsuzaki, M., Noguchi, J., Yasumatsu, N., and Nakahara, H. (2003). Structure-stability-function relationships of dendritic spines. Trends Neurosci *26*, 360-368.

Kato, T., Yamakawa, Y., Sakazaki, Y., Ito, J., Kato, H., Tsunooka, H., Masaoka, A., and Tanaka, R. (1981). Glial cell growth-promoting factor in astrocytoma (C6) cell extracts. Brain Res *254*, 596-601.

Kennedy, M.B. (2000). Signal-processing machines at the postsynaptic density. Science *290*, 750-754.

Kim, J., Liao, D., Lau, L., and Huganir, R. (1998). SynGAP: a synaptic RasGAP that associates with the PSD-95/SAP90 protein family. Neuron *20*, 683-691.

Kleinfeld, D., Kahler, K., and Hockberger, P. (1988). Controlled outgrowth of dissociated neurons on patterned substrates. J Neurosci *8*, 4098-4120.

Kotaleski, J., and Blackwell, K. (2010). Modelling the molecular mechanisms of synaptic plasticity using systems biology approaches. Nat Rev Neurosci *11*, 239-251.

LaMantia, A.-S. (2004). Plasticity of mature synapses and circuits. In Neuroscience, D. Purves, G. Augustine, D. Fitzpatrick, W. Hall, A.-S. LaMantia, J. McNamara, and S.M. Williams, eds. (Massachussets, Sinauer Associates, Inc.), pp. 575-612.

Lang, C., Barco, A., Zablow, L., Kandel, E., Siegelbaum, S., and Zakharenko, S. (2004). Transient expansion of synaptically connected dendritic spines upon induction of hippocampal long-term potentiation. Proc Natl Acad Sci U S A *101*, 16665-16670.

Lardi-Studler, B., and Fritschy, J. (2007). Matching of pre- and postsynaptic specializations during synaptogenesis. Neuroscientist *13*, 115-126.

Lee, H.K. (2006). Synaptic plasticity and phosphorylation. Pharmacology & Therapeutics *112*, 810-832.

Lelong, I., Petegnief, V., and Rebel, G. (1992). Neuronal cells mature faster on polyethyleneimine coated plates than on polylysine coated plates. J Neurosci Res *32*, 562-568.

Levi-Montalcini, R. (1987). The nerve growth factor 35 years later. Science *237*, 1154-1162.

Lewin, G., and Barde, Y. (1996). Physiology of the neurotrophins. Annu Rev Neurosci *19*, 289-317.

Lisman, J. (1989). A mechanism for the Hebb and the anti-Hebb processes underlying learning and memory. Proc Natl Acad Sci U S A *86*, 9574-9578.

Liu, B., Ma, J., Gao, E., He, Y., Cui, F., and Xu, Q. (2008). Development of an artificial neuronal network with post-mitotic rat fetal hippocampal cells by polyethylenimine. Biosens Bioelectron *23*, 1221-1228.

Liu, B., Ma, J., Xu, Q., and Cui, F. (2006). Regulation of charged groups and laminin patterns for selective neuronal adhesion. Colloids Surf B Biointerfaces *53*, 175-178.

Liu, Q., and Wong-Riley, M. (2005). Postnatal developmental expressions of neurotransmitters and receptors in various brain stem nuclei of rats. J Appl Physiol *98*, 1442-1457.

Majewska, A., Tashiro, A., and Yuste, R. (2000). Regulation of spine calcium dynamics by rapid spine motility. Journal of Neuroscience *20*, 8262-8268.

Malenka, R., and Nicoll, R. (1993). NMDA-receptor-dependent synaptic plasticity: multiple forms and mechanisms. Trends Neurosci *16*, 521-527.

Malinow, R., Hayashi, Y., Maletic-Savatic, M., Zaman, S., Poncer, J., Shi, S., Esteban, J., Osten, P., and Seidenman, K. (2010). Introduction of green fluorescent protein (GFP) into hippocampal neurons through viral infection. Cold Spring Harb Protoc *2010*, pdb.prot5406.

Mandell, J., and Banker, G. (1995). The microtubule cytoskeleton and the development of neuronal polarity. Neurobiol Aging *16*, 229-237; discussion 238.

Marcello, E., Epis, R., and Di Luca, M. (2008). Amyloid flirting with synaptic failure: towards a comprehensive view of Alzheimer's disease pathogenesis. Eur J Pharmacol *585*, 109-118.

Margeta, M., and Shen, K. (2010). Molecular mechanisms of synaptic specificity. Mol Cell Neurosci *43*, 261-267.

Matsubayashi, Y., Iwai, L., and Kawasaki, H. (2008). Fluorescent double-labeling with carbocyanine neuronal tracing and immunohistochemistry using a cholesterol-specific detergent digitonin. J Neurosci Methods *174*, 71-81.

Matsuzaki, M. (2007). Factors critical for the plasticity of dendritic spines and memory storage. Neurosci Res *57*, 1-9.

Matsuzaki, M., Honkura, N., Ellis-Davies, G., and Kasai, H. (2004). Structural basis of long-term potentiation in single dendritic spines. Nature *429*, 761-766.

McAllister, A., Katz, L., and Lo, D. (1999). Neurotrophins and synaptic plasticity. Annu Rev Neurosci *22*, 295-318.

McAllister, A., Lo, D., and Katz, L. (1995). Neurotrophins regulate dendritic growth in developing visual cortex. Neuron *15*, 791-803.

Murphy, R., Oger, J., Saide, J., Blanchard, M., Arnason, B., Hogan, C., and Pantazis, N. (1977). Secretion of nerve growth factor by central nervous system glioma cells in culture. J Cell Biol *72*, 769-773.

Müller, M., Gähwiler, B., Rietschin, L., and Thompson, S. (1993). Reversible loss of dendritic spines and altered excitability after chronic epilepsy in hippocampal slice cultures. Proc Natl Acad Sci U S A *90*, 257-261.

Neves, G., Cooke, S., and Bliss, T. (2008). Synaptic plasticity, memory and the hippocampus: a neural network approach to causality. Nat Rev Neurosci *9*, 65-75.

Niu, S., Yabut, O., and D'Arcangelo, G. (2008). The Reelin signaling pathway promotes dendritic spine development in hippocampal neurons. J Neurosci *28*, 10339-10348.

Noguchi, J., Matsuzaki, M., Ellis-Davies, G.C.R., and Kasai, H. (2005). Spine-neck geometry determines NMDA receptor-dependent Ca2+ signaling in dendrites. Neuron *46*, 609-622.

Nusser, Z., Lujan, R., Laube, G., Roberts, J.D.B., Molnar, E., and Somogyi, P. (1998). Cell type and pathway dependence of synaptic AMPA receptor number and variability in the hippocampus. Neuron *21*, 545-559.

O'Donovan, M. (1999). The origin of spontaneous activity in developing networks of the vertebrate nervous system. Curr Opin Neurobiol *9*, 94-104.

Okamoto, K., Nagai, T., Miyawaki, A., and Hayashi, Y. (2004). Rapid and persistent modulation of actin dynamics regulates postsynaptic reorganization underlying bidirectional plasticity. Nat Neurosci *7*, 1104-1112.

Okuda, S., Saito, H., and Katsuki, H. (1994). Divergent trophic actions of glioma conditioned media on cultured rat hippocampal neurons. Biol Pharm Bull *17*, 735-738.

Pan, F., and Gan, W. (2008). Two-photon imaging of dendritic spine development in the mouse cortex. Dev Neurobiol *68*, 771-778.

Papa, M., Bundman, M.C., Greenberger, V., and Segal, M. (1995). MORPHOLOGICAL ANALYSIS OF DENDRITIC SPINE DEVELOPMENT IN PRIMARY CULTURES OF HIPPOCAMPAL-NEURONS. Journal of Neuroscience *15*, 1-11.

Parnass, Z., Tashiro, A., and Yuste, R. (2000). Analysis of spine morphological plasticity in developing hippocampal pyramidal neurons. Hippocampus *10*, 561-568.

Parnavelas, J., Globus, A., and Kaups, P. (1973). Continuous illumination from birth affects spine density of neurons in the visual cortex of the rat. Exp Neurol *40*, 742-747.

Pfeiffer, B., and Huber, K. (2009). The state of synapses in fragile X syndrome. Neuroscientist *15*, 549-567.

Pickering, M., Pickering, B.W., Murphy, K.J., and O'Connor, J.J. (2008). Discrimination of cell types in mixed cortical culture using calcium imaging: A comparison to immunocytochemical labeling. Journal of Neuroscience Methods *173*, 27-33.

Polleux, F., and Gosh, A. (2008). Molecular determinants of dendrite and spine development. In Dendrites, G. Stuart, N. Spruston, and M. Häusser, eds. (New York, Oxford University Press), pp. 95-116.

Potter, S., and DeMarse, T. (2001). A new approach to neural cell culture for long-term studies. J Neurosci Methods *110*, 17-24.

Rao, A., Kim, E., Sheng, M., and Craig, A. (1998). Heterogeneity in the molecular composition of excitatory postsynaptic sites during development of hippocampal neurons in culture. J Neurosci *18*, 1217-1229.

Rao, S., and Winter, J. (2009). Adhesion molecule-modified biomaterials for neural tissue engineering. Front Neuroengineering *2*, 6.

Ray, J., Peterson, D., Schinstine, M., and Gage, F. (1993). Proliferation, differentiation, and long-term culture of primary hippocampal neurons. Proc Natl Acad Sci U S A *90*, 3602-3606.

Roerig, B., and Feller, M. (2000). Neurotransmitters and gap junctions in developing neural circuits. Brain Res Brain Res Rev *32*, 86-114.

Russo, S., Dietz, D., Dumitriu, D., Morrison, J., Malenka, R., and Nestler, E. (2010). The addicted synapse: mechanisms of synaptic and structural plasticity in nucleus accumbens. Trends Neurosci.

Ryan, T., and Grant, S. (2009). The origin and evolution of synapses. Nat Rev Neurosci.

Sabatini, B.L., Oertner, T.G., and Svoboda, K. (2002). The life cycle of Ca2+ ions in dendritic spines. Neuron *33*, 439-452.

Sala, C., Cambianica, I., and Rossi, F. (2008). Molecular mechanisms of dendritic spine development and maintenance. Acta Neurobiologiae Experimentalis *68*, 289-304.

Salama-Cohen, P., Arévalo, M., Meier, J., Grantyn, R., and Rodríguez-Tébar, A. (2005). NGF controls dendrite development in hippocampal neurons by binding to p75NTR and modulating the cellular targets of Notch. Mol Biol Cell *16*, 339-347.

Sanes, J.R., and Lichtman, J.W. (1999). Can molecules explain long-term potentiation? Nature Neuroscience *2*, 597-604.

Santos, S.D., Carvalho, A.L., Caldeira, M.V., and Duarte, C.B. (2009). REGULATION OF AMPA RECEPTORS AND SYNAPTIC PLASTICITY. Neuroscience *158*, 105-125.

Schubert, V., Da Silva, J., and Dotti, C. (2006). Localized recruitment and activation of RhoA underlies dendritic spine morphology in a glutamate receptor-dependent manner. J Cell Biol *172*, 453-467.

Segal, M. (2005). Dendritic spines and long-term plasticity. Nat Rev Neurosci *6*, 277-284.

Selkoe, D. (2002). Alzheimer's disease is a synaptic failure. Science *298*, 789-791.

Sheng, M., and Hoogenraad, C.C. (2007). The postsynaptic architecture of excitatory synapses: A more quantitative view. Annual Review of Biochemistry *76*, 823-847.

Shors, T., Chua, C., and Falduto, J. (2001). Sex differences and opposite effects of stress on dendritic spine density in the male versus female hippocampus. J Neurosci *21*, 6292-6297.

Sorra, K.E., and Harris, K.M. (2000). Overview on the structure, composition, function, development, and plasticity of hippocampal dendritic spines. Hippocampus *10*, 501-511.

Soussou, W., Yoon, G., Brinton, R., and Berger, T. (2007). Neuronal network morphology and electrophysiologyof hippocampal neurons cultured on surface-treated multielectrode arrays. IEEE Trans Biomed Eng *54*, 1309-1320.

Spitzer, N. (2002). Activity-dependent neuronal differentiation prior to synapse formation: the functions of calcium transients. J Physiol Paris *96*, 73-80.

Spitzer, N. (2006). Electrical activity in early neuronal development. Nature *444*, 707-712.

Stepanyants, A., Tamás, G., and Chklovskii, D. (2004). Class-specific features of neuronal wiring. Neuron *43*, 251-259.

Stephan, K., Baldeweg, T., and Friston, K. (2006). Synaptic plasticity and dysconnection in schizophrenia. Biol Psychiatry *59*, 929-939.

Sudhof, T.C. (2004). The synaptic vesicle cycle. Annual Review of Neuroscience *27*, 509-547.

Svoboda, K., and Yasuda, R. (2006). Principles of two-photon excitation microscopy and its applications to neuroscience. Neuron *50*, 823-839.

Swann, J., Al-Noori, S., Jiang, M., and Lee, C. (2000). Spine loss and other dendritic abnormalities in epilepsy. Hippocampus *10*, 617-625.

Südhof, T. (2008). Neuroligins and neurexins link synaptic function to cognitive disease. Nature *455*, 903-911.

Südhof, T.C. (2006). Synaptogenesis: When Long-Distance Relations Become Intimate. In Molecular mechanisms of synaptogenesis, A. Dityatev, and A. El-Husseini, eds. (New York, Springer Science+Business Media, LLC), pp. 1-9.

Tada, T., and Sheng, M. (2006). Molecular mechanisms of dendritic spine morphogenesis. Curr Opin Neurobiol *16*, 95-101.

Tahirovic, S., and Bradke, F. (2009). Neuronal polarity. Cold Spring Harb Perspect Biol *1*, a001644.

Takumi, Y., Ramirez-Leon, V., Laake, P., Rinvik, E., and Ottersen, O.P. (1999). Different modes of expression of AMPA and NMDA receptors in hippocampal synapses. Nature Neuroscience *2*, 618-624.

Tau, G., and Peterson, B. (2010). Normal development of brain circuits. Neuropsychopharmacology *35*, 147-168.

Thompson, S., Fortunato, C., McKinney, R., Müller, M., and Gähwiler, B. (1996). Mechanisms underlying the neuropathological consequences of epileptic activity in the rat hippocampus in vitro. J Comp Neurol *372*, 515-528.

Trinchese, F., Liu, S., Ninan, I., Puzzo, D., Jacob, J., and Arancio, O. (2004). Cell cultures from animal models of Alzheimer's disease as a tool for faster screening and testing of drug efficacy. J Mol Neurosci *24*, 15-21.

van Ooyen, A., and van Pelt, J. (1994). Activity-dependent neurite outgrowth and neural network development. Prog Brain Res *102*, 245-259.

van Spronsen, M., and Hoogenraad, C. (2010). Synapse pathology in psychiatric and neurologic disease. Curr Neurol Neurosci Rep *10*, 207-214.

Vicario-Abejón, C. (2004). Long-term culture of hippocampal neurons. Curr Protoc Neurosci *Chapter 3,* Unit 3.2.

Westermann, R., Hardung, M., Meyer, D., Ehrhard, P., Otten, U., and Unsicker, K. (1988). Neuronotrophic factors released by C6 glioma cells. J Neurochem *50*, 1747-1758.

Winter, J., Han, N., Jensen, R., Cogan, S., and Rizzo, J. (2009). Adhesion molecules promote chronic neural interfaces following neurotrophin withdrawal. Conf Proc IEEE Eng Med Biol Soc *2009*, 7151-7154.

Xie, Z., Huganir, R., and Penzes, P. (2005). Activity-dependent dendritic spine structural plasticity is regulated by small GTPase Rap1 and its target AF-6. Neuron *48*, 605-618.

Yamagata, M., Sanes, J.R., and Weiner, J.A. (2003). Synaptic adhesion molecules. Current Opinion in Cell Biology *15*, 621-632.

Yamamoto, N., Tamada, A., and Murakami, F. (2002). Wiring of the brain by a range of guidance cues. Prog Neurobiol *68*, 393-407.

Young, P., and Feng, G. (2004). Labeling neurons in vivo for morphological and functional studies. Curr Opin Neurobiol *14*, 642-646.

Yu, X., and An, L. (2002). A serum- and antioxidant-free primary culture model of mouse cortical neurons for pharmacological screen and studies of neurotrophic and neuroprotective agents. Cell Mol Neurobiol *22*, 197-206.

Yuste, R., and Denk, W. (1995). DENDRITIC SPINES AS BASIC FUNCTIONAL UNITS OF NEURONAL INTEGRATION. Nature *375*, 682-684.

Zander, J., Münster-Wandowski, A., Brunk, I., Pahner, I., Gómez-Lira, G., Heinemann, U., Gutiérrez, R., Laube, G., and Ahnert-Hilger, G. (2010). Synaptic and vesicular coexistence of VGLUT and VGAT in selected excitatory and inhibitory synapses. J Neurosci *30*, 7634-7645.

Zhang, L., and Poo, M. (2001). Electrical activity and development of neural circuits. Nat Neurosci *4 Suppl*, 1207-1214.

Zito, K., Scheuss, V., Knott, G., Hill, T., and Svoboda, K. (2009). Rapid Functional Maturation of Nascent Dendritic Spines. Neuron *61*, 247-258.

Ziv, N., and Garner, C. (2001). Principles of glutamatergic synapse formation: seeing the forest for the trees. Curr Opin Neurobiol *11*, 536-543.